Order Number 9315472

A theoretical study of spatial and temporal cytosolic calcium oscillations

Jafri, M. Saleet, Ph.D.

City University of New York, 1993

U·M·I
300 N. Zeeb Rd.
Ann Arbor, MI 48106

A THEORETICAL STUDY OF SPATIAL AND TEMPORAL CYTOSOLIC CALCIUM OSCILLATIONS

by

M. SALEET JAFRI

A dissertation submitted to the Graduate Faculty in biomedical sciences in partial fulfillment of the requirements for the degree of Doctor of Philosophy, The City University of New York.

1993

This manuscript has been read and accepted by the Graduate Faculty in Biomedical Sciences in satisfaction of the dissertation requirements for the degree of Doctor of Philosophy.

January 7, 1993
Date

Chair of Examining Committee

January 7, 1993
Date

Executive Officer

Craig J. Benham, PhD

George Nemethy, PhD

Michael Lacker, MD, PhD

Supervisory Comittee

The City University of New York

Abstract

A THEORETICAL STUDY OF SPATIAL AND TEMPORAL CYTOSOLIC CALCIUM OSCILLATIONS

by

M. SALEET JAFRI

Advisor: Professor Craig J. Benham

Cytosolic calcium oscillations occur in a wide variety of cells controlling cellular functions such as contraction, secretion and gene expression. In this dissertation mathematical models are used to study cytosolic calcium oscillations. A membrane model based on the electrophysiological properties of the endoplasmic reticulum membrane (ER) is proposed. The initial model includes equations for the cytosolic calcium concentration, the ER membrane potential, and the concentration of calcium binding proteins. It features a calcium induced calcium release channel in the ER, calcium pumps in the ER and plasma membrane, constant calcium entry in to the cytosol. The membrane model predicts that the frequency and amplitude can be modulated by controlling the rate of calcium entry into the cytosol or by varying the amount of active calcium binding sites. The model is then modified to include counterions, and a separate inositol 1,4,5-trisphosphate (IP_3) sensitive store which has its own pumps and calcium

release channel sensitive to IP_3. The modified model shows that the period of latency depends on the rate of calcium entry into the cytosol. It also shows that the pump rate out of the cytosol can modify the frequency and amplitude of oscillations. It predicts that the presence of counterions augments the oscillations in that the amplitude and width are increased. A diffusion term is added to the initial model to study the propagation of waves of elevated cytosolic calcium concentration in cells. The amplitude and speed of a calcium wave can be modulated by the rate of calcium influx, pump rates, and effective diffusion constant.

Acknowledgments

The completion of a PhD is not only the intellectual work of an individual but it is a composite of the interaction with peers in the field and the emotional support of friends and family. First, I would like to my advisor Craig Benham for his helpful discussion and advice when I needed it. I would also like to give particular thanks to my collaborator Boaz Gillo whose experimental research and discussion gave me the desire to study calcium oscillations in cells. I would also like to thank Charlie Peskin, Pedro Pasik, Arthur Sherman, and Sandor Vajda for their helpful discussion.

It is just as important to mention the friends and family that played a crucial role in my accomplishment. I first would like to thank my parents Salma and M. Haris Jafri for their support and sacrifice through the years. I would also like to thank my brothers and sisters, Samir, Ayesha, Ayfer, Shabeen and Deeba. I would like to particularly like to acknowledge the support of friends, Davis Hill, Ted Hsueh, Milagros Marchese, Janne Ravantti, and Hope Taub.

Finally, I would also like to thank CUNY and Mt. Sinai for giving me the facilities and the funding to persue my research area of interest.

Table of Contents

List of Tables

List of Figures

Introduction

This dissertation presents a mathematical study of cytosolic calcium oscillations. This introduction provides a brief background survey of the field. It first describes the phenomenon of cytosolic calcium oscillations and the experimental evidence for it. This is followed by a description of the various models that have been proposed to explain calcium oscillations.

Cytosolic Calcium oscillations

Calcium is used by the cell as a second messenger, that is, it is release as a result of an initiating chain of biochemical events and causes another set of biochemical events to occur. Calcium is maintained at a very low concentration in the cellular cytosol. In fact, highly elevated calcium will disrupt normal cell function. Cytosolic calcium ranges from 50-200 nM in a resting cell to up to 10 μM during cell activity (Berridge and Irvine, 1989). Cell activities that result from elevation of the cytosolic calcium concentration include contraction, secretion, and neuronal transmission (Jaffe, 1991).

Cytosolic calcium concentration can be measured both directly and indirectly. Direct measurement involves the use of fluorescent calcium-sensitive dyes, that is, compounds that emit fluorescence under excitation by certain

wavelengths of light when bound to calcium. These dyes are introduced into the cell cytosol by microinjection or by diffusion through the plasma membrane. A few such dyes are Fura-2, Fluo-3, Indo, and calcium green. Measurements of fluorescent intensities are made using whole cell fluorescence microscopy or confocal microscopy. Confocal microscopy provides high resolution images of spatial calcium distribution in cells. When using fluorescent dyes, one must realize that they serve as a buffer since they bind calcium, preventing a fraction of the calcium from fulfilling its biochemical role. The calcium dyes move more freely through the cytosol compared to native calcium binding proteins and increase the effective diffusion rate of calcium (Hanley, personal communication).

Cytosolic calcium concentration can also be measured indirectly by measuring the ionic current of a calcium-dependent channel in the plasma membrane, such as the calcium-dependent chloride channel in *Xenopus* oocytes (DeLisle et al., 1990; Parker and Ivorra 1990; Parker and Miledi, 1986) or rat pancreatic acinar cells (Wakui et al., 1990). In *Xenopus* oocytes, elevation of the cytosolic calcium concentration causes an increase in the chloride current. Studies using both indirect and direct methods have shown that the methods agree (Parker and Ivorra, 1990; Parker and Miledi, 1986). In *Xenopus* oocytes, waves of elevated calcium concentration are shown to propagate throughout the outer 20-40 μm of the cell. Target patterns and spiral

calcium waves have been observed in these oocytes (Girard et al., 1992; Lechleiter et al., 1992; Lechleiter et al., 1991; Parker and Yao, 1991).

Oscillations in the cytosolic calcium concentration ($[Ca]_{cyt}$) regulate a variety of cellular functions in different systems, such as secretion in the pituitary (Schlegal et al., 1987) and parotid glands (Gray, 1988), contraction of smooth muscle (Ambler et al., 1988; Benham et al., 1986), and cardiac inotrophy and induction of arrhythmias (Lakatta et al., 1986). Calcium oscillations also occur in other types of cells, where their functions remain unknown. Examples include fibroblasts (Harootunian et al., 1988), hepatocytes (Rooney et al., 1991), endothelial cells (Jacob et al., 1988) and oocytes (Gillo et al., 1987; DeLisle et al., 1990).

In experiments with non-excitable cells, calcium oscillations are evoked in two ways. The application of extracellular calcium (Harootunian et al., 1988; Stern et al., 1988) is responsible for calcium entry into the cytosol through plasmalemmal calcium channels. Alternatively, application of calcium mobilizing neurotransmitters (Dascal et al., 1985; Wakui and Petersen, 1990) causes release from intracellular stores mediated by a secondary messenger, such as inositol 1,4,5-trisphosphate (IP_3; Berridge and Irvine, 1989). In excitable cells, calcium entry is mediated by voltage-sensitive calcium channels in the plasmalemmal and by the Na/Ca exchange pump.

In vivo, exposure of the aforementioned cells to a calcium mobilizing neurotransmitter induces a complex series of events that results in calcium release from the ER. First, the neurotransmitter binds to a cell surface receptor which activates a G protein. This in turn activates a phospholipase C which cleaves phosphotidylinositol 4,5-bisphosphate into IP_3 and 1,2-diacylglycerol. The IP_3 diffuses in the cytosol and binds to the IP_3 receptor on the ER membrane, which results in calcium release into the cytosol. The 1,2-diacylglycerol activates protein kinase C (PKC) with the help of calcium. The activated PKC then phosphorylates various other proteins in the cell and regulates their activity (Darnell et al., 1990).

Although the ER compartment is small compared to the volume of the cytosol, the amount of calcium sequestered there is large due to a higher free calcium concentration and the presence of calcium binding proteins. The total concentration of calcium in the ER is approximately three orders of magnitude higher than that of the cytosol (Somlyo et al., 1981). This is more than adequate to account for the calcium fluxes observed during oscillations.

Releasable intracellular calcium stores have been shown by direct and indirect methods to be in the ER (Jacob et al., 1988; Berridge and Irvine, 1989; Somlyo et al., 1981). Jacob and co-workers have shown that the plasma membrane potential plays no role in calcium oscillations. They observed calcium

oscillations in human endothelial cells while the plasma membrane potential was held constant using voltage clamp techniques. Calcium oscillations also have been observed in cells in an extracellular medium containing no calcium (Gillo et al., 1987).

Theoretical Models

Three basic mechanisms have been proposed to explain cytosolic calcium oscillations. A molecular model (Meyer and Stryer, 1988; Swillens and Mercan, 1990) assumes that IP_3 binding to the calcium release channel in the ER is the driving force behind the oscillations. A second model, the compartmental calcium-exchange model (Kuba and Takeshita, 1981; Goldbeter et al., 1990; Somogyi and Stucki, 1991), is based on fluctuations in the calcium concentration in both the cytosol and the ER lumen. The variation of this model proposed by Goldbeter and co-workers (1990), adds a constant calcium flux into the cytosol from IP_3-sensitive stores of the ER. It posits a balance between the cytosolic and ER luminal calcium concentrations, so that the depletion of the latter causes the closing of the ER calcium channel, thereby inhibiting calcium-dependent calcium release into the cytosol. The formulation by Somogyi and Stucki (1991) differs from the original compartmental calcium-exchange model in that it requires cooperative binding of IP_3 and calmodulin to the ER calcium release channel. In a third

model, Keizer and DeYoung (1992) have proposed that both calcium and IP_3 must bind to the calcium channel for calcium release to occur.

The models by Swillens and Mercan, Meyer and Stryer, and Keizer and Deyoung all postulate that there is only one calcium pool in the ER from which calcium is released. The model by Goldbeter and co-workers assumes two pools of calcium. One pool releases calcium in response to calcium binding to the calcium-release channel, and the other pool releases calcium in response to IP_3 binding to a different calcium-release channel.

We propose another possible physiological mechanism to explain calcium oscillations, which is based on the interplay between the calcium channels and calcium pumps that are found in the ER membrane. In our model the driving force behind the oscillations is the electrochemical gradient across the ER membrane. Calcium oscillations occur when the elevation in cytosolic calcium triggers calcium-dependent calcium release from the ER through calcium binding to the calcium release channel. The resulting increase in cytosolic calcium accelerates the rate of release into the cytosol in an autocatalytical manner. The termination of release occurs when the electrochemical calcium gradient is diminished by the increase of cytosolic calcium to the point where the rate of calcium removal by the action of calcium pumps exceeds the rate of movement of calcium through the channel. Since the

pump rate is dependent on calcium binding, as the cytosolic calcium concentration decreases the pump rate also decreases. Eventually, the pump rate will fall enough so that the calcium entry into the cytosol once again dominates the changes in cytosolic calcium. Oscillations occur as this cycle repeats itself. It is important to note that the cytosolic calcium entry that triggers these events is constant and need not oscillate. Okada and co-workers (1982) offered a similar mechanism in which the calcium oscillations occurred as a result of the movement of calcium across the plasma membrane. Jacob and co-workers (1988), however, showed that in certain cells the plasma membrane potential played no role in cytosolic calcium oscillations, although they did not exclude the role of ER membrane potential fluctuations.

This study develops this membrane mechanism for generating cytosolic calcium oscillations. Equations describing changes in cytosolic calcium and ER membrane potential are solved. The potential role of buffering in the control of cytoplasmic calcium oscillations is included. The model is applied to simulate the propagation of calcium waves in the cytosol.

The first chapter develops the membrane model for temporal cytosolic calcium oscillations. Chapter Two further refines the membrane model by adding the effect of ions other than calcium that move passively across the endoplasmic reticulum (ER) membrane, and by separating the calcium fluxes

from the inositol 1,4,5-trisphosphate sensitive compartment. It explores the effects of varying the calcium pump rates and the phenomenon of latency which is the delay of the onset of the oscillations. Chapter Three presents the spatio-temporal model and describes calcium waves in the cell. In this model, calcium waves propagate by the diffusion of calcium which initiates calcium-induced calcium release. Chapter Four is a mathematical treatment of the temporal and spatio-temporal models. It explores the existence of travelling wave solutions of the system of equations for the spatio-temporal model and solves exactly a piecewise linear version of the spatio-temporal model equations.

Chapter One

Chapter 1 describes a membrane model of cytosolic calcium oscillations. This chapter is a slightly modified reproduction of a paper by M. S. Jafri, S. Vajda, P. Pasik, and B. Gillo entitled "A membrane model for cytosolic calcium oscillations: a study using *Xenopus* oocytes." from *Biophys. J.* (1992) 63:235-246. In this paper I developed the basic model and generated several simulations. S. Vajda aided in the initial parameter estimation necessary to obtain oscillations, which I then adjusted to physiological values. P. Pasik made the electron micrographs and helped me devise the stereologic methods. Stereologic methods are the techniques used to derive three dimensional information such as volumes from the two dimensional image of an electrom micrograph. I made the stereologic measurements from the micrographs and performed calculations to derive relative volumes of the intracellular compartments. B. Gillo performed the electrophysiological experiments and wrote the experimental sections. All the sections of the paper are included because they contribute to the completeness of this work.

ABSTRACT

Cytosolic calcium oscillations occur in a wide variety of cells and are involved in different cellular functions. We describe these calcium oscillations by a mathematical model based on the putative electrophysiological properties of the endoplasmic reticulum (ER) membrane. The salient features of our membrane model are calcium-dependent calcium channels and calcium pumps in the ER membrane, constant entry of calcium into the cytosol, calcium dependent removal from the cytosol, and buffering by cytoplasmic calcium binding proteins. Numerical integration of the model allows us to study the fluctuations in the cytosolic calcium concentration, the ER membrane potential and the concentration of free calcium binding sites on a calcium binding protein. The model demonstrates the physiological features necessary for calcium oscillations and suggests that the level of calcium flux into the cytosol controls the frequency and amplitude of oscillations. The model also suggests that the level of buffering affects the frequency and amplitude of the oscillations. The model is supported by experiments indirectly measuring cytosolic calcium by calcium induced chloride currents in *Xenopus* oocytes as well as cytosolic calcium oscillations observed in other preparations.

INTRODUCTION

Oscillations in the cytosolic calcium concentration ($[Ca]_{cyt}$) regulate a variety of cellular functions in different systems, such as the secretion in the pituitary (Schlegal et al., 1987) and parotid glands (Gray, 1988), the contraction of smooth muscle (Ambler et al., 1988; Benham et al., 1986), and cardiac inotrophy and induction of arrhythmias (Lakatta et al., 1986). These oscillations also occur in cells where their function remains unknown, such as fibroblasts (Harootunian et al., 1988), endothelial cells (Jacob et al., 1988) and oocytes (Gillo et al., 1987; DeLisle et al., 1990). Experimentally, calcium oscillations are evoked through the application of extracellular calcium (Harootunian et al., 1988; Stern et al., 1988) or calcium mobilizing neurotransmitters (Wakui and Petersen, 1990). These stimuli are responsible for calcium entry into the cytosol through plasmalemmal calcium channels or release from intracellular stores mediated by a secondary messenger, such as inositol trisphosphate (IP_3; Berridge and Irvine, 1989).

Recently, two classes of mathematical models have been proposed to explain the mechanism for cytosolic calcium oscillations: (1) a molecular model (Meyer and Stryer, 1988; Swillens and Mercan, 1990) which uses IP_3 binding as the driving force behind the oscillations, and (2) a compartmental calcium-exchange model (Kuba and Takeshita,

1981; Goldbeter et al., 1990; Somogyi and Stucki, 1991) which is based on the fluctuations in the calcium concentration in both the cytosol and the ER lumen. The model proposed by Goldbeter and co-workers (1990) adds a constant calcium flux into the cytosol from IP_3-sensitive stores. It relies on the balance between the cytosolic and ER luminal calcium so that the depletion of the latter causes the closing of the ER calcium channel, thereby inhibiting the calcium dependent calcium release. The formulation by Somogyi and Stucki (1991) differs from the original compartmental calcium-exchange model in that it requires cooperative binding of IP_3 and calmodulin to the ER calcium release channel.

We propose another possible physiological mechanism to explain calcium oscillations which is based on the interplay between the calcium channels and the calcium pumps in the ER membrane. Okada and co-workers (1982) offered a similar mechanism in which the calcium oscillations occurred as a result of the movement of calcium across the plasma membrane. Jacob and co-workers (1988), however, showed that in certain cells the plasma membrane potential played no role in cytosolic calcium oscillations, although they did not exclude the role of ER membrane potential fluctuations. In our model the driving force behind the oscillations is the electrochemical gradient across the ER membrane. Calcium oscillations would occur when the elevation in cytosolic calcium triggers calcium dependent calcium release from the

ER. The rate of release will increase autocatalytically due to the additional increase in cytosolic calcium. The termination of release occurs when the electrochemical gradient of calcium is diminished by the increase of cytosolic calcium so that the rate of calcium removal by the action of calcium pumps exceeds the rate of movement of calcium through the channel. Since the pump rate is dependent on calcium binding, as the cytosolic calcium concentration decreases the pump rate also decreases. Eventually, the pump rate will fall enough so that the calcium entry into the cytosol once again dominates the changes in cytosolic calcium. This cycle repeats itself and oscillations occur. It is important to note that the cytosolic calcium entry that triggers these events is constant and need not oscillate.

In this study, we present our membrane model as a different mechanism to describe cytosolic calcium oscillations by means of equations that represent the changes in cytosolic calcium and ER membrane potential. In addition, we simulate the potential role of buffering in the control of cytoplasmic calcium oscillations. The model is applied to simulate calcium-evoked chloride current oscillations in *Xenopus* oocytes and may also explain calcium oscillations in other systems.

THE MODEL

Glossary of Terms

Variables

$[Ca]_{cyt}$ = cytosolic calcium concentration

[P] = concentration of buffer protein binding sites

V = ER membrane potential

Functions

I_{Ca} = calcium current through ER channel

E_{Ca} = reversal potential across ER for calcium

Parameters

R = ideal gas constant

T = absolute temperature

F = Faraday's constant

$[Ca]_{ER}$ = ER calcium concentration

g_{Ca} = calcium conductance through ER calcium channel per unit area

$\overline{g_{Ca}}$ = maximal calcium conductance per area

S = surface area of ER membrane

K_{diss} = dissociation constant off channel protein

V_{cyt} = volume of cytosolic compartment

k_{pump} = pump rate into the ER

k = pump rate out of cytosol into extracellular space or another compartment

q = flux of calcium into cytosol

C_m = ER membrane capacitance per area

k_{off} = off rate for buffer protein binding sites

k_{on} = on rate for buffer protein binding sites

$[P_{total}]$ = total concentration of calcium binding sites

The model is based on the following assumptions:

1) The ER membrane is excitable, that is, it separates charge and has ionic currents flowing across it. Calcium is the only ion that significantly contributes capacitative current to evoke changes in the ER membrane potential (Meissner, 1983; Oetliker, 1982; Stephenson et al., 1981).
2) The plasma membrane potential has no influence on the oscillations (Jacob et al., 1988; Harootunian et al., 1988; Gillo et al., 1987).
3) The oscillations occur as a result of competition between the calcium-dependent calcium release from the ER and the uptake from the cytosol into the ER by a calcium dependent pump.
4) There is a constant calcium entry into the cytosol from either intracellular sources through calcium release mediated by a second messenger, such as IP_3, or extracellular sources through plasma membrane calcium channels.
5) There is calcium-dependent efflux from the cytosol into the extracellular space by a plasmalemmal

calcium pump.

6) The calcium oscillations in *Xenopus* oocytes that are measured by the calcium-dependent chloride current in the plasma membrane occur primarily in the cytosolic compartment which is approximated by a spherical shell comprised of the outer 1 μm of the oocyte (see the section on electron microscopy and stereology).

7) Cytosolic calcium is bound by calcium binding proteins.

The oocyte has a complex buffering system consisting of calcium binding proteins and calcium stores. The main cytosolic calcium binding protein is calmodulin which has a binding constant of 10^{-6} M^{-1} (Robertson et al., 1981). Calmodulin has four calcium binding sites that herein are treated as independent sites. The balance equation for free calmodulin is given by

$$\frac{d[P]}{dt} = k_{off}([P_{total}] - [P]) - k_{on}([Ca]_{cyt}[P]) \qquad (1)$$

where [P] is the concentration of free calmodulin calcium binding sites, $[P_{total}]$ is the total amount of calmodulin calcium binding sites in the cell, $[Ca]_{cyt}$ is the cytosolic calcium concentration, and k_{on} and k_{off} are the on and off

rates from the binding sites. The concentration of calmodulin in a resting *Xenopus* oocyte is ~34 μM (Cartaud et al., 1980). Calmodulin has four binding sites per molecule which yields a total of ~136 μM calcium binding sites. We use 120 μM as the total amount of calcium binding sites. The dissociation constant of calcium from calmodulin ranges from .2 to 18 μM (Robertson et al., 1981, Lin et al., 1974, Wolff et al., 1977). We use a value of 1 μM with 5 $\mu M^{-1}s^{-1}$ for k_{on} and 5 s^{-1} for k_{off}.

The membrane model assumes that the ER membrane has electrophysiological properties similar to the plasma membrane. The ER membrane is depolarized by the calcium current through the calcium channel and repolarized by the calcium pump (figure 1.1).

The calcium current across the ER membrane is given by

$$I_{Ca} = g_{Ca}(E_{Ca} - V), \qquad (2)$$

where g_{Ca} is the ER membrane calcium conductance per unit area, E_{Ca} is the reversal potential for calcium, and V is the potential difference across the ER. For simplicity, we assume that the ER luminal calcium concentration ($[Ca]_{ER}$) remains constant at 5 mM (Somlyo et al., 1981). The reversal potential for calcium (E_{Ca}) is calculated by using the Nernst equation.

$$E_{Ca} = \frac{RT}{zF} \ln\left(\frac{[Ca]_{ER}}{[Ca]_{cyt}}\right). \qquad (3)$$

Data on the ER calcium channel is derived from experiments on the sarcoplasmic reticulum (SR) since no such information is available on the ER. The conductance is simplified (equation 4) as cooperative binding given by Hill's equation with Hill coefficient n = 2 (Meissner et al., 1986; Chay and Keizer, 1983). The concentration of SR luminal calcium (trans) has been shown to have no effect on the duration of channel opening (Lai et al., 1988). Thus, there is no inhibition by trans calcium. It has also been shown that highly elevated cis calcium (>10 μM) inhibits calcium release through this channel (Meissner et al., 1986). However, this calcium concentration is above the physiological observed level during calcium oscillations and may contribute to the inhibition of the calcium oscillations at high calcium concentrations. In our model, we attribute the inhibition by high cis calcium to the decrease of the electrochemical gradient. Hence, the conductance is given by

$$g_{Ca} = \overline{g_{Ca}} S \frac{\left(\frac{[Ca]_{cyt}}{K_{diss}}\right)^2}{1 + \left(\frac{[Ca]_{cyt}}{K_{diss}}\right)^2}, \qquad (4)$$

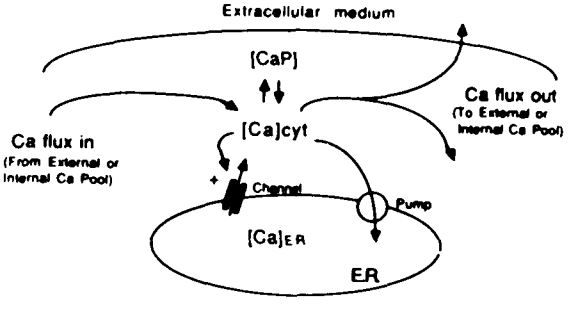

Figure 1.1. Schematic representation of the calcium oscillation components involved in the membrane model. Notice that an increase in $[Ca]_{cyt}$ triggers calcium release from the ER. The calcium bound to cytosolic calcium binding proteins is represented by [CaP].

where $\overline{g_{Ca}}$ is the maximal ER membrane conductance per unit area, and S is the ER surface area (see below). The dissociation constant of calcium from the channel protein is represented by K_{diss}. K_{diss} should be in the range of 2-10 μM (Meissner et al., 1986). We choose a value of 5 μM for K_{diss}.

The pump is assumed to depend linearly on the $[Ca]_{cyt}$ since the physiological range is on the linear part of the Michaelis-Menten curve (Ogawa et al., 1981; Gandhi and Ross, 1988). In equation 5 below, k_{pump} is the pump rate from the cytosol into the ER. Ogawa and co-workers (1981) measured a maximal pump rate of 1 mM s^{-1} with a K_m of 1 μM for SR calcium uptake in frog skeletal muscle. The rate constant calculated when $[Ca]_{cyt}$ is 1 μM is 250 s^{-1}. For the oocyte, the rate constant will be considerably slower, i.e. 69.8 s^{-1} since the oscillations are slow compared to those occurring during a muscle twitch.

We can now write the complete balance equation for $[Ca]_{cyt}$.

$$\frac{d[Ca]_{cyt}}{dt} = \frac{I_{Ca}}{2FV_{cyt}} - k_{pump}[Ca]_{cyt} + \frac{q}{V_{cyt}} - k[Ca]_{cyt} + k_{off}([P_{total}]-[P]) - k_{on}[Ca]_{cyt}[P], \quad (5)$$

where V_{cyt} is the cytosolic compartment volume (see below), k is the rate constant of calcium efflux from the cytosol across the plasma membrane, and F is Faraday's constant. The factor 2 in the denominator is the charge on a calcium ion. The

calcium flux q into the cytosol remains constant during the course of an oscillation. In different simulations, which are described in the results, the value of q is varied to produce different behavior.

The third equation fcr the model, that of the ER membrane potential, is given by

$$SC_m \frac{dV}{dt} = I_{Ca} - 2FV_{cyt} k_{pump} [Ca]_{cyt}, \qquad (6)$$

where C_m is the membrane capacitance per unit area and V is the potential difference across the membrane. The first term on the right hand side of the equation is the capacitative current due to calcium movement through the channel. The second term is the electrogenic current generated by the ER calcium pump. The complete model is given in equations (1) through (6) where equations (1), (5), and (6) are the differential equations for the system.

EXPERIMENTAL PROCEDURES

Materials.

Collagenase type 1A and other reagents and chemicals were obtained from the Sigma Chemical Co. (St. Louis, MO).

Oocyte culture.

Xenopus laevis (Xenopus One, Ann Arbor, MI or NASCO, Ft. Atkinson, WI) were maintained at 18-20°C and a day-night cycle of 15 h/ 9 h. A section of ovary was removed surgically from female frogs under percutaneous tricaine anesthesia and the oocytes defolliculated for two hours with 2 mg/ml collagenase in calcium-free ND96 solution (96 mM NaCl, 2 mM KCl, 1 mM $MgCl_2$, 5 mM Hepes, pH = 7.5). Oocytes were examined under a dissecting microscope and healthy-looking stage V and stage VI cells (Dumont, 1972) were selected and maintained at 21°C in enriched ND96 (supplemented with 1.8 mM $CaCl_2$, 2.5 mM sodium phosphate, 100 U/ml penicillin and 100 μg/ml streptomycin) for 1-3 days prior to recording.

Electrophysiology.

Cells were placed in a 0.5 ml bath which was constantly perfused with medium and then they were penetrated with two 0.5 - 1 MΩ, 3 M KCL filled glass electrodes attached to a DAGAN 8500 amplifier, using an 8100 probe (Dagan Corp., Minneapolis, MN). An IBM PC/AT system employing the TL-1

interface and pClamp software from Axon Instruments (Burlingame, CA) was used for maintaining voltage-clamp conditions. Cells were usually held at -70 mV unless otherwise stated. The current in the voltage-clamp circuit was registered on a chart recorder (Yokogawa, Tokyo, Japan).

The composition of the "calcium-free medium" used to incubate and perfuse the oocytes was 86 mM NaCl, 2 mM KCl, 15 mM $MgCl_2$, 0.2 mM EGTA and 5 mM Hepes, pH = 7.5. For acute application of calcium, 5 mM $CaCl_2$ was substituted for 5 mM $MgCl_2$ (no EGTA) to maintain the osmolarity unchanged. This solution is referred to as "calcium-containing medium".

Intracellular Application of Substances.

Two techniques were used to introduce reagents into the oocyte cytosol. For acute calcium injection, hereby referred to as "injection", a pressure system was used. For this purpose, a cell under voltage-clamp had a third micropipette introduced. Pipettes were obtained by breaking the tip to 2-4 μm diameter under microscopic control. The 50 mM calcium solution was introduced into the pipette tip by applying negative pressure to the open side. The filled pipette was connected by a rigid tube to a controller which delivered pulses of compressed nitrogen for specified time intervals (Picospritzer II, General Valve Corporation, Fairfield, NJ). Before insertion into and after withdrawal from the cell, the pipette tip was immersed in a drop of mineral oil and observed

under a microscope with an eye piece micrometer. The pressure was adjusted to obtain a drop of drug with a volume of less than 0.4% of the volume of the oocyte (100-200 μm diameter which is equivalent to 50-200 pmol/cell). From the calcium concentration and the drop diameter the amount of calcium actually injected could be determined.

Preloading the cell (>10 minute exposure) with IP_3, referred to as "loading", was made with a microdispenser (Drumond, Broomall, PA) through a pulled glass capillary tube with the tip broken at 10 μm diameter. A drop of mineral oil was added to the tube prior to introduction of the microdispenser plunger, and 1-2 μl solution was added by backfilling. Thirty to 50 nl of the solution were introduced into the cells after penetration.

Electron Microscopy and Stereology

Recently developed techniques of microfluorescence measurement of calcium signals in *Xenopus* oocytes found that maximal fluorescence intensity is recorded approximately 10 μm beneath the plasma membrane (Takehashi et al., 1987). In fact, calcium oscillations were observed 5 μm below the surface membrane (Parker and Ivorra, 1990). In our work, we monitor the changes in cytosolic calcium using the native calcium-sensitive chloride channel. Thus, we assume that changes in calcium concentration occur in the submembranal region. Deep injections of calcium over 100 μm deep (see

experimental section below) do not immediately activate the chloride channels. This suggests that the measured calcium oscillations are a result of calcium elevation closer to the membrane. Taken together we confine our analysis of the cytosolic volume and the ER surface area to the cytosolic compartment, that is, the volume of the cytosol close to the plasma membrane. We assume that it well represents the region where the calcium oscillations occur.

Immature denuded oocytes were prepared for transmission electron microscopy according to published protocols (Gardiner and Grey, 1983; Charbonneau and Grey, 1984). Oocytes were fixed for two hours in 2.5% glutaraldehyde in ND96 at 4°C, then washed and cut by fine scalpel into the two hemispheres. Only animal hemispheres were used, as it is known that they contain the larger number of Ca mobilizing related components (Gardiner and Grey, 1983). Animal hemispheres were post-fixed for 1 hour in 1% OsO_4 in 50% ND96 at 4°C. After washing in buffer, specimens were dehydrated in graded ethanol with 1% uranyl acetate in the 70% stage. Finally, they were embedded in Epon-Araldite with the equatorial face resting on the flat embedding vessel. After polymerization, the specimen was glued on its side on a blank resin block and sectioned perpendicular to the flat face. Ultrathin sections (silver interference color) were collected on formvar-coated slot grids, after discarding the first 400 μm. In this way, sections were taken from the equatorial region of the animal

hemisphere. After counterstaining with uranyl and lead salts, grids were examined with a Hitachi 12A electron microscope and micrographs taken at 12000 magnification and further enlarged in printing to 30,000 magnification (plate 1.1).

The cytosolic compartment consists of the region between the cortical granules and the plasma membrane which is approximated by a spherical shell about 1 μm in thickness. Its volume (W) is easily estimated using the difference in volume of two spheres

$$W = \frac{4}{3}\pi\,(r^3-(r-1)^3)\,, \qquad (7)$$

where r is the cell radius in microns.

The value of the ER surface area (S) is derived from area and length measurements on the electron micrographs obtained through planimetry and the application of the fundamental stereologic principle. The fundamental stereologic principle (Delesse, 1847) states that the fraction V_1 of a volume V_2 occupied by randomly distributed components is equal to the fraction A_1 of the area A_2 of a plane of section of volume V_2 covered by transections of those components, that is,

$$\frac{A_1}{A_2} = \frac{V_1}{V_2}\,. \qquad (8)$$

Plate 1.1. Electron micrograph of *Xenopus* oocyte, x30000. The ER structures and cytosolic compartment borders are inked to emphasize the cross-sectional areas that are used in the calculation of the cytosolic compartment volume and the ER surface area.

The following morphometric measurements were made on the oocyte cortical cytosol appearing in 4 electron micrographs:

a_{tot} = total cross-sectional area of the cortical cytosol (area between the cortical granules and the plasma membrane including the ER)

a_{ER} = cumulative cross-sectional area of the ER in the cortical cytosol

L_{ER} = cumulative long axes of the ER cisterns in the cortical cytosol.

The following calculations were made to estimate the ER surface area to cytosolic volume ratio:

$$a_{cyt} = a_{tot} - a_{ER} \tag{9}$$

where a_{cyt} is the area of the cortical cytosol. Then,

$$r_{mean} = \frac{1}{2}\frac{a_{ER}}{L_{ER}} \tag{10}$$

where r_{mean} is the mean radius of ER cisterns, and

$$v_{ER} = \frac{\pi a_{ER}^{2}}{4 L_{ER}} \tag{11}$$

where v_{ER} is the volume of the ER. The surface area of the ER is given by

$$s_{ER} = \pi a_{ER} + n\frac{\pi a_{ER}^2}{4L_{ER}^2} \qquad (12)$$

where n is the number of ER cisterns present in the sample. Using the fundamental stereologic principle, the cytosolic volume in the sample is

$$v_{cyt} = \frac{a_{cyt}v_{ER}}{a_{ER}} \ . \qquad (13)$$

Finally, the value of the ER surface area (Table 1.1) for the entire compartment is

$$S = \frac{s_{ER}}{v_{cyt}} W. \qquad (14)$$

NUMERICAL METHODS

The membrane model (equations 1 through 6) was numerically integrated using the ROW4D program (Valko and Vajda, 1985) on a Convex C220 computer. A description of the ROW4D program is given in the Numerical Methods section of Chapter 2. The values of the physiological parameters used in the model are presented in Table 1.1. When other parameter values are used in the computations they are mentioned in the corresponding figure caption. The value of the calcium entry into the cytosol (q) was adjusted to produce the frequency and amplitude of oscillations observed experimentally.

Table 1.1

Parameter values for the model

Parameter		*Value*
C_m	=	$1\ \mu F\ cm^{-2}$
F	=	$96500\ coulombs(mol\ e^{-})^{-1}$
$\overline{g_{Ca}}$	=	$340\ \mu S\ cm^{-2}$
K_{diss}	=	$5\ \mu M$
k_{pump}	=	$69.8\ s^{-1}$
k	=	$20.2\ s^{-1}$
S	=	$6.16 \times 10^{-3}\ cm^2$
V_{cyt}	=	$5.84 \times 10^{-5}\ \mu l$
q	=	$2.92 \times 10^{-10}\ \mu mol\ s^{-1}$
P_{total}	=	$120\ \mu M$
k_{off}	=	$5\ s^{-1}$
k_{on}	=	$1\ \mu M^{-1}\ s^{-1}$
$[Ca]_{ER}$	=	$5000\ \mu M$
V_0	=	$12.9\ mV$
R	=	$8.314\ J°K^{-1}\ mole^{-1}$
T	=	$300\ K$
r	=	$600\ \mu m$

These parameters are used in the simulations unless otherwise stated.

EXPERIMENTAL RESULTS

Current fluctuations due to intracellular application of calcium.

Shallow injection of calcium into the oocyte (~100 μM) evokes a two component chloride current with a fast component that lasts less than a minute and a slow component that appears after 3-4 minutes (Dascal et al., 1985). The slow component consists of current fluctuations with a small increase in the total current over the base line. However, with increasing the depth of injection (>~200 μm) and the injection of a series of small doses, the rapid transient is not detected and more homogenous calcium diffusion in the cell is achieved (Gillo et al., 1987).

All the experiments were performed in calcium-free medium to avoid the effect of the extracellular calcium pool. Figure 1.2A shows the response to acute injection (see methods) of 100 pmol of calcium, 200 μm below the cell surface membrane. After a delay of ~2 minutes, the spike-like calcium induced chloride current appears. The mean interval between the single spikes is 20-30 seconds. A series of spikes on a slow time base can be seen in figure 1.3A. In figure 1.2B, a series of calcium injections is applied to the oocyte to bring in a total of 400 pmol; the frequency of the oscillations is

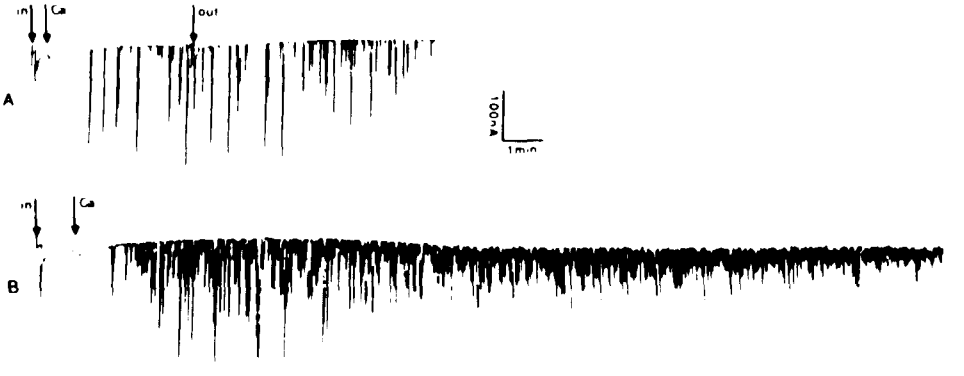

Figure 1.2. Chloride current fluctuations elicited by intracellular injection of calcium in calcium-free medium. The "in" and "out" arrows mark the insertion and withdrawal of the injection pipette. A. A total of 100 pmol of calcium is injected at 200 μm into the cell. B. A total of 400 pmol of calcium is injected at 200 μm into the cell in consecutive small doses.

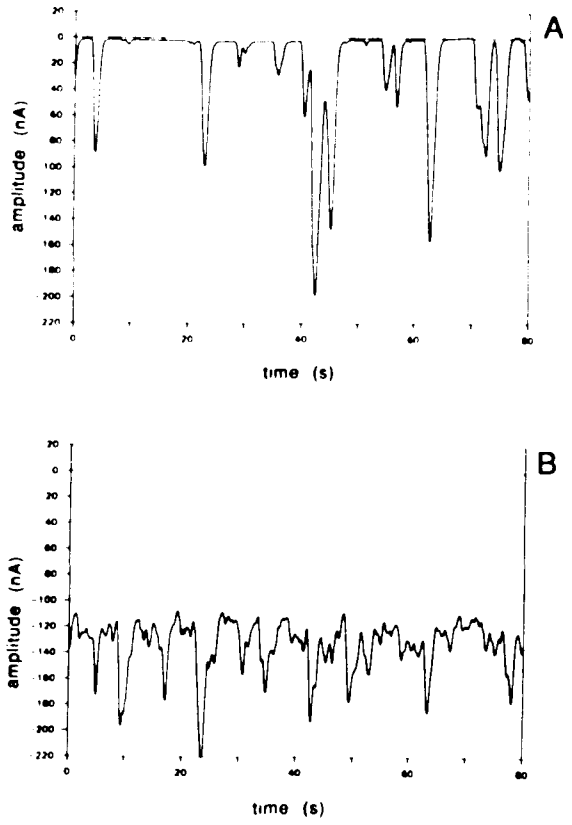

Figure 1.3. Intracellular injection of calcium on an expanded time scale of a current fluctuation. A. Cell injected with a low dose of calcium (100 pmol) exhibits spike-like chloride current fluctuations. B. High frequency current fluctuations observed ten minutes after a high dose (400 pmol) calcium injection.

dramatically increased. As the response progressed, the frequency of the spikes increased and the amplitude decreased, eventually becoming high frequency oscillations. Figure 1.3B shows the high frequency low amplitude oscillations on a slow time scale, taken from the same oocyte as in figure 1.2B, 10 minutes after the injection of calcium. The faster oscillations superimposed on these oscillations are not modelled. The oscillations persist indefinitely; we have recorded for as long as 30 minutes with no significant diminution of the oscillations. The model suggests that for sustained oscillations there must be a constant calcium flux into the cytosol. This flux is probably due to the sequestration of the initial calcium bolus by intracellular stores and subsequent slow continuous release of calcium from these stores into the cytosol. This also implies that the pumping of calcium out of the cell is relatively small in spite of the fact that the cell is perfused in calcium-free medium. Indeed, Dascal and Boton (1990) reported that repetitive deep injection of calcium into the oocyte loaded the intracellular pool for as long as ninety minutes.

Current fluctuations due to extracellular application of calcium.

Injection of IP_3 or application of calcium-mobilizing neurotransmitter to oocytes increases the cell membrane permeability to calcium either at resting membrane potential (Snyder et al., 1988) or by hyperpolarizing steps (Parker et al., 1987).

Loading the oocyte with a high dose of IP_3 (>2 pmol) and maintaining it in calcium-free extracellular medium increases the membrane permeability to calcium for more than an hour. Exposing the cell to a brief (3-5 s) extracellular calcium application evokes a large depolarizing response which results from calcium flux via the open channels. Upon calcium washout, damped current oscillations emerge and decay rapidly (figure 1.4). No calcium oscillations occurred upon longer exposure . However, calcium oscillations are observed after washout. It appears as if the high level of calcium entry into the cytosol attenuates the current oscillations. Thus, we show that cytosolic calcium oscillations can be stimulated by extracellular as well as intracellular application of calcium. Furthermore, no oscillations occur when overloading the cytosol with calcium.

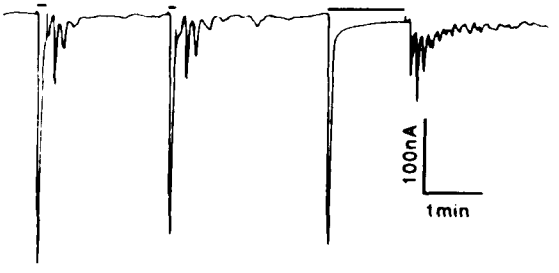

Figure 1.4. Chloride current fluctuation evoked by extracellular application of calcium to a IP_3-loaded cell. Oocyte is preloaded with 2.5 pmol IP_3. After fifteen minutes 5 mM Ca is applied during the period indicated by the horizontal bars. The current fluctuations die rapidly with calcium washout.

NUMERICAL RESULTS

We assume that calcium oscillations in *Xenopus* oocytes can be measured by the chloride current across the plasma membrane because the chloride channels are calcium gated. This has been shown in studies involving observation of calcium oscillations using a calcium sensitive fluorescent dye and monitoring of the chloride current oscillations (Parker and Miledi, 1986; DeLisle et al., 1990; Parker and Ivorra, 1990). Osipchuk and co-workers (1990) have shown a positive correlation between the cytosolic calcium concentration and the chloride current using microfluorometry and whole cell patch clamp in pancreatic acinar cells. Moreover, the native chloride current seems to better resolve small fluctuations of the cytosolic calcium concentration then calcium binding fluorescent dyes.

The spikes of our simulated calcium oscillations have a rising phase that is not observed in the chloride current records. This is probably due to a threshold phenomenon. The chloride channels open when the $[Ca]_{cyt}$ reaches a certain threshold level. The existence of the threshold phenomenon has been suggested previously to explain the latency phenomenon (Berridge et al., 1988). The variation in the current records (figure 1.3) might be due to the spatial inhomogeneity of the oscillations

(Parker and Ivorra, 1990; Lechleiter et al., 1991). Calcium release from a nearby segment of ER can cause a measurable chloride current which appears in the record as intermediate small oscillations.

The membrane model reproduces the oscillatory phenomena observed when calcium is injected into an oocyte. The injection is deep in the oocyte and gradually enters the cortical cytosolic compartment. The model reflects this source of calcium (the flux into the compartment) by the parameter q. The ER membrane potential oscillates around its equilibrium value of 89.3 mV (potential difference of the ER lumen to the cytosol). The equilibrium value for the percentage of free calcium binding sites is 95.3%. These values are found by solving the system for the dynamic variables when the derivatives are set to zero (equations 1,5 & 6). The model reproduces the shape and frequency of oscillations found in Xenopus oocytes (figures 1.5 & 1.6).

Harootunian and co-workers (1988) showed that fibroblasts depolarized by gramicidin, which allows calcium entry into the cell via voltage gated calcium channels, have an increasing frequency and decreasing amplitude of oscillations when exposed to increasing concentrations of extracellular calcium. Similarly, increases in extracellular calcium in the heart cause an increase in the frequency of spontaneous calcium oscillations through calcium entry (Stern et al., 1988).

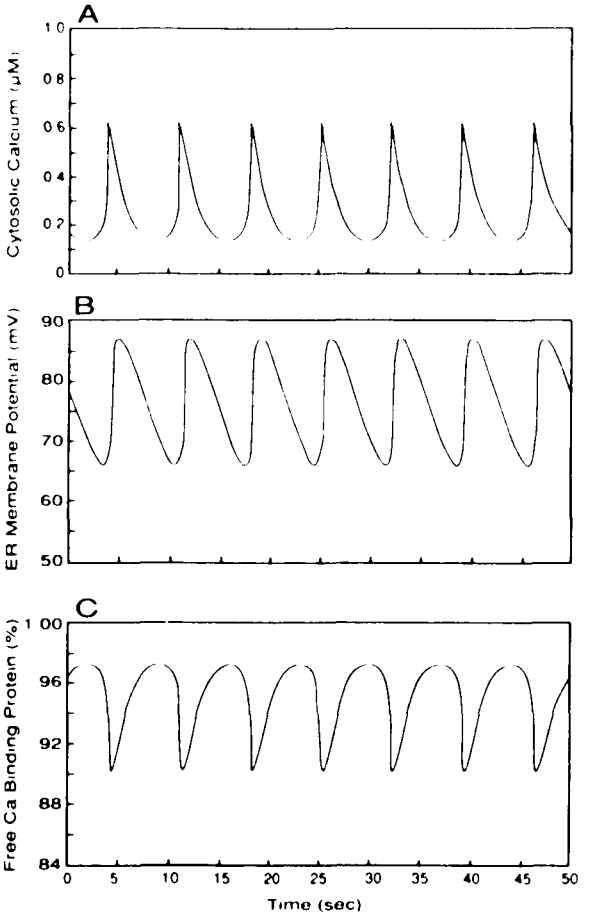

Figure 1.5. Simulation of intracellular calcium injection induced oscillations of A. $[Ca]_{cyt}$ B. ER membrane potential and C. Percentage free calcium binding sites on calcium binding protein for a small constant flux of calcium into the cytosol ($q = 2.49 \times 10^{-10}$ μmol/s).

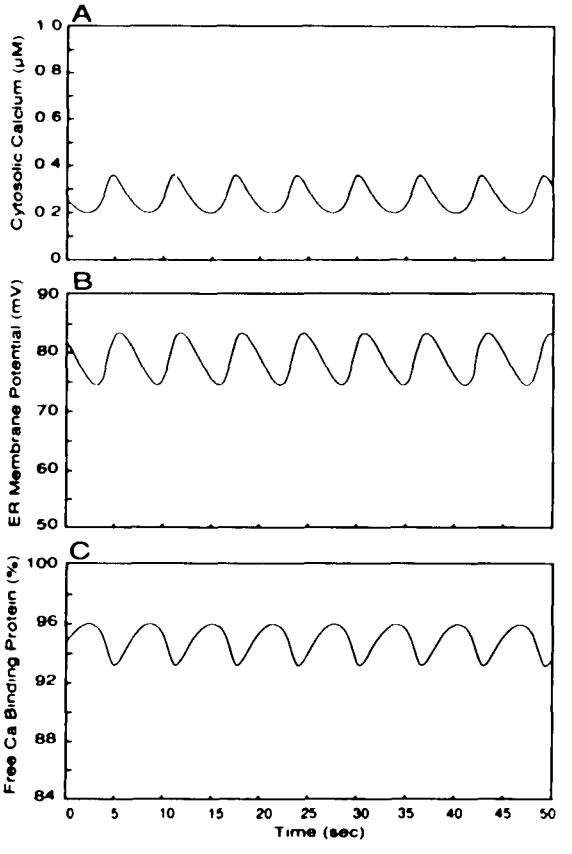

Figure 1.6. Simulation of intracellular calcium injection induced oscillations of A. $[Ca]_{cyt}$ and B. ER membrane potential and C. Percentage free calcium binding sites on calcium binding protein for a large constant flux of calcium into the cytosol ($q = 2.15 \times 10^{-10}$ μmol s^{-1}).

We model this phenomenon by increasing the value of q, the constant flux into the cytosol. When q is increased the amplitude decreases and the frequency increases. These relationships are shown in figure 1.7. For low values of q the model shows spiking of the calcium concentration (figure 1.5) and for high values of q, the oscillations have low amplitude and high frequency. As the value of q rises beyond 2.5 x 10^{-8} μmol s^{-1}, the oscillations cease asthey also do when q becomes zero. In fact, DeLisle and co-workers (1990) find that calcium oscillations stop when an oocyte is bathed in 6 mM calcium, and the oscillations resume when the bath concentration is lowered to .1 mM. Similarly, Wakui and Petersen (1990) showed that acetylcholine-induced calcium oscillations in pancreatic acinar cells cease to oscillate when the cells are exposed to ionomycin which floods the cytosol with calcium from the extracellular space and that the oscillations resume after the ionomycin is removed.

We performed simulations in which the effect of the buffer was removed to show that the oscillations in the model were due to the calcium dependent calcium release mechanism rather than binding and release from the buffer. This was accomplished by setting the total amount of buffer, and the k_{on} and k_{off} for the buffer all to zero. The resulting oscillations increased in both

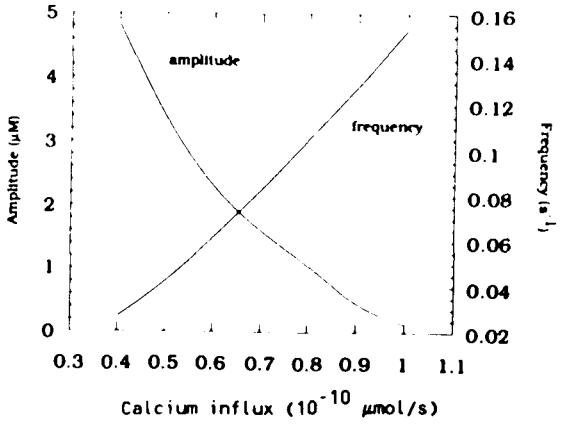

Figure 1.7. The effects of varying the constant flux into the cytosol (q) on the amplitude and frequency of the oscillations in cytosolic calcium. The influx shown is normalized with 2.92 μmol/s being the unit flux.

amplitude and frequency (figure 1.8). A similar result was obtained in simulations by increasing the total amount of calcium binding sites, P_{total} (figure 1.9). This finding is comparable to that of Petersen and co-workers (1991), who also observed a decrease in the amplitude and frequency of the cytosolic calcium oscillations upon addition of citrate to pancreatic acinar cells as our model would predict.

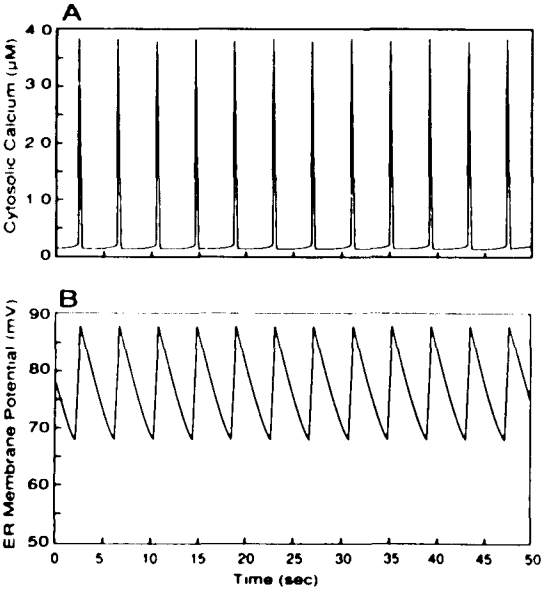

Figure 1.8. Simulation of the oscillations in A. $[Ca]_{cyt}$ and B. ER membrane potential after removal of the buffer (P_{total})=0, k_{on}=0, and k_{off}=0). Note the increase in the amplitude and frequency of the oscillations.

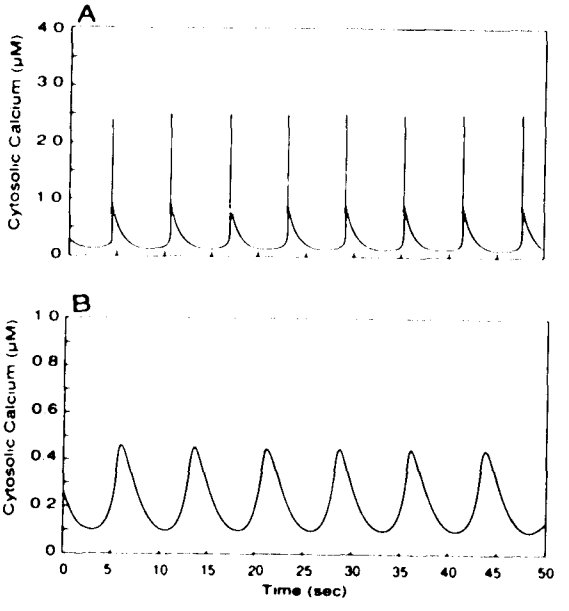

Figure 1.9. Simulation of the calcium oscillations with different concentrations of calcium binding sites A. 80 μM and B. 140 μM. Note that with increased buffer the oscillations have a decresed amplitude and frequency.

DISCUSSION

A system of mathematical equations describing an oscillatory phenomenon arbitrarily far from equilibrium was established to explain a group of oscillating chemical reactions (Prigogine, 1968; Lavenda et al., 1971; Lefever and Nicolis, 1970). A model of this type includes the following mathematical features: a positive feedback term for the oscillating species, a constant flux of this species, a species dependent removal term and a balance equation for a second species which becomes small when the first species becomes large.

Earlier classes of models for cytosolic calcium oscillations, namely the molecular model (Meyer and Stryer, 1988; Swillens and Mercan, 1990) and the compartmental calcium-exchange model (Kuba and Takeshita, 1981; Goldbeter et al., 1990; Somogyi and Stucki, 1991), result in mathematical formulations which include the features discussed in the preceding paragraph. The main differences between the two classes are the physiological assumptions which determine the meaning of the terms in the differential equations. The dynamic variables in the molecular model are the $[Ca]_{cyt}$ and the cytosolic IP_3 concentration, that is, it assumes that the cytosolic calcium as well as the cytosolic IP_3 levels are changing.

However, cytosolic calcium oscillations are observed in pancreatic acinar cells (Wakui et al., 1990) and in *Xenopus* oocytes (Taylor et al., 1988; DeLisle et al., 1990) injected with a non-degradable analog of IP_3. This suggests that, in a large number of preparations, the cytosolic IP_3 concentration remains relatively constant during the calcium oscillations and therefore the latter cannot be explained by IP_3 fluctuations. Furthermore, cytosolic calcium oscillations in hepatocytes are independent of IP_3 formation (Rooney et al., 1991).

IP_3 is believed to cause calcium release from intracellular stores. We propose that the constant level of IP_3 causes a constant release of calcium, which results in the occurrence of oscillations. Similarly, direct intracellular or extracellular application of calcium allows calcium entry into the cell cytosol which generates cytosolic calcium oscillations. The calcium entry from both sources is described by the constant flux q in the differential equations.

The dynamic variables of the compartmental calcium-exchange model (Goldbeter et al., 1990) are the cytosolic calcium concentration and the ER luminal calcium concentration. In this model, the positive feedback for calcium (Ca-dependent Ca release channel) is activated by a rise in calcium in both the cytosol and the ER lumen. The channel is closed by depletion of the $[Ca]_{ER}$. This,

however, conflicts with the finding of Lai and co-workers (1988) that SR luminal calcium has no effect on the duration for which a channel stays in the open state. In contrast, our membrane model uses the reduction of the electrochemical gradient to terminate the calcium release from the ER.

Electron microprobe analysis has shown that during tetanic contraction in skinned striated muscle, magnesium and potassium ions move into the sarcoplasmic reticulum (SR), and calcium is released (Somlyo et al., 1981). Although the contribution of these counterions is not insignificant, they together have about half the charge of the calcium ions. For simplicity, the present model considers only the contribution of the calcium ions since adding the potassium and magnesium ions would involve the addition of two more dynamic variables to our model. This omission may not be critical to the qualitative behavior of the model because the counterion effect serves to maintain an electrochemical gradient which allows calcium release down the gradient. This presence of counter ions is modelled in chapter 2.

Our model demonstrates the local temporal behavior of cytosolic calcium concentration. It does not describe the spatial inhomogeneity. For example, calcium released from the ER can trigger calcium-dependent calcium release in the adjacent ER and hence calcium release can be propagated along the sheets of ER as shown by Lechleiter

and co-workers (1991) in *Xenopus* oocytes. The spatial properties of calcium oscillations are modelled in chapter 3.

As an initial test of the membrane model we studied the calcium-evoked chloride current oscillations in *Xenopus* oocytes. The experiment was performed in calcium-free medium to exclude the effect of an extracellular calcium source. In response to an injection of a low calcium dose, the current oscillations were high-amplitude, low frequency spikes. A high dose initially elicited high-frequency spikes. As time progressed, the oscillations increased in frequency with a decreased amplitude. These changes in the behavior of the calcium oscillations can be modelled by an increase in the calcium entry into the compartment, represented by q. Considering the large dose of calcium necessary to evoke oscillations (0.1-0.4 mM final concentration) and the elimination of the fast component (figure 1.2), we infer that most of the calcium is sequestered into the intracellular stores and by calcium binding proteins before oscillations begin. With no other source of calcium we propose that the gradual conversion from transient spikes to high frequency oscillations results from overloading of the pumps or depletion of ATP which leads to an increase in $[Ca]_{cyt}$ via increased calcium entry into the oscillatory cytosolic compartment. The

same mechanism has been recently proposed for potentiation of the calcium evoked chloride current by repetitive calcium injection in *Xenopus* oocytes (Dascal and Boton, 1990). Similarly, Wakui and co-workers (1990) obtained calcium oscillations in pancreatic acinar cells by infusion of 100 μM calcium.

The model predicts that as calcium entry into the cytosol increases, the oscillation frequency increases and its amplitude decreases. This is supported by a similar observation in fibroblasts depolarized by gramicidin (Harootunian et al., 1988) and exposed to extracellular calcium and in cardiac myocytes exposed to extracellular calcium (Stern et al., 1988). Gillo and co-workers (1987) showed that shallow injection of IP_3 (high local dose) produce very small oscillations compared to deep injection (low dose; see also above). The same relationship is observed in a response to a calcium-mobilizing hormone in RNA-injected oocytes (gonadotropin releasing hormone; S. Sealfon, personal communication). Moreover, the transition from sinusoidal-like to transient spiking behavior for the oscillations can be achieved by decreasing q. The various forms of oscillations that appear in a variety of preparations have been reviewed recently (Berridge and Irvine, 1989; Rooney and Thomas, 1991). Furthermore, the model predicts that when the constant calcium entry is

too small or too large no oscillations will occur.

When the total amount of calcium binding sites is increased (and q is held constant) the calcium oscillations decrease in amplitude and frequency. The decrease in amplitude occurs because the calcium released from the ER is sequestered by the additional buffer. The fall in frequency occurs because the rise of cytosolic calcium to threshold is slower due to the increased buffering effect, that is, there is a smaller increase in free cytosolic calcium. This threshold is the point at which calcium- dependent calcium release becomes the predominant process. This finding is supported by the work of Petersen and co-workers (1991). When citrate is added to pancreatic acinar cells the amplitude and frequency of the cytosolic calcium oscillations decrease. Our model predicts that removal of buffer will result in an increase of amplitude and frequency of the oscillations. In addition, with a decrease in amount of buffer, the form of the oscillations will change from sinusoidal to a transient spiking pattern.

Oscillations are observed in IP_3 loaded cells exposed to extracellular calcium. IP_3 loading increases the plasmalemmal permeability to calcium. This shows that the source of calcium flux can be extracellular as well as intracellular.

The model demonstrates that a constant calcium entry

into the cytosol is sufficient for the occurence of oscillations. Moreover, this flux serves as a mechanism by which the frequency and amplitude can be regulated. The source of calcium can be the result of numerous physiological origins such as IP_3 mediated release, flux from external sources, etc. The degree of binding of calcium by intracellular calcium binding proteins can also regulate the form, amplitude and frequency of cytosolic calcium oscillations. These two factors can be used in concert to reproduce a wide variety of oscillations. This suggest a possible mechanism by which a cell can produce the different types of oscillations described in the review by Rooney and Thomas (1991).

The membrane model demonstrates that the salient features needed to produce cytosolic calcium oscillations are calcium dependent calcium release, a calcium dependent removal and a source of constant calcium entry. In order to extend the model to simulate calcium oscillations observed under different conditions, the differential equations will be further extended in the following chapters to include terms for other observed physiological mechanisms for calcium regulation. Further experimentation is needed to validate the physiological assumptions that define the model.

ACKNOWLEDGEMENTS

We are greatly thankful to S. Mundamattom who performed the electrophysiological experiments. We would like to give special thanks to Dr. S. C. Sealfon and Dr. A. Sherman for their helpful remarks and discussion.

REFERENCES

Ambler, S. K., P. Poenie, R. Y. Tsien, and P. Taylor. 1988. Agonist-stimulated oscillations and cycling of intracellular free calcium in individual cultured muscle cells. *J. Biol. Chem.* 263:1952-1959.

Benham, C. D. and T. B. Bolton. 1986. Spontaneous transient outward currents in single visceral and vascular smooth muscle cells of the rabbit. *J. Physiol.* 381:385-406.

Berridge, M. J., P. H. Cobbold, and K. S. R. Cuthbertson. 1988. Spatial and temporal aspects of cell signalling. *Phil. Trans. R. Soc. Lond. B.* 320:325-343.

Berridge, M. J., and R. F Irvine. 1989. Inositol phosphate and cell signalling. *Nature.* 341:197-205.

Cartaud, A., R. Ozon, M. P. Walsh, J. Haiech, and J. G. Demaille. 1980. *Xenopus Laevis* oocyte calmodulin in the process of meiotic maturation. *J. Biol. Chem.* 255:9404-9408.

Charbonneau, M. and R. D. Grey. 1984. The onset of activation responsiveness during maturation coincides with the formation of the cortical endoplasmic reticulum in oocytes of *Xenopus laevis. Developmental Biology.* 102:90-97.

Chay, T. R., and J. Keizer. 1983. Minimal model for membrane oscillations in the pancreatic ß-cell. *Biophys. J.* 42:181-190.

Dascal, N., and R. Boton. 1990. Interaction between

injected Ca^{2+} and intracellular Ca^{2+} stores in *Xenopus* oocytes. *FEBS*. 267:22-24.

Dascal, N., B. Gillo, and Y. Lass. 1985. Role of calcium mobilization in mediation of acetylcholine responses in *Xenopus laevis* oocytes. *J. Physiol*. 366:299-314.

Delesse, M. A. 1847. Procede mecanique pour determiner la composition des roches. *Comput. Rend. Acad. Sci*. 25:544-547.

DeLisle S., K. Krause, G. Denning, B. V. L. Potter, and M. J. Welsh. 1990. Effect of inositol trisphosphate and calcium on oscillation elevations of intracellular calcium in *Xenopus* oocytes. *J. Biol. Chem*. 265:11726-11730.

Dumont, J. N. 1972. Oogenesis in *Xenopus laevis* (Daudin). *J. Morphol*. 136:153-180.

Gandhi, C. R., and D. H. Ross. 1988. Characterization of a high-affinity Mg^{2+}-independent Ca^{2+}-ATPase from rat brain synaptosomal membranes. *J. Neurochem*. 50:248-256.

Gardiner, D. M. and R. D. Grey. 1983. Membrane junctions in *Xenopus* eggs: their distribution suggests a role in calcium regulation. *J. Cell Biol*. 96:1159-1163.

Gillo, B., Y. Lass, E. Nadler, and Y. Oron. 1987. The involvement of inositol 1,4,5-trisphosphate and calcium in the two-component response to acetylcholine in *Xenopus* oocytes. *J. Physiol*. 392:349-361.

Goldbeter, A., G. Dupont, and M. J. Berridge. 1990. Minimal model for signal induced Ca^{2+} oscillations and for their frequency encoding through protein phosphorylation. *Proc. Natl. Acad. Sci. USA*. 87:1461-1465.

Gray, P. T. A. 1988. Oscillations of free cytosolic calcium evoked by cholinergic and catecholaminergic agonists in rat parotid acinar cells. *J. Physiol. (London)*. 406:35-53.

Harootunian, A. T., J. P. Y. Kao, and R. Y. Tsien. 1988. Agonist-induced calcium oscillations in depolarized fibroblasts and their manipulation by photoreleased $Ins(1,4,5)P_3$, Ca^{++}, and Ca^{++} buffer. *Cold Spring Harbor Symposia on Quantitative Biology*. 53:935-943.

Jacob, R., J. E. Merritt, T. J. Hallam, and T. J.

Rink. 1988. Repetitive spikes in cytoplasmic calcium evoked by histamine in human endothelial cells. *Nature*. 335:40-45.

Kuba, K. and Takeshita. 1981. Simulation of intracellular Ca^{2+} oscillations in a sympathetic neurone. *J. Theor. Biol*. 93:1009-1031.

Lai, F. A., H. P. Erickson, E. Rosseau, Q. Liu, and G. Meissner. 1988. Purification and reconstitution of the calcium release channel from skeletal muscle. *Nature*. 331:315-319.

Lakatta, E. G., M. C. Capogrossi, A. A. Kort, and M. D. Stern. 1986. Spontaneous myocardial calcium oscillations: overview with emphasis on ryanodine and caffeine. *Fed. Proc*. 44:2977-2983.

Lavenda, B., G. Nicolis, and M. Herschkowitz-Kaufman. 1971. Chemical instabilities and relaxation oscillations. *J. Theor. Biol*. 32:283-292.

Lechleiter, J., S. Girard, E. Peralta, and D. Clapham. 1991. Spiral calcium wave propagation and annihilation in *Xenopus laevis* oocytes. *Science*. 252:123-126.

Lefever, R. and G. Nicolis. 1970. Chemical instabilities and sustained oscillations. *J. Theor. Biol*. 30:267-284.

Lin N. Y., Y. P. Liu, W. Y. Cheung. 1974. Cyclic 3′:5′-nucleotide phosphodiesterase: purification, characterization, and active form of the protein activator from bovine brain. *J. Biol. Chem*. 249:4943-4954.

Meissner, G. 1983. Monovalent ion and calcium ion fluxes in sarcoplasmic reticulum. *Molecular and Cellular Biochemistry*. 55:65-82.

Meissner, G., E. Darling, and J. Eveleth. 1986. Kinetics of rapid Ca^{2+} release by sarcoplasmic reticulum. effects of Ca^{2+}, Mg^{2+}, and adenine nucleotides. *Biochem*. 25:236-244.

Meyer, T., and L. Stryer. 1988. Molecular model for receptor-stimulated calcium spiking. *Proc. Natl. Acad. Sci. USA*. 85:5051-5055.

Oetliker, H. 1982. An appraisal of the evidence for a sarcoplasmic reticulum membrane potential and its

relation to calcium release in skeletal muscle. *Journal of Muscle Research and Cell Motility*. 3:247-272.

Ogawa, Y., N. Kurebayashi, A. Irimajiri, and T. Hanai. 1981. Transient kinetics for Ca uptake by fragment sarcoplasmic reticulum from bullfrog skeletal muscle with reference to the rate of relaxation in living muscle. Adv. Physiol. Sci. 5:417-435.

Okada, Y., W. Tsuchiya, and T. Yada. 1982. Calcium channel and calcium pump involved in oscillatory hyperpolarizing responses of L-strain mouse fibroblasts. *J. Physiol*. 327:440-461.

Osipchuk, Y. V., M. Wakui, D. I. Yule, D. V. Gallacher, and O. H. Petersen. 1990. Cytoplasmic Ca^{2+} oscillations evoked by receptor stimulation, G-protein activation, internal application of inositol trisphosphate of Ca^{2+}: simultaneous microfluorometry and Ca^{2+} dependent Cl^- current recording in single pancreatic acinar cells. *EMBO J*. 9:697-704.

Parker, I. and I. Ivorra. 1990. Localized all-or-none calcium liberation by inositol trisphosphate. *Science*. 250:977-979.

Parker, I. and R. Miledi. 1986. Changes in intracellular calcium and in membrane currents evoked by injection of inositol trisphosphate into *Xenopus* oocytes. *Proc. R. Soc. Lond. B*. 228:307-315.

Parker, I., K. Sumikawa, and R. Miledi. 1987. Activation of a common effector system by different brain neurotransmitter receptors in *Xenopus* oocytes. *Proc. R. Soc. Lond*. 231:37-45.

Petersen, C. C. H., E. C. Toescu, and O. H. Petersen. 1991. Different patterns of receptor-activated cytoplasmic Ca^{2+} oscillations in single pancreatic acinar cells: dependence on receptor type, agonist concentration and intracellular Ca^{2+} buffering. *EMBO J*. 10:527-533.

Prigogine, I. 1968. *Introduction to Thermodynamics of Irreversible Processes*. 3rd ed. Wiley Interscience. New York.

Robertson, S. P., J. D. Johnson, and J. D. Potter. 1981. The time-course of Ca^{2+} exchange with calmodulin, troponin, parvalbumin, and myosin in response to transient increases in Ca^{2+}. *Biophys. J*. 34:559-569.

Rooney, T. A., D. C. Renard, E. J. Sass, and A. P. Thomas. 1991. Oscillatory cytosolic calcium waves independent of stimulated inositol 1,4,5-trisphosphate formation in hepatocytes. *J. Biol. Chem.* 266:12272-12282.

Rooney, T. A. and A. P. Thomas. 1991. Organization of intracellular calcium signals generated by inositol lipid-dependent hormones. *Pharmac. Ther.* 49:223-237.

Schlegal, W., B. P. Winger, P. Mollard, F. Wuarin, G. R. Zahnd, C. B. Wolheim, and B. Dufy. 1987. Oscillations of cytosolic Ca^{2+} in pituitary cells due to action potentials. *Nature (London).* 329:719-721.

Snyder, P. M., K. H. Krause, and M. J. Welsh. 1988. Inositol Trisphophate isomers, but not inositol 1,3,4,5 tetrakisphosphate, induces calcium influx in *Xenopus laevis* oocytes. *J. Biol. Chem.* 263: 11048-11051.

Somlyo, A. V., H. Gonzalez-Serratos, H. Shuman. G. McClellan, and A. P. Somlyo. 1981. Calcium release and ionic changes in the sarcoplasmic reticulum of tetanized muscle: an electron-probe study. *J. Cell Biol.* 90:577-594.

Somogyi, R. and J. W. Stucki. 1991. Hormone-induced calcium oscillations in liver cells can be explained by a simple one pool model. *J. Biol. Chem.* 266:11068-11077.

Stephenson, D. G., I. R. Wendt, and Q. G. Forrest. 1981. Non-uniform ion distribution and electrical potential in carcoplasmic regions of skeletal muscle fibres. *Nature.* 289:690-692.

Stern, M. D., M. C. Capogrossi, and E. G. Lakatta. 1988. Spontaneous calcium release from the sarcoplasmic reticulum in myocardial cells: mechanisms and consequences. *Cell Calcium.* 9:247-258.

Swillens, S. and D. Mercan. 1990. Computer simulation of a cytosolic calcium oscillator. *Biochem. J.* 271:835-838.

Takahashi, T., E. Neher, and B. Sakmann. 1987. Rat brain serotonin receptors in *Xenopus* oocytes are coupled by intracellular calcium to endogenous channels. *Proc. Natl. Acad. Sci. USA.* 84:5063-5067.

Taylor, W. C., W. J. Berridge, K. D. Brown, A. M. Cooke, and B. V. L. Potter. 1988. Dl-myo-inositol 1,4,5-trisphosphate mobilizes intracellular calcium in Swiss 3T3 cells and *Xenopus* oocytes. *Biochem. Biophys. Res.*

Comm. 150:626-632.

Valko, P. and S. Vajda. 1985. An extended ODE solver for sensitivity calculations. *Comput. Chem.* 8:255-271.

Wakui, M., Y. V. Osipchuk, and O. H. Petersen. 1990. Receptor-activated cytoplasmic Ca^{2+} spiking mediated by inositol trisphosphate is due to Ca^{2+}-induced Ca^{2+} release. *Cell.* 63:1025-1032.

Wakui, M. and O. H. Petersen. 1990. Cytoplasmic Ca^{2+} oscillations evoked by acetylcholine or intracellular infusion of inositol trisphosphate or Ca^{2+} can be inhibited by internal Ca^{2+}. *FEBS.* 263:206-208.

Wakui, M., V. L. Potter, and O. H. Petersen. 1989. Pulsatile intracellular calcium release does not depend on fluctuations in inositol trisphosphate concentration. *Nature.* 339:317-320.

Wolff, D. J., P. G. Poirier, C. O. Brostrom, and M. A. Brostrom. 1977. Divalent cation binding properties of bovine brain Ca^{2+}-dependent regulator protein. *J. Biol. Chem.* 252:4108-4117.

Chapter Two

Abstract

In the previous chapter, an initial model was proposed to describe a mechanism for cytosolic calcium oscillations (Jafri, M. S., S. Vajda, P. Pasik, and B. Gillo. 1992. A membrane model for cytosolic calcium oscillations: a study using *Xenopus* oocytes. *Biophys. J.* 63:235-246). Here we report several extensions of the original model which provide a quantitatively more accurate treatment. In this chapter we have shown that the oscillations can occur at lower endoplasmic reticulum (ER) membrane potentials, consistent with physiological values. Here we include the effects of counterions, which produce smoother oscillations over a wider parameter range. We predict that reduction of the ER calcium pump (Ca-ATPase) rate can cause the termination of cytosolic calcium oscillations in an active cell, and induce oscillations in a resting cell. This result is consistent with experiments with thapsigargin, a Ca-ATPase activity inhibitor. We simulate the latency phenomenon and offer a plausible explanation for it.

Introduction

Our recently proposed model for cytosolic calcium

oscillations (Jafri et al., 1992) is based on the electrophysiological properties of the ER membrane. The model includes calcium-dependent calcium release through a calcium channel in the ER membrane, the ER Ca-ATPase that pumps calcium back into the ER, calcium dependent removal from the ER by the plasmalemmal calcium pump, and calcium entry into the cytosol from the IP_3-sensitive store and other possible sources. Analysis of the model concluded that frequencies and amplitudes of calcium oscillations can be modulated by the rate of calcium entry, and also by the concentrations of calcium binding proteins.

Several models for the mechanism governing calcium oscillations have been proposed recently, as described in the introduction to Chapter 1 (for a review, see Dupont and Goldbeter, 1992). They fall into two basic categories: (a) molecular models and (b) compartmental or pool models. The compartmental models have either one or two pools of calcium. The one-pool models assume calcium and IP_3 cause calcium to be released from a single store in the ER. The two-pool models divide the ER into IP_3-sensitive and IP_3-insensitive stores. Calcium-dependent calcium release occurs from the IP_3-insensitive store. It does not depend upon the presence of IP_3, but only upon the binding of calcium to a channel protein. Calcium release from the IP_3-sensitive store is caused by binding of IP_3 to the IP_3-sensitive calcium channel.

Our model is a two-pool model. It differs from the

others in that in incorporates the electrophysiological properties of the ER membrane and cytosolic calcium buffering. We have postulated in our previous work (Jafri, et al., 1992) that the mechanisms behind the oscillations in both excitable and non-excitable cells might differ only in the mode of calcium entry into the cytosol. In excitable cells, calcium entry is typically due to the opening of plasmalemmal voltage-gated calcium channels. In non-excitable cells the calcium entry is typically due to IP_3-mediated calcium release as a result of agonist-stimulated IP_3 production. The entry of calcium slowly raises the cytosolic calcium concentration, which causes an increase in calcium-dependent calcium release from the ER in a positive feedback loop. Thus, calcium release is amplified until the electrochemical gradient across the ER membrane has been lowered sufficiently to slow calcium release. During this process the calcium-dependent calcium pumps are increasing their rates in response to elevated cytosolic calcium. This decreases cytosolic calcium to its base level, and the process repeats (Figure 2.1).

In this paper we investigate additional properties of our model and develop it further to include counterions. Counterions are positive ions that move across the ER membrane in response to the changes in ER membrane potential caused by the calcium fluxes across the ER membrane. They move passively with fixed conductance. It has been shown

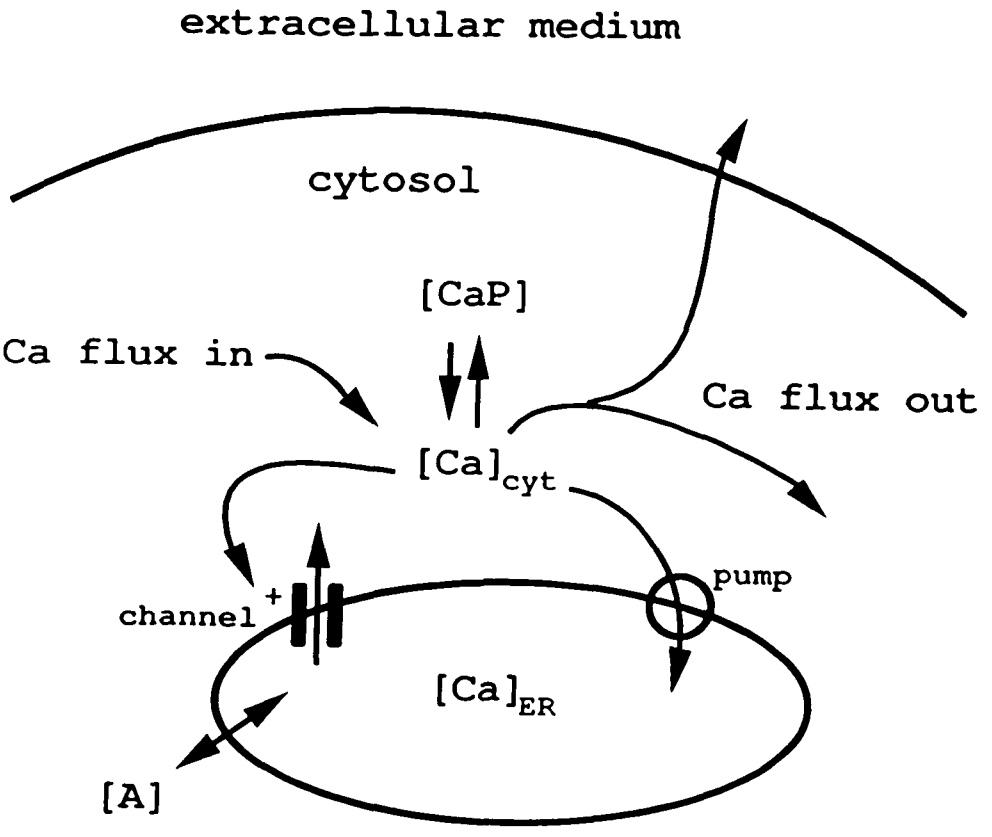

Figure 2.1. Schematic representation of the model for cytosolic calcium oscillations. Notice that an increase of $[Ca]_{cyt}$ triggers calcium release from the ER through the calcium-dependent calcium release channel. The calcium bound to calmodulin is denoted by [CaP]. [A] is the counterion concentration.

that in the hepatocyte, upon release of calcium from the ER, K^+ ions move into the ER lumen (Joseph and Williamson, 1986). Somlyo and co-workers (1981) made the same observation in the sarcoplasmic reticulum (SR) of skeletal muscle cells. It also has been observed that Mg^{2+} moves into the ER in response to ER calcium release in the bee photoreceptor (Baumann et al., 1991). We will now present the model with its modifications.

Glossary of New Terms

This model uses the terms and parameters presented in the Glossary of Terms in Chapter 1. In addition, the following new quantities arise:

Variables

$[A]_{cyt}$ = cytosolic counterion concentration

Functions

I_A = counterion current across the ER membrane

E_A = counterion reversal potential across the ER membrane

Parameters

V_{ER}	=	volume of ER lumen
V_{total}	=	$V_{ER} + V_{cyt}$
$[A]_{ER}$	=	counterion concentration in the ER lumen
$[A_{total}]$	=	total concentration of counterions

THE MODEL

The model builds on our previous membrane model (Jafri et al., 1992), with several modifications. An additional differential equation models changes in counterion concentration. Explicit terms model the calcium release from $_{IP3}$-sensitive store (IP_3-mediated calcium release) and uptake by a calcium pump to refill this store.

The model is based on the following assumptions (the new or modified assumptions are starred (*)):

1*) The ER membrane is excitable, that is, it separates charge and has ionic currents flowing across it. Calcium is the only ion that is actively transported across the ER membrane by a pump.

2) The plasma membrane potential has no influence on the calcium oscillations.

3) The oscillations occur as a result of competition between the calcium-dependent calcium release from

the ER and the uptake from the cytosol into the ER by a calcium dependent pump.

4) There is a constant calcium entry into the cytosol from either intracellular sources through calcium release mediated by a second messenger, such as IP_3, or extracellular sources through plasma membrane calcium channels.

5) There is calcium-dependent efflux from the cytosol into the extracellular space by a plasmalemmal calcium pump.

6) The calcium oscillations in *Xenopus* oocytes that are measured by the calcium-dependent chloride current in the plasma membrane occur primarily in the cytosolic compartment which is approximated by a spherical shell comprised of the outer 1 μm of the oocyte.

7) Cytosolic calcium is bound by calcium binding proteins.

8*) There are counterions that move across the ER membrane as a result of the calcium ion movement across the membrane (Baumann et al., 1991; Meissner, 1983; Somlyo et al., 1981).

The mathematical model consists of four differential equations (equations 1,5,6,7) described below. Equation 1 is unchanged from the previous model. Equations (5) and (6) are

modifications of those in Chapter 1 to include counterion terms and specific terms for the contribution of the IP_3-sensitive store of the ER to the cytosolic calcium concentration. Equation 7 is new. The dynamic variables in these equations are the cytosolic calcium concentration ($[Ca]_{cyt}$), the ER membrane potential (V), the concentration of calcium binding sites ([P]), and the cytosolic counterion concentration ($[A]_{cyt}$). The remaining equations 1,2,3,4,8,9,10) provide values for the functions contained in the differential equations.

Calmodulin is the main calcium binding protein in the cytosol. It has four binding sites per molecule, which we treat as identical. The balance equation for the number of free binding sites is

$$\frac{d[P]}{dt} = k_{off}([P_{total}] - [P]) - k_{on}([Ca]_{cyt}[P]). \qquad (1)$$

where [P] is the concentration of free calmodulin calcium binding sites, $[P_{total}]$ is the total amount of calmodulin calcium binding sites in the cell, $[Ca]_{cyt}$ is the cytosolic calcium concentration, and k_{on} and k_{off} are the on and off rates of the calcium binding sites. The calmodulin concentration has been measured to be ~34 μM (Cartaud et al., 1980) in resting mature oocytes. Thus, the total concentration of calmodulin calcium binding sites in the cell is ~136 μM. We

use 120 μM as the total concentration of calcium binding sites. Measured values of the equilibrium constant for the disassociation of calcium from calmodulin (disassociation constant) ranges from 0.2 to 18 μM (Robertson et al., 1981, Lin et al., 1974, Wolff et al., 1977). We use a disassociation constant value of 1 μM in the model with k_{on} and k_{off} values of 5 $\mu M^{-1}s^{-1}$ and 5 s^{-1}, respectively.

We assume that the ER membrane has electrophysiological properties similar to the plasma membrane. The ER membrane is depolarized by the calcium current and repolarized by the movement of calcium by the pump. These changes of ER membrane potential are opposed by the flow of counterions in both directions (figure 2.1).

As before, The calcium current across the ER membrane is given by

$$I_{Ca} = g_{Ca}(E_{Ca} - V) . \qquad (2)$$

where g_{Ca} is the ER membrane calcium conductance per unit area, E_{Ca} is the reversal potential for calcium, and V is the potential difference across the ER. We use the convention that positive ions flowing into the cytosol constitute a negative current. The unbuffered ER calcium concentration is ~5mM (Somlyo et al., 1981). This, however, measures the total amount of calcium in the ER lumen including free and

buffered calcium. In the cell, only the free calcium contributes to the reversal potential. For simplicity, we assume that the free ER luminal calcium concentration ($[Ca]_{ER}$) remains constant at 15 μM. This implies that movement of calcium on and off the ER calcium binding proteins is fast compared to calcium movement across the ER. The reversal potential for calcium (E_{Ca}) is calculated by using the Nernst equation,

$$E_{Ca} = \frac{RT}{zF} \ln\left(\frac{[Ca]_{ER}}{[Ca]_{cyt}}\right) \qquad (3)$$

where R is the ideal gas constant, F is Faraday's constant, Z is the charge on the calcium ion, and T is the absolute temperature.

Much of the information here is inferred from experimental results on the calcium-dependent calcium release (ryanodine) channel obtained from sarcoplasmic reticulum (SR) membrane preparations. The conductance is simplified as cooperative binding given by Hill's equation with Hill coefficient n = 2.

$$g_{Ca} = \overline{g_{Ca}} S \frac{\left(\frac{[Ca]_{cyt}}{K_{diss}}\right)^2}{1 + \left(\frac{[Ca]_{cyt}}{K_{diss}}\right)^2} \quad (4)$$

where $\overline{g_{Ca}}$ is the maximal ER membrane conductance per unit area, K_{diss} is the disassociation constant of calcium from the ryanodine channel, and S is the ER surface area. We use a value of 3.4 pS per square micron for $\overline{g_{Ca}}$ (Jafri et al., 1992). The disassociation constant of calcium from the ryanodine channel ranges from 2-10 μM (Meissner et al., 1986). We use a value of 5 μM for K_{diss}. We use a value of 6.16×10^{-3} cm_2 for the ER surface area (S).

We can now write the complete balance equation for $[Ca]_{cyt}$.

$$\frac{d[Ca]_{cyt}}{dt} = \frac{I_{Ca}}{2FV_{cyt}} - k_{pump}[Ca]_{cyt} + \frac{q_0}{V_{cyt}} - k[Ca]_{cyt} + \frac{q_{IP}}{V_{cyt}} - k_{IP}[Ca]_{cyt} + k_{off}([P_{total}] - [P]) - k_{on}[Ca]_{cyt}[P] \quad (5)$$

where V_{cyt} is the cytosolic compartment volume, k is the rate constant of calcium efflux from the cytosol across the plasma membrane, k_{pump} is the pump rate for the ER Ca-ATPase, and q_0 is the rate of calcium entry into the cytosol which we approximate at 2.92×10^{-10} μM per second. The pump rate into the IP_3-sensitive store is k_{IP} and q_{IP} is the rate of calcium

influx into the cytosol from this store. The factor 2 in the denominator is the charge of the calcium ion. We use a value of 5.84 x 10^{-5} μl for V_{cyt}. In our calculations (Jafri et al., 1992) we obtained a value of 6.1 μm^{-1} for the ratio of

which is comparable to the value of 13 μm^{-1} obtained by Mobley and Eisenberg (1975) in the terminal cisternae of frog skeletal muscle.

The pump rate ER calcium ATPase (k_{pump}) is assumed to depend linearly on $[Ca]_{cyt}$ since the physiological range of $[Ca]_{cyt}$ is on the almost linear part of the Michaelis-Menten curve (Ogawa, et al., 1981, Ghandi and Ross, 1988). We make the same approximation for the plasmalemmal calcium pump rate (k). Thus, we use 20.2 s^{-1} and 69.8 s^{-1} for the initial values of k and k_{pump}, respectively.

The third equation for the model, that of the ER membrane potential, is given by

$$SC_m \frac{dV}{dt} = I_{Ca} - 2FV_{cyt}k_{pump}[Ca]_{cyt} + I_A \qquad (6)$$

where C_m is the membrane capacitance per unit area, V is the potential difference across the membrane and I_A is the current due to the movement of counterions across the ER membrane (described below). The first term on the right hand side of the equation is the capacitative current due to the calcium movement through the channel. The second term is the electrogenic current generated by the ER calcium ATPase.

The counterions are positive ions that move across the ER membrane in the opposite direction of calcium to balance the charge movement due to calcium fluxes across the ER membrane. The balance equation for the cytosolic counterion concentration ($[A]_{cyt}$) is given by

$$\frac{d[A]_{cyt}}{dt} = \frac{I_A}{FV_{cyt}}, \qquad (7)$$

where the current across the ER membrane due to the counterions is

$$I_A = g_A (E_A - V), \qquad (8)$$

and the reversal potential for the counterions is described by

$$E_A = \frac{RT}{F} \ln \left(\frac{[A]_{ER}}{[A]_{cyt}}\right). \qquad (9)$$

The "conductance" (g_A) of the counterions is assumed to be constant. The ER luminal counterion concentration ($[A]_{ER}$) is not modelled explicitly. Instead, it is expressed as

$$[A]_{ER} = \frac{V_{total}[A_{total}] - V_{cyt}[A_{cyt}]}{V_{ER}}, \qquad (10)$$

where $[A_{total}]$ is the total counterion concentration, V_{ER} is the volume of the ER lumen and

$$V_{total} = V_{ER} + V_{cyt}. \qquad (11)$$

The complete model is given in equations (1) through (11).

Methods

The model (Equations 1 through 11) was numerically integrated using the ROW4D program (Valko and Vajda, 1985) on a Convex C220 computer. The ROW4D program uses a semi-implicit Runge-Kutta method introduced by Rosenbrock and modified by Gottwald and Wanner (1981). This method is simpler than the Gear program with comparable performance (Seifert, 1987)

The values of physiological parameters used in the model are presented in Table 2.1. When other parameter values are used in the computations they are mentioned in the figure legend. The value for the counterion conductance (g_A) is not known. It was approximated using the ratio of the total magnesium flux to the total calcium flux measured to be 0.7

in the bee photoreceptor (Baumann et al., 1991). Using a cytosolic counterion concentration of 5 mM, the conductance was increased from zero until the ratio of 0.7 had been achieved. If the cytosolic counterion [A_{cyt}] has concentration of 5 mM then the cytosolic magnesium concentration is 2.5 mM since it has a valence of +2.

The numerical experiments involving latency started the simulation at a resting concentration of .085 μM and made a step change in the influx (q_{IP}) to imitate the onset of IP_3-induced calcium release. The simulations to mimic the effects of thapsigargin, a pharmacological agent that inhibits the activity of certain calcium pumps, were performed by allowing step decreases in the pump rate.

Table 2.1

Parameter values for the model

Parameter		*Value*
C_m	=	$1\ \mu F\ cm^{-2}$
F	=	$96500\ coulombs(mol\ e^{-})^{-1}$
$\overline{g_{Ca}}$	=	$340\ \mu S\ cm^{-2}$
K_{diss}	=	$5\ \mu M$
k_{pump}	=	$69.8\ s^{-1}$
k	=	$10.0\ s^{-1}$
k_{IP}	=	$10.2\ s^{-1}$
S	=	$6.16\ x\ 10^{-3}\ cm^2$
V_{cyt}	=	$5.84\ x\ 10^{-3}\ \mu l$
q_0	=	$1.0\ x\ 10^{-10}\ \mu mol\ s^{-1}$
q_{IP}	=	$1.92\ x\ 10^{-10}\ \mu mol\ s^{-1}$
P_{total}	=	$120\ \mu M$
k_{off}	=	$5\ s^{-1}$
k_{on}	=	$1\ \mu M^{-1}\ s^{-1}$
$[Ca]_{ER}$	=	$5000\ \mu M$
V_0	=	$12.9\ mV$
R	=	$8.314\ J°K^{-1}\ mole^{-1}$
T	=	$300\ K$
r	=	$600\ \mu m$
V_{ER}	=	$4.02\ x\ 10^{-6}\ \mu l$
g_A	=	$10\ x\ 10^{-6}\ S cm-2$
$[A_{total}]$	=	$10\ mM$

These parameters are used in the simulations unless otherwise stated.

Results and Discussion

Changes in the ER membrane potential

Experiments with potentiometric dyes have shown that the SR membrane potential in skeletal muscle is between ~15-20 mV (Stephenson et al., 1981) at rest and rises to ~40 mV during calcium uptake (Meissner, 1983). In this model we reduce the value of the ER calcium concentration to 15 μM. This results in a lower ER membrane potential (figure 2.2) which is closer to the experimentally measured values. With this modification the model displays all the behavior seen in the previous model (Jafri, et al., 1992). To be specific, an increase in calcium influx into the cytosol results in higher frequency and lower amplitude oscillations. Also, as the buffer concentration increases the oscillations have decreased amplitude and increased frequency.

The effects of counterions on cytosolic calcium oscillations

Counterions are ions that move across the ER membrane in response to the movement of charge through channels. The net effect of counterions is to reduce the actual amount of net charge that crosses the ER. The existence of counterion currents involving Mg^{2+}, H^{+}, and K^{+} has been postulated to be (Somlyo et al., 1981) to explain the large amount of charge due to calcium that can cross the ER during tetanus without electrical breakdown of the ER membrane. In hepatocytes

(Joseph and Williamson, 1986) and skeletal muscle (Somlyo et al., 1981) K^+ was found to enter the ER (or SR in muscle) during calcium release. Baumann and co-workers (1991) determined Mg^{2+} to be the counterion during calcium release from the ER in bee photoreceptor cells.

We model the counterion by a generic univalent positive ion A^+. When we allow a total counterion concentration of 5 mM the calcium oscillations increase very slightly in amplitude and width in comparison to the results without counterions as shown by figures. As the counterion concentration is raised the oscillations increase slightly in amplitude and width (figure 2.3). The amplitude of the membrane potential oscillations decreases with increasing counterion concentration. The range of values of the calcium entry (q) also increases with this modification.

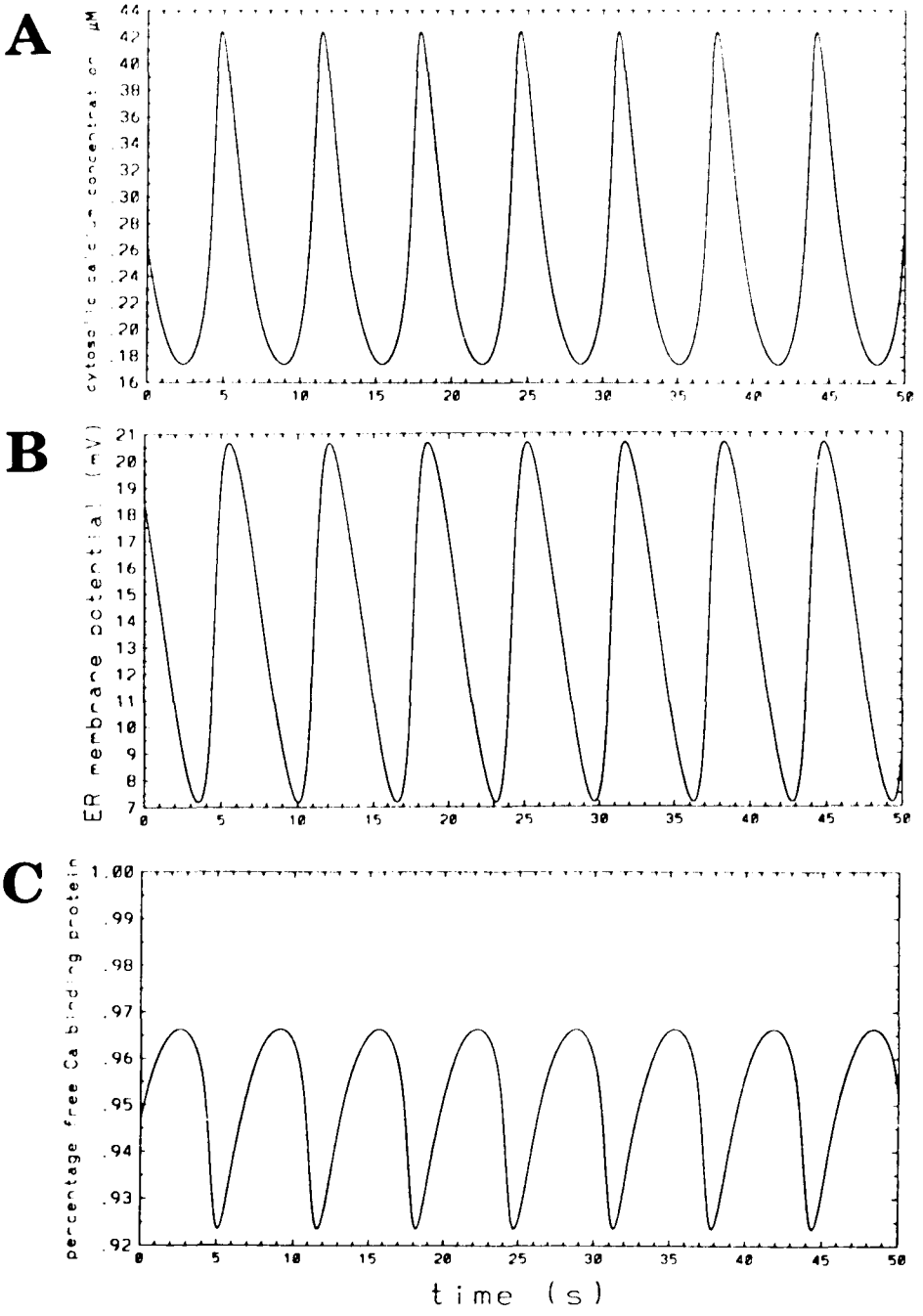

Figure 2.2. Simulation of cytosolic calcium oscillations without counterions. A. $[Ca]_{cyt}$ B. ER membrane potential C. percentage free calcium calmodulin calcium binding sites. The total rate of calcium entry is q = 2.92 x 10^{-10} μmol/s ($q = q_0 + q_{IP}$).

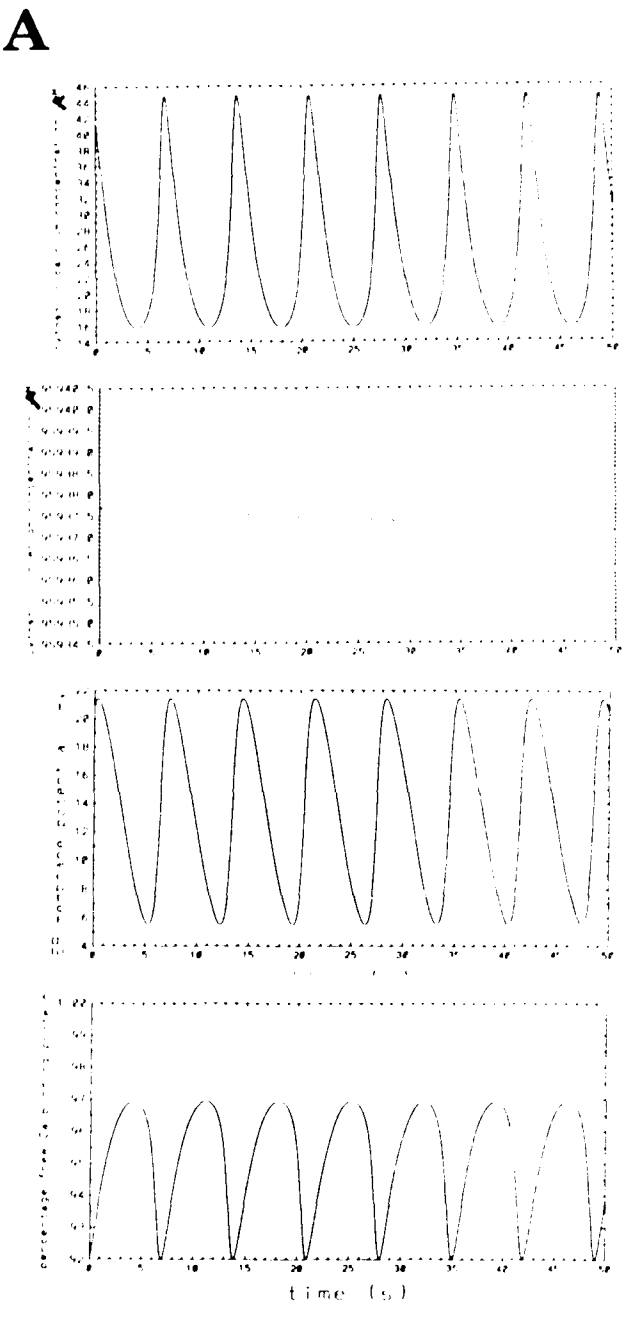

Figure 2.3. As the counterion concentration is raised the oscillations become smoother with increased amplitude. A. The total counterion concentration [A_{total}] = 5 mM. This concentration corresponds to magnesium being the counterion.

B

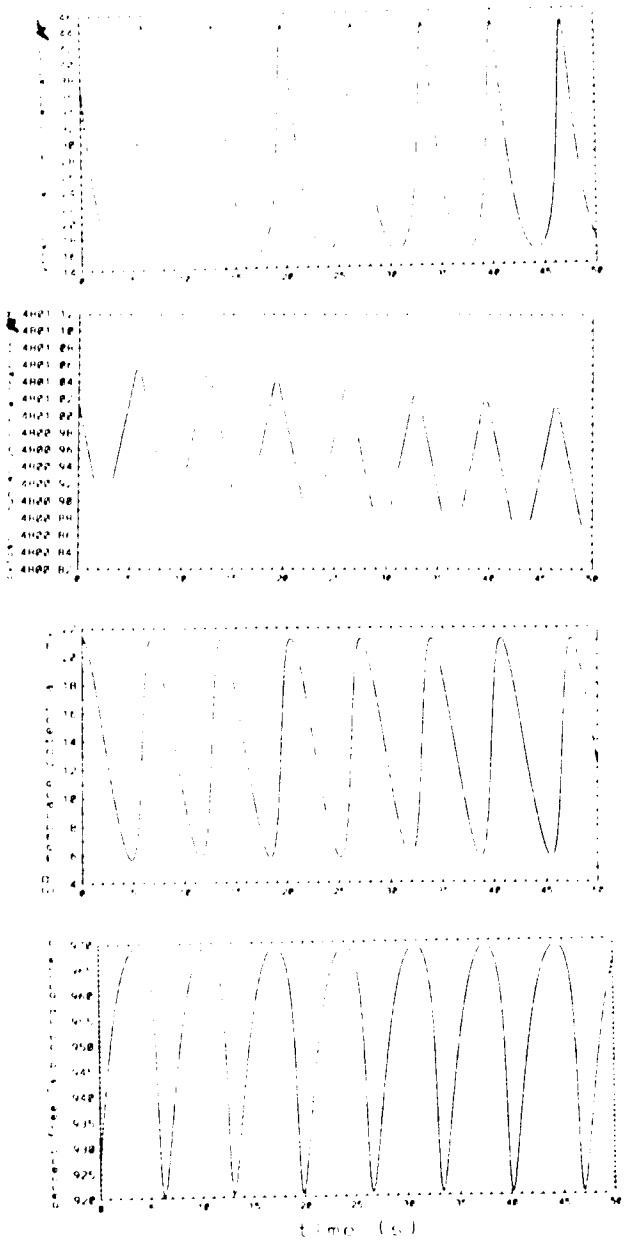

Figure 2.3. B. The total counterion concentration [A_{total}] = 100 mM. This concentration corresponds to potassium being the counterion.

Latency

It has been observed (Tanaka et al., 1992; Rooney et al., 1989) that with increasing dose of neurotransmitter the period of time between the response and the dose increases. This phenomenon is called latency. The model exhibits a similar latency effect and offers a plausible explanation for the phenomenon.

We start the simulation with the cell at a resting value of $[Ca]_{cyt}$. At time zero, the calcium entry (q) is raised to a given value. The larger the value of q the shorter the period of latency (figure 2.4). Figure 2.5 shows that the dependence of the length of the period of latency on q. In fact, when we plot latency vs. period of the oscillations (figure 2.6) we get a qualitatively similar figure to that obtained by Rooney and co-workers (1989) experimentally. For higher values of q the oscillations cease and the latency quickly approaches a limiting value ~1.2 seconds. They are not shown in figure 2.4 since the period of the oscillations is fluctuating.

These simulations model the final step of signal transduction, that is, the calcium has already been released from the IP_3-sensitive store and has diffused to the channel. These latency values are somewhat smaller than those measured experimentally for the following reason. When the cell is exposed to neurotransmitter a cascade of events occur resulting in an increase of IP_3 production. The increase in IP_3 concentration in the cytosol results in an increase in the

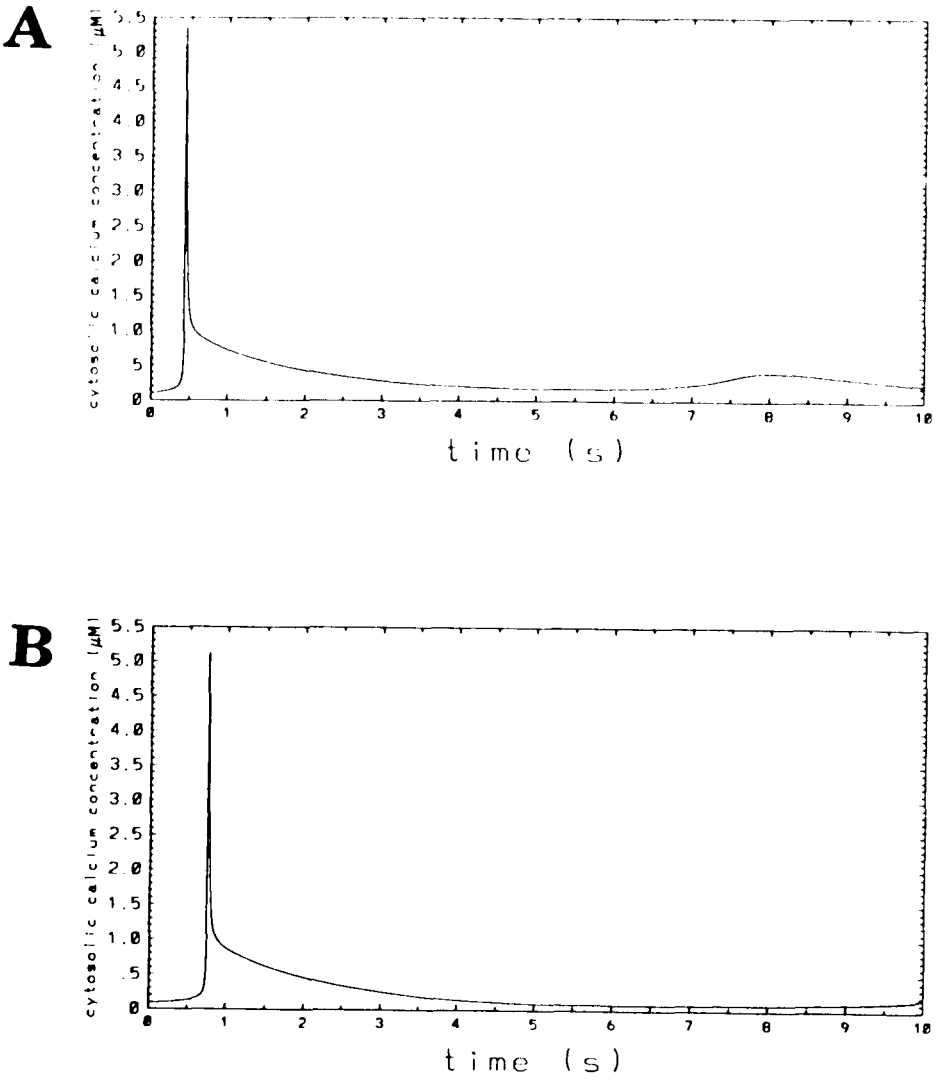

Figure 2.4. A step change of the total influx ($q = q_0 + q_{IP}$) to A. 3.0×10^{-10} μmol/s and B. 2.4×10^{-10} μmol/s to a cell with resting $[Ca]_{cyt}$ = . Notice that the period of latency is longer for a lower rate of calcium entry q. In the physiological system the calcium entry is due to IP_3 mediated calcium release in response to agonist. The latency period predicted here will be shorter than that found in experiments since in experiments the latency period will include time for the transduction of agonist stimulation to IP_3 production.

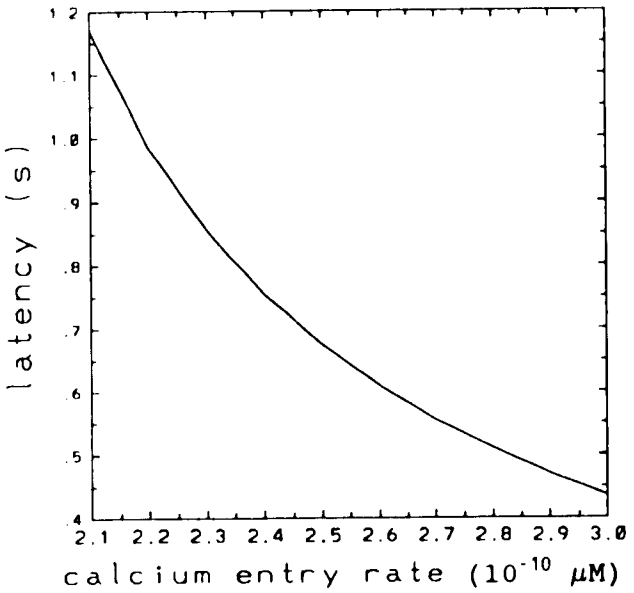

Figure 2.5. The dependence of latency period on the value of the total calcium entry q. As q increases the length of the latency period reaches a minimum.

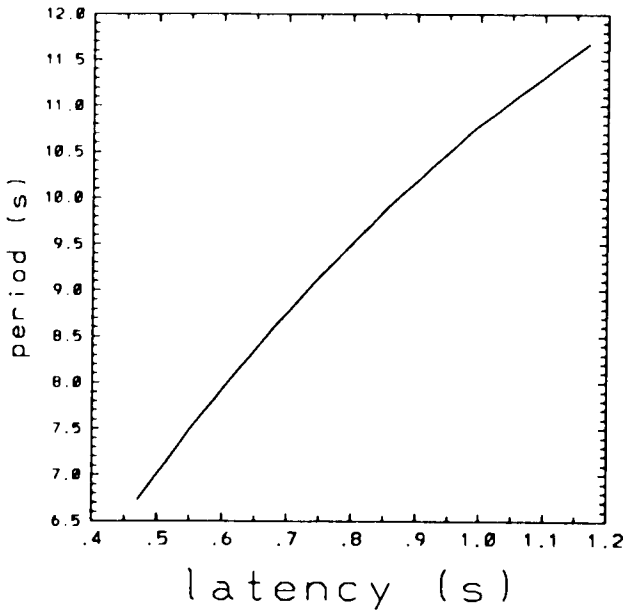

Figure 2.6. The correlation of latency period and period of the oscillations. There is a limiting minimal value of the latency as the period of oscillations decreases that is not shown since the oscillations as q increases past the range shown and the period of oscillations therefore was not measurable.

release of calcium from the IP_3-sensitive stores, which we model as q. The increased q causes the cytosolic calcium to reach threshold more rapidly resulting in a shorter latency period. This is the same phenomenon that results in higher frequency oscillations as q increases.

The effects of varying pump rate on cytosolic calcium oscillations

Intracellular application of thapsigargin blocks the ER Ca-ATPase. Foskett and coworkers (1991a, 1991b) have shown the calcium pump of the IP_3-sensitive store in the ER is affected and the store emptied. The model can simulate this phenomenon by reducing the pump rate into the IP_3-sensitive store (k_{IP}). Calcium oscillations have been shown to be triggered or terminated by the addition of thapsigargin. This can be simulated by varying the amount of the reduction of the pump rate into the IP_3-sensitive store of the ER (k_{IP}). The reduction from 45 s^{-1} to 15 s^{-1} of the pump rate (k_{IP}) into the IP_3-sensitive store caused the onset of calcium oscillations. Figure 2.7 shows that further reduction of the pump rate (k_{IP}) to 5 s^{-1} abolishes oscillations. Osada and coworkers (1992) observed the absence of calcium oscillations upon application of calcium mobilizing hormone to thapsigargin treated hepatocytes. Similarly, Foskett and coworkers (1991a, 1991b) observed an elevation of cytosolic calcium without oscillations upon application of thapsigargin. Their data

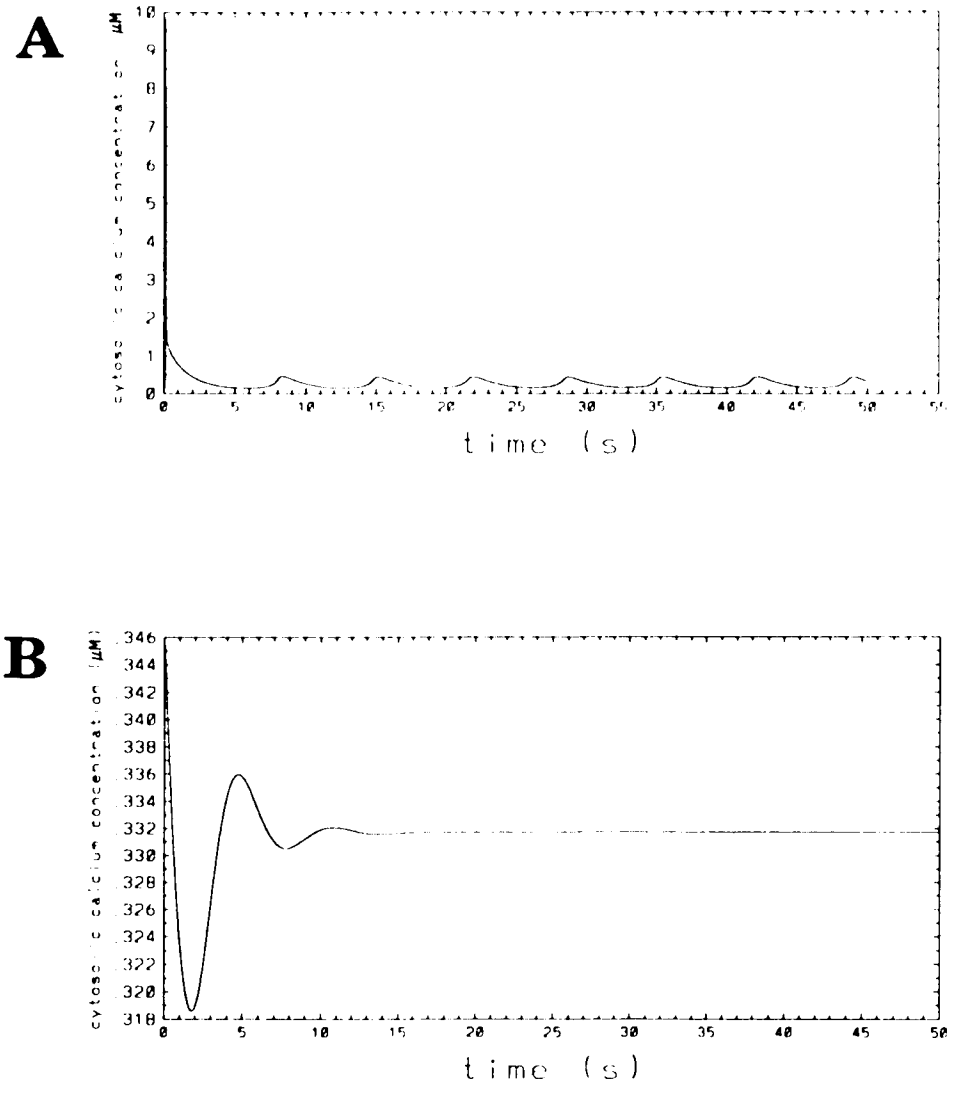

Figure 2.7. A simulation of the effects of thapsigargin on calcium oscillations. Application of thapsigargin to a quiscent cell at time = 0 s can result in spontaneous oscillatons or simply a rise in cytosolic calcium. When the value of k_{IP} were reduced to 15.2 s^{-1} from 45.2 s^{-1} oscillations resulted (panel A.). When the value of k_{IP} was further reduced to 5.2 s^{-1} the oscillations stopped (panel B). The pump rate into the ER (k) is held constant at 10 s^{-1}. (q = 3.0 x 10^{-10} μmol/s)

does not exclude some effect on the calcium pump (Ca-ATPase) of the ER of the IP_3-insensitive ER store. In fact, in skeletal muscle all the Ca-ATPase of the SR is affected (Sagara and Inesi, 1991; Wrzosek et al., 1992). When the pump rate into the IP_3-insensitive store (k_{pump}) is reduced, the release of calcium into the cytosol is unaffected while the re-uptake is slower (not shown). A similar effect was observed by Wrzosek and co-workers (1992).

The model with counterions still exhibits the same behavior as the simpler model (Jafri et al., 1992). The period of latency is shown to increase to a limiting value as the rate of calcium entry into the cytosol increases. By lowering $[Ca]_{ER}$ to more accurately represent the free ER calcium concentration, we have lowered the ER membrane potential into a range that agrees with the experimental evidence available. It is important to note that the lowering of the ER membrane potential and the latency phenomenon are also observed in the original model.

References

Baumann, O., B. Walz, A. V. Somlyo, and A. P. Somlyo. 1991. Electron probe microanalysis of calcium release and magnesium uptake by endoplasmic reticulum in bee photoreceptors. *Proc. Natl. Acad. Sci.* 88:741-744.

Cartaud, A., R. Ozon, M. P. Walsh, J. Haiech, and J. G. Demaille. 1980. *Xenopus Laevis* oocyte calmodulin in the process of meiotic maturation. *J. Biol. Chem.* 255:9404-9408.

Dupont, G. and A. Goldbeter. 1992. Oscillations and waves of cytosolic calcium: insights from theoretical models. *BioEssays*. 14:

Foskett, J. K., C. M. Roifman, and D. Wong. 1991. Activation of calcium oscillations by thapsigargin in parotid acinar cells. *J. Biol. Chem.* 266:2778-2782.

Foskett, J. K. and D. Wong. 1991. Free cytoplasmic Ca^{2+} concentration oscillations in thapsigargin treated parotid acinar cells are caffeine- and ryanodine-sensitive. *J. Biol. Chem.* 266:14535-14538.

Gandhi, C. R., and D. H. Ross. 1988. Characterization of a high-affinity Mg^{2+}-independent Ca^{2+}-ATPase from rat brain synaptosomal membranes. *J. Neurochem.* 50:248-256.

Gottwald, B. A., and G. Wanner. 1981. A reliable Rosenbrock-integrator for stiff differential equations. *Computing*. 26:335-357.

Jafri, M. S., S. Vajda, P. Pasik, and B. Gillo. 1992. A membrane model for cytosolic calcium oscillations: a study using *Xenopus* oocytes. *Biophys. J.* 63:235-246.

Joseph, S. K. and J. R. Williamson. 1986. Characteristics of inositol trisphosphate-mediated Ca^{2+} release from permeabilized hepatocytes. *J. Biol. Chem.* 261:14658-14664.

Lin N. Y., Y. P. Liu, W. Y. Cheung. 1974. Cyclic 3′:5′-nucleotide phosphodiesterase: purification, characterization, and active form of the protein activator from bovine brain. *J. Biol. Chem.* 249:4943-4954.

Meissner, G. 1983. Monovalent ion and calcium ion fluxes in sarcoplasmic reticulum. *Molecular and Cellular Biochemistry*. 55:65-82.

Meissner, G., E. Darling, and J. Eveleth. 1986. Kinetics of rapid Ca^{2+} release by sarcoplasmic reticulum. effects of Ca^{2+}, Mg^{2+}, and adenine nucleotides. *Biochem.* 25:236-244.

Mobley, B. A., and B. R. Eisenberg. 1975. Sizes of components in from skeletal muscle measured by methods of stereology. *J. Gen. Physiol.* 66:31-45.

Ogawa, Y., N. Kurebayashi, A. Irimajiri, and T. Hanai. 1981. Transient kinetics for Ca uptake by fragment sarcoplasmic reticulum from bullfrog skeletal muscle with reference to the rate of relaxation in living muscle. *Adv. Physiol. Sci.* 5:417-435.

Osada, S., S. Saji, T. Nakamura, and Y. Nozawa. 1992. Cytosolic calcium oscillations induced by hepatocyte growth factor (HGF) in single fura-2-loaded cultured hepatocytes: effects of extracellular calcium and protein kinase C. *Biochem. et Biophys. Acta.* 1135:229-232.

Robertson, S. P., J. D. Johnson, and J. D. Potter. 1981. The time-course of Ca^{2+} exchange with calmodulin, troponin, parvalbumin, and myosin in response to transient increases in Ca^{2+}. *Biophys. J.* 34:559-569.

Rooney, T. A., E. J. Sass, and A. P. Thomas. 1989. Characterization of cytosolic calcium oscillations induced by phenylephrine and vasopressin in single fura-2-loaded hepatocytes. *J. Biol. Chem.* 264:17131-17141.

Sagara, Y. and G. Inesi. 1991. Inhibition of the sarcoplasmic reticulum Ca^{2+} transport ATPase by thapsigargin at subnanomolar concentrations. *J. Biol. Chem.* 266:13503-13506.

Seifert, P. 1987. Computational experiments with algorithms for stiff ODEs. *Computing.* 163-176.

Somlyo, A. V., H. Gonzalez-Serratos, H. Shuman. G. McClellan, and A. P. Somlyo. 1981. Calcium release and ionic changes in the sarcoplasmic reticulum of tetanized muscle: an electron-probe study. *J. Cell Biol.* 90:577-594.

Stephenson, D. G., I. R. Wendt, and Q. G. Forrest. 1981. Non-uniform ion distribution and electrical potential in sarcoplasmic regions of skeletal muscle fibres. *Nature.* 289:690-692.

Tanaka, y., N. Hayashi, A. Kaneko, T. Ito, E. Miyoshi, Y. Sasaki, H. Fusamoto, and T. Kamada. 1992. Epidermal growth factor induces dose-dependent calcium oscillations in single

fura-2-loaded hepatocytes. *Hepatology*. 16:179-486.

Valko, P. and S. Vajda. 1985. An extended ODE solver for sensitivity calculations. *Comput. Chem.* 8:255-271.

Wolff, D. J., P. G. Poirier, C. O. Brostrom, and M. A. Brostrom. 1977. Divalent cation binding properties of bovine brain Ca^{2+}-dependent regulator protein. *J. Biol. Chem.* 252:4108-4117.

Wrzosek, A., H. Schneider, S. Grueninger, and M. Chiesi. 1992. Effect of thapsigargin on cardiac muscle cells. *Cell Calcium*. 13:281-292.

Chapter Three

Abstract

Spatial calcium waves have been observed in *Xenopus* oocytes through the use of confocal fluorescence microscopy. The waves assume many patterns including plane waves, target patterns, and spirals. Modification of the membrane model presented in Chapter 1 (Jafri et al., 1992) to include diffusion terms in two-dimensions reproduces planar and circular propagating waves. A one-dimensional model is used to study the properties of these waves. The model predicts that increasing the buffering capacity of the cytosol decreases the wave amplitude and speed. A decrease in the wave speed is also predicted when the net calcium entry rate into the cytosol decreases. The model also predicts that as the diffusion constant is increased the wave speed and amplitude increase.

Introduction

The development of confocal microscopy has enabled experimenters to resolve the spatial distribution of calcium in the cytosol. Waves of elevated calcium concentration have been observed that have various forms in different cell types. They commonly occur as circular waves originating

from a specific locus, or plane waves that move across the cell. Calcium waves are seen in rat gonadotropes (Rawlings et al., 1991), *Xenopus* oocytes (Girard et al., 1992; Lechleiter and Clapham, 1992; Lechleiter et al., 1991: Parker and Yao, 1991), pancreatic acinar cells (Nathanson et al., 1992), vascular smooth muscle cells (Blatter and Wier, 1992; Neylon et al., 1990), cardiac myocytes (Ishide et al., 1992; Tamakatsu and Wier, 1990a,b) and hepatocytes (Thomas et al., 1991). In *Xenopus* oocytes, spiral waves also are seen (Girard et al., 1992; Lechleiter and Clapham, 1992; Lechleiter et al., 1991).

When a cell is exposed to calcium mobilizing hormone or neurotransmitter, inositol 1,4,5-trisphosphate (IP_3) is produced after a chain of biochemical events. The IP_3 binds to the IP_3-receptor channel in the IP_3-sensitive store in the endoplasmic reticulum (ER), resulting in calcium release into the cytosol. The newly introduced calcium diffuses to the nearby calcium-induced calcium release channels and triggers calcium release into the cytosol from the IP_3-insensitive store of the ER. This rise in calcium is larger in magnitude then the initial increase from the IP_3-sensitive store. This calcium diffuses to other calcium-induced calcium release channels, causing further calcium release into the cytosol. Thus, a calcium wave propagates in the cell.

A spatio-temporal model of cytosolic calcium concentration is developed that explains calcium movement and

its resulting signalling in the cell. The model builds on the original membrane model developed earlier by Jafri an co-workers (1992; see Chapter 1).

The Model

Glossary of Terms

In addition to the functions, parameters, and variables used in the earlier model described in Chapter 1, this treatment also uses the following parameter:

D = diffusion constant of calcium in the cytosol

The spatio-temporal model is a modification of the basic membrane model (Jafri et al., 1992) with terms added to describe diffusion in one or two dimensions (figure 3.1). The model makes the same assumptions as the previous model in Chapter 1.

The model assumes that the ER membrane is excitable. It separates charge and has ionic currents flowing across it (Meissner, 1981). Calcium is the only ion that significantly contributes capacitative current to evoke changes in the ER membrane potential. The ER membrane is depolarized by the calcium current and repolarized by the calcium pump (figure 3.1). The plasma membrane potential has no influence on the oscillations (Jacob et al., 1988; Harootunian et al., 1988). The oscillations occur as a result of competition between the

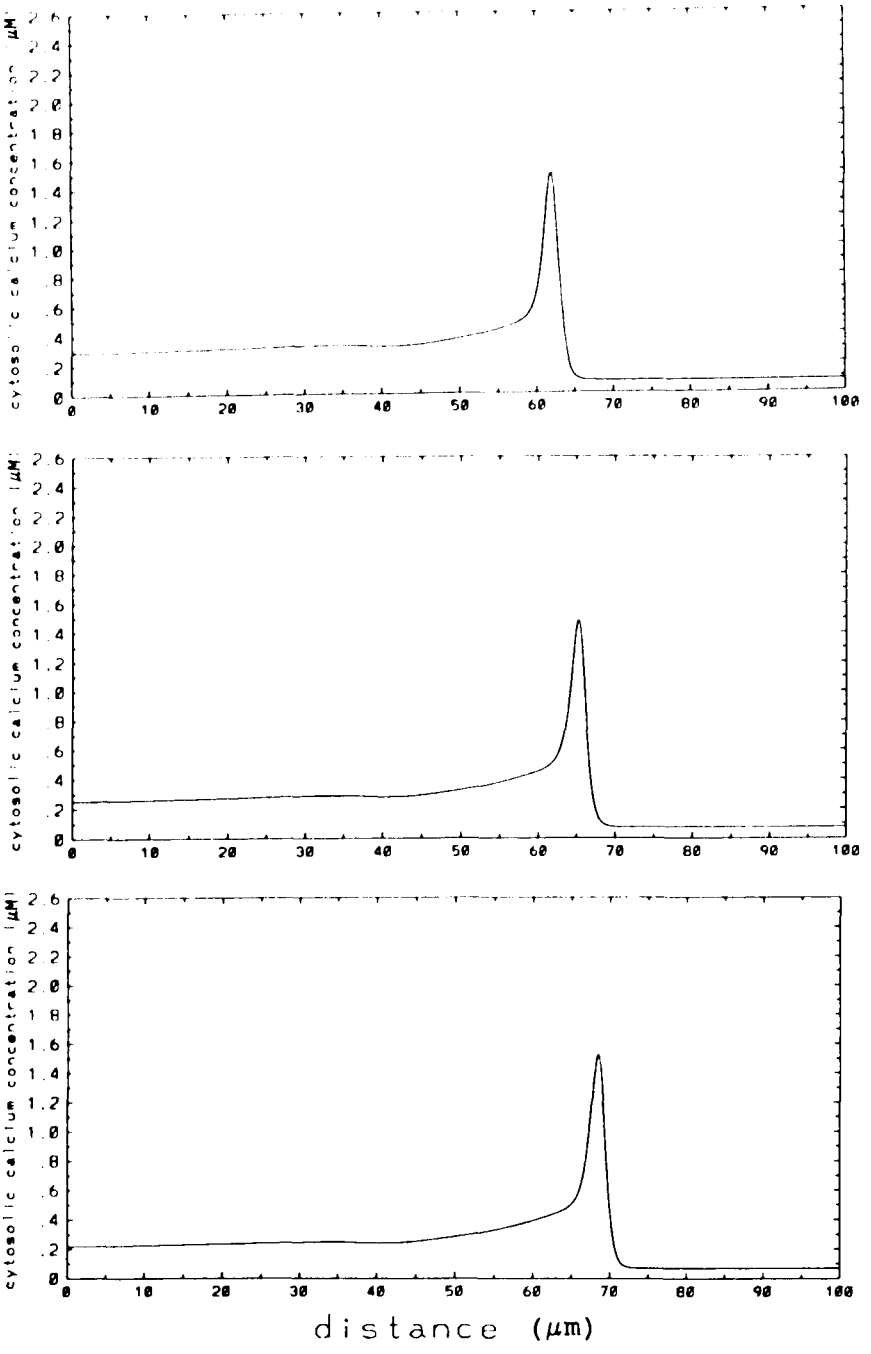

Figure 3.1. Simulation of a one-dimensional propagating calcium wave in a *Xenopus* oocyte. Note that the wave speed is ~34 μm/s and the amplitude is 1.5 μM. The time interval between frames is 0.1 s. The parameter values for the simulation are shown in Table 3.1.

calcium-dependent calcium release from the ER and the uptake from the cytosol into the ER by a calcium dependent pump. There is a constant calcium entry into the cytosol from either intracellular sources through calcium release mediated by a second messenger, such as IP_3 from the IP_3-sensitive stores of the ER. There is calcium-dependent efflux from the cytosol into IP_3-sensitive store by a ER calcium pump.

The calcium oscillations in *Xenopus* oocytes seen by fluorescent confocal microscopy occur in the outer 20-40 μm of the cytosol. We consider a slice of this space which we call the cytosolic compartment which is approximated by a spherical shell comprised of the outer 1 μm of the oocyte (Jafri et al, 1992).

Cytosolic calcium is bound by calcium binding proteins. Calcium and buffer diffuse through the cytosol. Since the concentration of free calcium binding protein is 10^5 times larger than the concentration of free calcium in the cytosol and the calcium binding protein initially is distributed homogeneously, it never builds up a concentration gradient and does not diffuse. Hence, we ignore the diffusion of calcium binding protein in the cytosol.

Three differential equations model the changes in cytosolic calcium ($[Ca]_{cyt}$), ER membrane potential (V), and concentration of free cytosolic calcium binding sites ([P]). They are as follows:

$$\frac{d[Ca]_{cyt}}{dt} = \frac{I_{Ca}}{2FV_{cyt}} - k_{pump}[Ca]_{cyt} + \frac{q}{V_{cyt}} - k[Ca]_{cyt} + \quad (1)$$
$$+ D\nabla^2([Ca]_{cyt}) + k_{off}([P_{total}] - [P]) - k_{on}[Ca]_{cyt}[P],$$

$$SC_m\frac{dV}{dt} = I_{Ca} - 2FV_{cyt}k_{pump}[Ca]_{cyt}, \quad (2)$$

and

$$\frac{d[P]}{dt} = k_{off}([P_{total}] - [P]) - k_{on}([Ca]_{cyt}[P]) \quad (3)$$

where the calcium current (I_{Ca}) across the ER membrane is given by

(4)

the reversal potential for calcium (E_{Ca}) is calculated by using the Nernst equation

$$E_{Ca} = \frac{RT}{zF}\ln(\frac{[Ca]_{ER}}{[Ca]_{cyt}}), \quad (5)$$

and the conductance (g_{Ca}) is given by

$$g_{Ca} = \overline{g_{Ca}} S \frac{\left(\frac{[Ca]_{cyt}}{K_{diss}}\right)^2}{1 + \left(\frac{[Ca]_{cyt}}{K_{diss}}\right)^2}. \qquad (6)$$

Note that in equation (1) there is now a term for the diffusion of calcium. In equations 1-3 above, k_{pump} is the pump rate from the cytosol into the ER, V_{cyt} is the cytosolic compartment volume, k is the rate constant of calcium efflux from the cytosol across the plasma membrane, and F is Faraday's constant. The factor z = 2 in the denominator is the charge on a calcium ion. The calcium flux q into the cytosol remains constant during the course of an oscillation. In different simulations, which are described in the results, the value of q is varied to produce different behavior.

Calmodulin is the major cytosolic calcium binding protein and has four biding sites per molecule. In the balance equation for free calcium binding sites [P] is the concentration of free calmodulin calcium binding sites, $[P_{total}]$ is the total concentration of calmodulin calcium binding sites in the cell, and k_{on} and k_{off} are the on and off rates from the binding sites. In equation 2, S is the ER surface area and C_m is the membrane capacitance per unit area. For simplicity in equation 5, we assume that the ER luminal calcium concentration ($[Ca]_{ER}$) remains constant at 5 mM (Somlyo et al., 1981). In equation 6, the dissociation constant of calcium from the channel protein is represented by K_{diss} and

the maximal unit ER calcium conductance is denoted by $\overline{g_{Ca}}$.

The first term on the right hand side of equation 2 is the capacitative current due to calcium movement through the channel. The second term is the electrogenic current generated by the ER calcium pump.

Numerical Methods

The equations for the one spatial dimensional model were solved using an Euler method that was implicit in space. The two spatial dimension model was solved using the above method with the split time scale. The Euler method was chosen because it allowed the non-linear equation (1) to be solved explicitly. The space derivative was expanded implicitly to improved stability.

The computations were performed on a CONVEX C3460 computer. The graphics generated for the two dimensional simulations were viewed on a Silicon Graphics Personal IRIS 4D/20 using NCAR Graphics and printed with a QMS Colorscript 100 Model 30i color printer. The one dimensional simulation graphics were viewed on a Sun Microsystems Sparcstation2 with NCAR Graphics.

The parameter values used for the simulations are given in Table 3.1. When different values were used, they are given in the figure legends.

Results

One Dimensional Simulations

When given an initial square pulse of calcium this model produced a travelling wave of calcium having wave speed of ~34 μm/s (figure 3.1) and amplitude of 1.5 μM. (Here the term amplitude refers to the maximum concentration of the travelling wave.) Experimental measurements of the wave speed range from 10-25 μm/s in the oocyte (Girard et al., 1992; Lechleiter and Clapham, 1992; Lechleiter et al., 1991; Parker and Yao, 1991; Busa and Nuccitelli, 1985). Temporal oscillations of the cytosolic calcium concentration were still observed under the same conditions as described in Chapter 1.

The effects of varying various physiological parameters was studied. When the buffer concentration (number of total calcium binding sites) ($[P_{total}]$) was raised the amplitude of the calcium wave decreased as did the speed of the wave. Figure 3.2 shows that when $[P_{total}]$ is decreased to 105 mM from 120 mM the wave speed increases to ~53 μm/s and the amplitude increases to 2.5 μM.

Increasing the rate of calcium entry into the cytosol (q) or decreasing the pump rate out of the cytosol (k) both increases the wave speed and amplitude. When q is raised to 2.9×10^{-10} μmol/s the wave speed increases to ~45 μm/s and the amplitude increases to 2.0 μM (figure 3.3). Analogously,

decreasing the pump rate to 31.2 s^{-1} increases the wave speed to ~55 μm/s and increases the amplitude to 2.4 μM (figure 3.4). Decreasing the diffusion constant of calcium (D) decreases the wave speed of the calcium wave. Figure 3.5 shows travelling when D is 26 $\mu m^2 s^{-1}$. Notice that the wave speed is decreased to 26 μm/s while the amplitude is relatively unchanged.

Two Dimensional Simulations

The model was able to reproduce plane waves of elevated calcium (figure 3.6). Circular waves of elevated calcium originating from one or more foci (figure 3.7) were also simulated. Confocal fluorescent microscopy in Xenopus oocytes has been able to record images of plane wave, circular wave, and target patterns.

When two circular or plane waves collide they annihilate each other (figure 3.7). The model suggests that this is a result of a refractory period that follows the wave. In the refractory region of the cytosol the calcium is slightly elevated, but region cannot support a propagating wave. Once the level of calcium falls sufficiently a new wave can propagate. The refractory region is also seen in the one-dimensional model. The wave speed and amplitude of the simulations are comparable to that of the one dimensional simulations and lie in the physiological range.

Table 3.1

Parameter values for the model

Parameter		*Value*
C_m	=	$1\ \mu F\ cm^{-2}$
F	=	$96500\ coulombs(mol\ e^{-})^{-1}$
$\overline{g_{Ca}}$	=	$340\ \mu S\ cm^{-2}$
K_{diss}	=	$5\ \mu M$
k_{pump}	=	$69.8\ s^{-1}$
k	=	$42\ s^{-1}$
S	=	$6.16 \times 10^{-3}\ cm^2$
V_{cyt}	=	$5.84 \times 10^{-5}\ \mu l$
q	=	$2.92 \times 10^{-10}\ \mu mol\ s^{-1}$
P_{total}	=	$120\ \mu M$
k_{off}	=	$5\ s^{-1}$
k_{on}	=	$1\ \mu M^{-1}\ s^{-1}$
$[Ca]_{ER}$	=	$5000\ \mu M$
V_0	=	$12.9\ mV$
R	=	$8.314\ J°K^{-1}\ mole^{-1}$
T	=	$300\ K$
r	=	$600\ \mu m$
D	=	$40\ \mu m^2\ s^{-1}$

These parameters are used in the simulations unless otherwise stated.

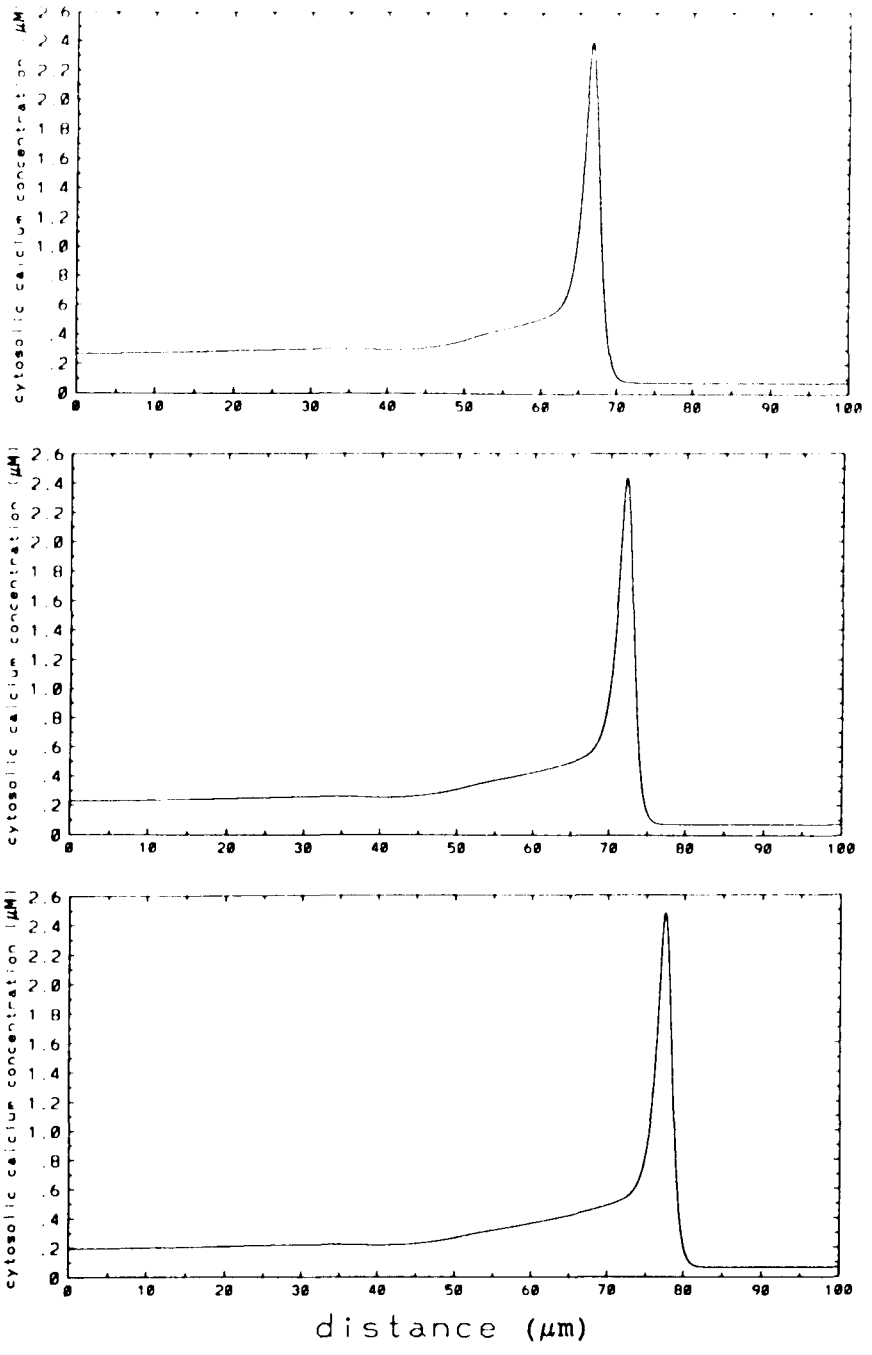

Figure 3.2. The effect of decreasing the buffer content in the cytosol. The wave speed increases to 53 μm/s and amplitude increases to 2.5 μM. The time interval between frames is 0.1 s. (P_{total} = 105 mM)

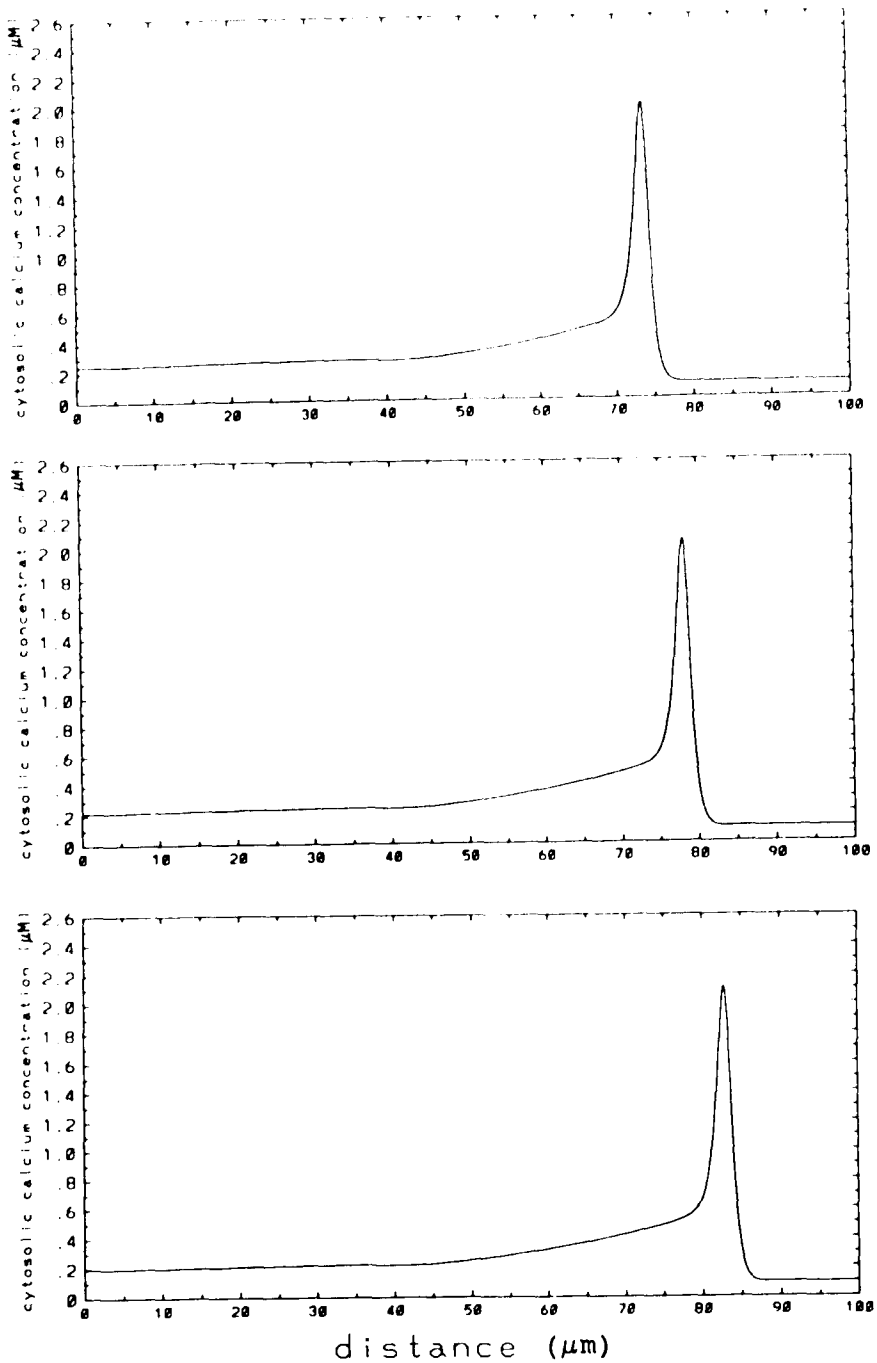

Figure 3.3. The effects of increasing the rate of calcium influx in the cell (q = 2.9 x 10^{-10} μmol/s). The wave speed increases to 45 μm/s and the amplitude increases to 2.0 μM. The time interval between frames is 0.1 s.

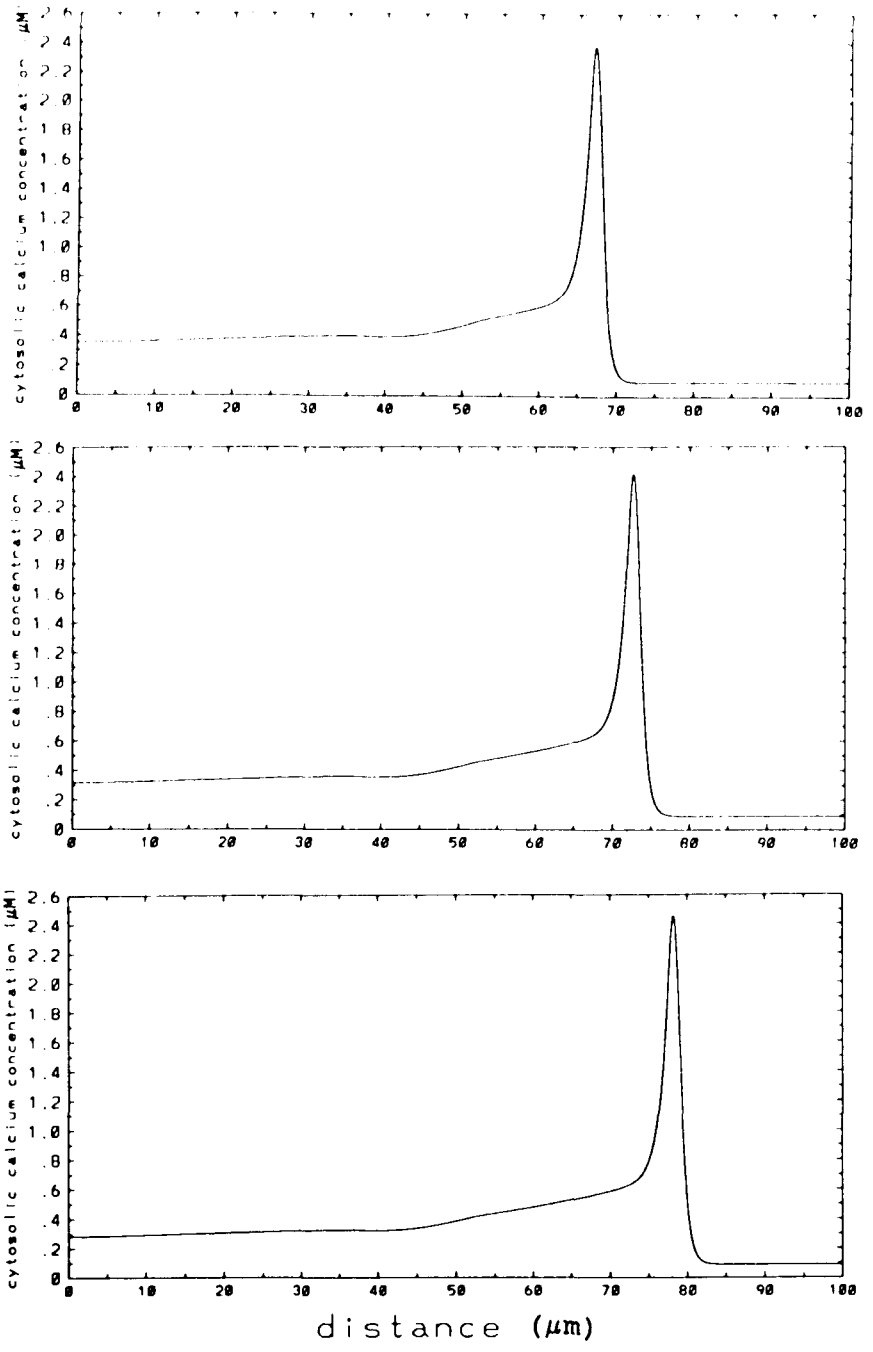

Figure 3.4. The effects of decreasing the pump rate out of the cytosol (k = 31.2 s^{-1}). The wave speed increases to 55 μm/s and the amplitude increases to 2.4 μM.

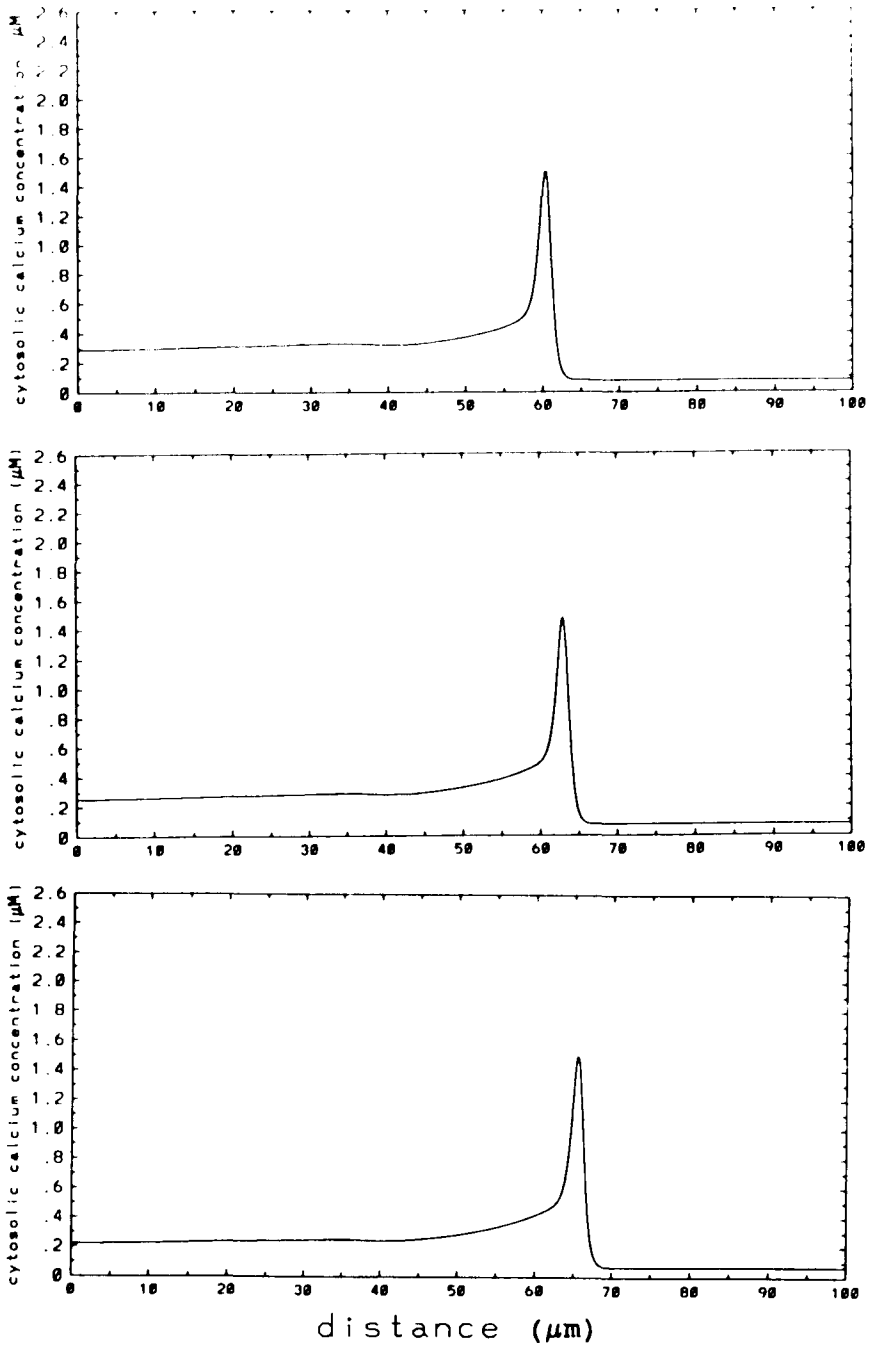

Figure 3.5. Decreasing the value of the effective diffusion constant (D) to 26 $\mu m^2 s^{-1}$ causes a decrease in the wave speed with little effect on the amplitude as compared to figure 3.1. The wave speed decreases to 26 $\mu m/s$. The time interval between frames is 0.1 s.

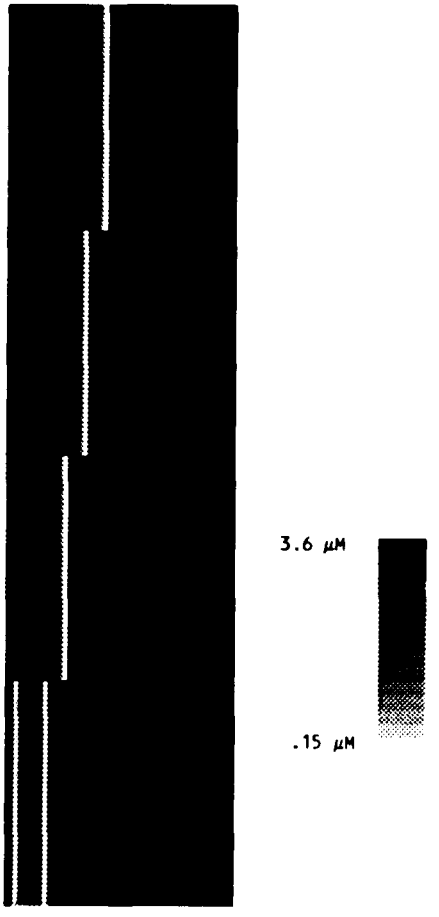

Figure 3.6. A plane wave propagating at a wave speed of ~34 μm/s. The red on the right of the scale bar is high calcium and the grey on the left side is low calcium. Notice that there is a refractory region of slightly elevated calcium that follows the wave. The region in 100 μm by 100 μm. The time interval between frames is 0.1 s.

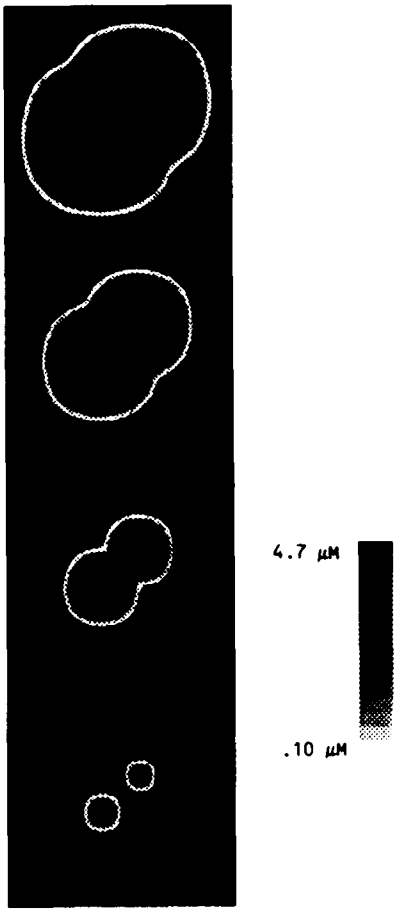

Figure 3.7. Two circular waves propagating out from a central locus in a 100 μm by 100 μm region. The locus toward the lower left corner was a 3 μm by 3 μm region of elevated calcium. The other locus measured 2 μm by 2 μm. The scale bar below the region shows high calcium concentration in red and low calcium concentration in gray. The time interval between frames is 0.1 s.

Discussion

In the cell, both calcium and buffer freely diffuse throughout the cytoplasm. The effective diffusion rate of calcium has been measured to be ~26 $\mu m^2 s^{-1}$ and increases to ~40 $\mu m^2 s^{-1}$ in the presence of fluorescent calcium dyes. The effective diffusion rate is small due to the large amount of buffering in the cytosol. The diffusion constant increases with the addition of dye because the dye moves more freely than the buffer proteins carrying bound calcium with it (M. Hanley, personal communication). This is confirmed by experimental observations. When using microscopy with fluorescent calcium binding dyes, the velocity of wave propagation was observed to be 18-25 $\mu m/s$ (Girard et al., 1992; Lechleiter and Clapham, 1992; Lechleiter et al., 1991; Parker and Yao, 1991). Busa and Nuccitelli (1985) measured the wave to be ~10 $\mu m/s$ using indirect methods. The dependence of the wave speed on D in the model supports this hypothesis. Figure 3.4 shows that with the experimentally estimated effective diffusion constant without calcium binding fluorescent dyes ($D = 26\ \mu m^2 s^{-1}$), the wave speed is ~26 $\mu m/s$. In the presence of the calcium binding dyes the estimated effective constant rises to $D = 40\ \mu m^2 s^{-1}$. The model predicts a wave speed of 34 $\mu m/s$. Further study of buffering influence on the effective diffusion constant is needed.

In both the one-dimensional and two-dimensional

simulations the calcium wave was assumed to start in a region, rather than a point source. In the one-dimensional model the wave was 1 μm long. The region was 2 μm by 2 μm and 3 μm by 3 μm in the two-dimensional model. This is supported by the work of Parker and Yao (1992) who observed that there was fine structure in the sources of the oscillation foci, having dimensions of a few microns rather that point sources.

The model shows that the propagation of calcium waves in *Xenopus* oocytes can be explained by diffusion of calcium triggering calcium-induced calcium release from the IP_3-insensitive store of the ER. There must be a source of calcium entry into the cytosol at the locus where the wave starts. We assume this is due to a steady release of calcium from the IP_3-sensitive store of the ER caused by the presence of IP_3. The rest of the region where the wave propagates can have a much lower basal level of calcium entry into the cytosol. The locus where the calcium entry is highest sets the frequency for the pulsating foci.

References

Blatter, L. A. and W. G. Wier. 1992. Agonist-induced $[Ca^{2+}]_i$ waves and Ca^{2+} release in mammalian vascular smooth muscle cells. *Am. J. Physiol.* 263:H576-H586.

Busa, W. B. and R. Nuccitelli. 1985. An elevated free cytosolic Ca^{2+} wave follows fertilization in eggs of the frog, *Xenopus laevis*. *J. Cell. Bio.* 100:1325-1329.

Girard, S., A. Lückoff, J. Lechleiter, J. Sneyd, and D. Clapham. 1992. Two-dimensional model of calcium waves reproduces the patterns observed in *Xenopus* oocytes. *Biophys. J.* 61:509-517.

Harootunian, A. T., J. P. Y. Kao, and R. Y. Tsien. 1988. Agonist-induced calcium oscillations in depolarized fibroblasts and their manipulation by photoreleased $Ins(1,4,5)P_3$, Ca^{++}, and Ca^{++} buffer. *Cold Spring Harbor Symposia on Quantitative Biology*. 53:935-943.

Ishide, N., M. Miura, M. Sakurai, and T. Takishima. 1992. Initiation and development of calcium waves in rat myocytes. *Am. J. Physiol.* 263:H327-H332.

Jacob, R., J. E. Merritt, T. J. Hallam, and T. J. Rink. 1988. Repetitive spikes in cytoplasmic calcium evoked by histamine in human endothelial cells. *Nature*. 335:40-45.

Jafri, M. S., S. Vajda, P. Pasik, and B. Gillo. 1992. A membrane model for cytosolic calcium oscillations: a study using *Xenopus* oocytes. *Biophys. J.* 63:235-246.

Lechleiter, J. D. and D. E. Clapham. 1992. Molecular mechanisms of intracellular calcium excitability in *X. laevis* oocytes. *Cell*. 69:283-294.

Lechleiter, J., S. Girard, E. Peralta, and D. Clapham. 1991. Spiral calcium wave propagation and annihilation in *Xenopus laevis* oocytes. *Science*. 252:123-126.

Meissner, G. 1983. Monovalent ion and calcium ion fluxes in sarcoplasmic reticulum. *Molecular and Cellular Biochemistry*. 55:65-82.

Nathanson, M. H., P. J. Padfield, A. J. O'Sullivan, A. D. Burgstahler, and J. D. Jamieson. 1992. Mechanism of Ca^{2+} wave

propagation in pancreatic acinar cells. *J. Biol. Chem.* 267:18118-18121.

Neylon, C. B., J. Hoyland, W. T. Mason, and R. F. Irvine. 1990. Spatial dynamics of intracellular calcium in agonist-stimulated vascular smooth muscle cells. *Am. J. Physiol.* 259:C675-C686.

Parker, I. and Y. Yao. 1991. Regenerative release of calcium from functionally discrete subcellular stores by inositol trisphosphate. *Proc. R. Soc. Lond. B.* 246:269-274.

Rawlings, S. R> D. J> Berry, and D. A. Leong. 1991. Evidence for localized calcium mobilization and influx in single rat gonadotropes. *J. Cell. Biol.* 266:22755-22760.

Tamakatsu, T. and W. G. Wier. 1990a. Calcium waves in mammalian heart: quantification of origin, magnitude, waveform, and velocity. *FASEB.* 4:1519-1525.

Tamakatsu, T. and W. G. Wier. 1990b. High temporal resolution video imaging of intracellular calcium. *Cell Calcium.* 11:111-120.

Chapter Four

Abstract

Detailed description of the analytic calculations contained in Chapters 1 and 3 are given in this section. The section begins with the reduction of the model given in Chapter 1 to a dimensionless system, followed by a bifurcation analysis the parameters. Next, this chapter describes the simplification of the one dimensional model presented in Chapter 3 to a piecewise linear model and finds a solution for a travelling wave solution. A comparison of the mathematical properties of this model to the model by Goldbeter and co-workers (1990) is made.

Introduction

Several models of cytosolic calcium oscillations have been proposed recently. They attempt to clarify the underlying physiological mechanisms behind this phenomenon. They have been described earlier in this dissertation. A mathematical analysis of the model by Goldbeter and co-workers has been performed by Sneyd and co-workers (1992). Those results will be compared to those found here. The analytical work presented here provides the ground work for the numerical simulations presented in Chapters 1-3.

Reduction of the membrane model to a dimensionless system.

Consider the system described in Chapter 1

$$\frac{d[Ca]_{cyt}}{dt} = \frac{I_{Ca}}{2FV_{cyt}} - k_{pump}[Ca]_{cyt} + \frac{q}{V_{cyt}} - k[Ca]_{cyt} + k_{off}([P_{total}] - [P]) - k_{on}[Ca]_{cyt}[P] \quad (1)$$

$$\frac{d[P]}{dt} = k_{off}([P_{total}] - [P]) - k_{on}([Ca]_{cyt}[P]) \quad (2)$$

$$SC_m\frac{dV}{dt} = I_{Ca} - 2FV_{cyt}k_{pump}[Ca]_{cyt} \quad (3)$$

where

$$I_{Ca} = g_{Ca}(E_{Ca} - V) \quad (4)$$

and

$$E_{Ca} = \frac{RT}{zF}\ln\left(\frac{[Ca]_{ER}}{[Ca]_{cyt}}\right) \quad (5)$$

and

The system (equations 1-6) will now be reduced to

$$g_{Ca} = \overline{g_{Ca}} S \frac{\left(\frac{[Ca]_{cyt}}{K_{diss}}\right)^2}{1 + \left(\frac{[Ca]_{cyt}}{K_{diss}}\right)^2}. \tag{6}$$

dimensionless form. Letting

$$\begin{aligned} u &= \frac{[Ca]_{cyt}}{K_{diss}}, \\ v &= \frac{V}{V_0}, \\ w &= \frac{P}{[P_{total}]}, \\ \tau &= \frac{t}{t_0}, \end{aligned} \tag{7}$$

the system reduces to

$$\frac{du}{d\tau} = f(u,v) + \mu - \beta_1 u + g(u,w) \tag{8}$$

$$\delta_1 \frac{dv}{d\tau} = f(u,v) \tag{9}$$

$$\delta_2 \frac{dw}{d\tau} = g(u,w) \tag{10}$$

where

$$f(u,v) = \alpha \frac{u^2}{1+u^2}(\sigma(\Gamma - \ln(u)) - v) - \beta_2 u \qquad (11)$$

$$g(u,w) = \pi_1(1-w) - \pi_2 u w \qquad (12)$$

and

$$\alpha = \frac{S\overline{g_{Ca}}V_0 t_0}{2FV_{cyt}K_{diss}} \qquad \beta_1 = kt_0 \qquad \beta_2 = k_{pump}t_0$$

$$\mu = \frac{qt_0}{K_{diss}V_{cyt}} \qquad \pi_1 = \frac{K_{off}[P_{total}]\,t_0}{K_{diss}} \qquad \pi_2 = k_{on}[P_{total}]\,t_0 \qquad (13)$$

$$\delta_1 = \frac{SC_mV_0}{2fV_{cyt}K_{diss}} \qquad \delta_2 = \frac{[P_{total}]}{K_{diss}}.$$

This next section studies the properties of the system described in Chapter 3.

Steady state analysis

Consider the equilibrium state where

$$\frac{du}{d\tau} = 0$$
$$\frac{dv}{d\tau} = 0 \qquad (14)$$
$$\frac{dw}{d\tau} = 0$$

We get

$$\begin{aligned} g(u^*, w^*) &= 0 \\ f(u^*, v^*) &= 0 \\ \mu - \beta_1 u^* &= 0 \end{aligned} \tag{15}$$

then the steady state values u^*, v^*, and w^* of u, v, and w, are

$$\begin{aligned} u^* &= \frac{\mu}{\beta_1} \\ v^* &= \sigma(\Gamma - \ln(u^*)) - \frac{\beta_2}{\alpha}\frac{1 + u^{*2}}{u^*} \\ w^* &= \frac{\pi_1}{\pi_1 + \pi_2 u^*} \end{aligned} \tag{16}$$

Bifurcation Analysis

In the system consisting of equations 9-12, the stability of the system depends on the equation

$$H = -\beta_1 + f_u(u^*, v^*) + g_u(u^*, w^*) + \frac{1}{\delta_1} f_v(u^*, v^*) + \frac{1}{\delta_2} g_z(u*, w^*) \tag{17}$$

Solving for the roots of the equation H = 0 as a function of a chosen parameters will find the bifurcation points for that parameter. The parameters μ and β_1 are two such parameters. When μ is increased or β_1 is decreased a Hopf bifurcation

point is approached. When μ is decreased or β_1 is increased a homoclinic point is approached. Figures 4.1 and 4.2 show the graphs of H as a function of μ and β_1, respectively. Thus, the quantity μ - ß1u serves as a bifurcation parameter. As this quantity increases, a Hopf bifurcation point is crossed and the oscillations cease. As the quantity decreases a homoclinic point is approached.

Equation (13) gives the physiological parameters that comprise μ and β_1. In terms of the physiology, as the calcium entry (q) increases the oscillations decrease in amplitude and increase in frequency. The oscillations cease when a Hopf bifurcation is crossed at $q = 3.36 \times 10^{-10}$ μmol/s. As q approaches zero the amplitude of the oscillations gets large as does the period between oscillations. As the pump rate out of the cytosol (k) increases a Hopf bifurcations is crossed. The oscillations increase in frequency and decrease in amplitude as k is decreases toward the bifurcation point of $k = 17.7$ s^{-1}.

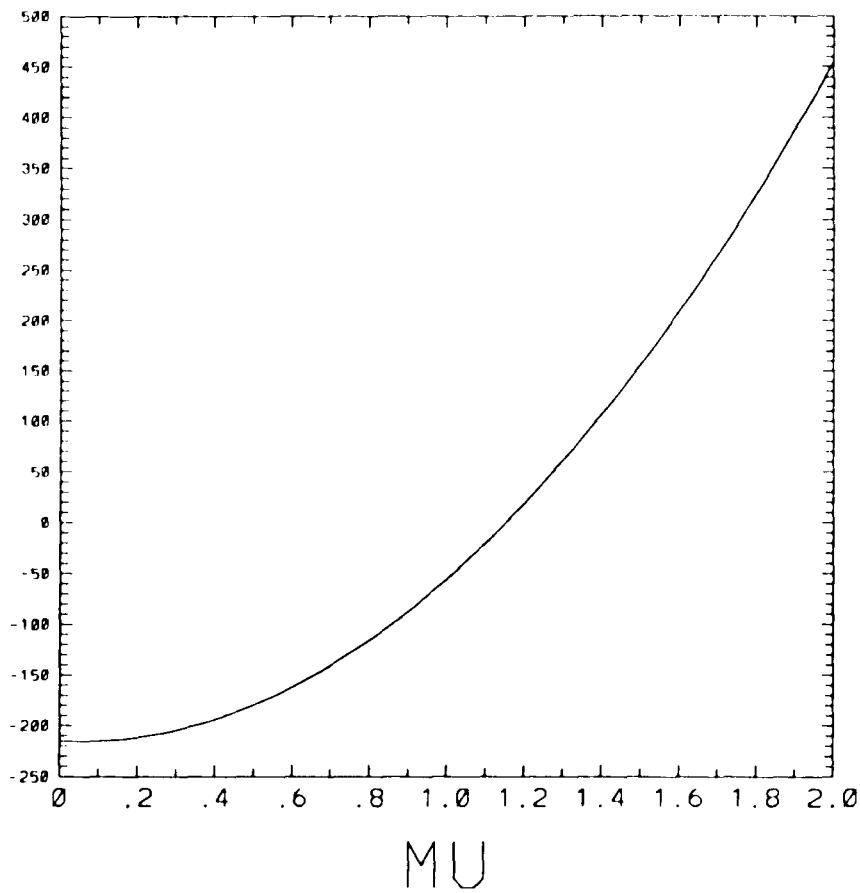

Figure 4.1. A plot of the H as a function of μ. The bifurcation point for the parameter μ occurs at $\mu = 1.15$ when $H = 0$. When $H < 0$ the oscillations occur.

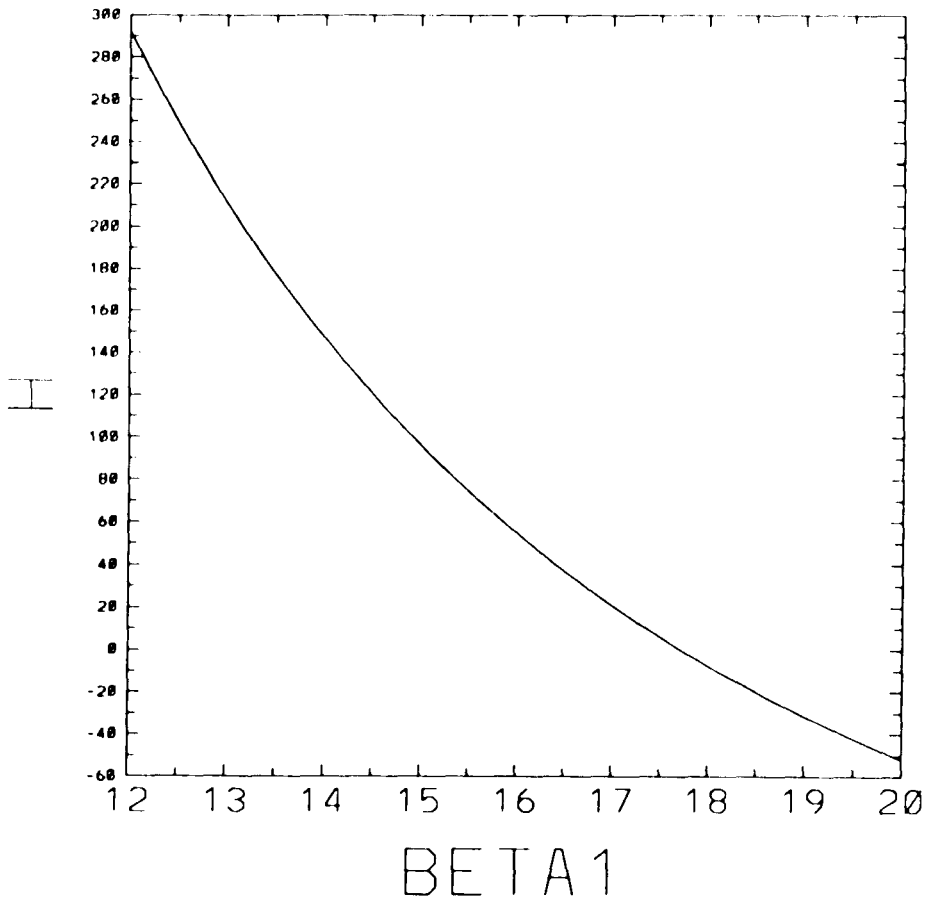

Figure 4.2. A plot of H as a function of β_1. The bifurcation point occurs at $\beta_1 = 17.7$ when $H = 0$. When $H < 0$ the oscillations occur.

Piecewise linear analysis of the system

In this section the system of equations governing the spatial wave case treated in Chapter 3 is analyzed. The dimensionless system of equations (8-12) is reduced to a piecewise linear system using the method developed by Peskin (1986). The equations governing t the system with diffusion are as follows:

$$\begin{aligned} \epsilon \frac{du}{d\tau} &= f(u,v) + \mu - \beta_1 u + g(u,w) + \epsilon^2 D \frac{d^2u}{dx^2} \\ \delta_1 \frac{dv}{d\tau} &= f(u,v) \\ \delta_2 \frac{dw}{d\tau} &= g(u,w) \end{aligned} \qquad \textbf{(18)}$$

The ϵ in front of the $\frac{du}{dt}$ makes explicit the fact that u varies rapidly compared to v. The ϵ^2 in front of the $\frac{d^2u}{dx^2}$ arises from the appropriate selection of length (l) to scale x, that is, $\epsilon = \frac{\sqrt{t_0}}{l}$ so that $\epsilon^2 D$ is dimensionless. Since δ_2 is large compared to δ_1 (24 and 1.41 respectively) we can assume that w is fast compared to u and v. Thus it is always

at equilibrium, that is,

$$\delta_2 \frac{dw}{d\tau} = g(u,w) = 0 \qquad (19)$$

Thus the system becomes

$$\frac{du}{d\tau} = f(u,v) + \mu - \beta_1 x \qquad (20)$$

$$\delta_1 \frac{dv}{d\tau} = f(u,v) \qquad (21)$$

The function f(u,v) describes the net flux of calcium across the ER membrane. We will make a piecewise linear approximation of the function f(u,v) called $\bar{f}(u,v)$. When f(u,v) (f(u,v) > 0) is positive the net calcium flux is out of the ER into the cytosol. During this phase, $\bar{f}(u,v) = f^+$ where f^+ is a constant. When the net calcium flux is into the ER, that is, when f(u,v) < 0, f(u,v) = f^-. The dependence of $\bar{f}(u,v)$ on u is included in the new function since the value of u determines in which phase $\bar{f}(u,v)$ lies.

In order to get a good piecewise linear approximation for f(u,v), the limiting behavior of f(u,v) is used to determine the values for f^+ and f^-. The variable u can be rescaled by its maximal value so that u lies between 0 and 1 (u can never be negative).

$$\lim_{u\to 1} f(u,v) = \sigma\Gamma - \frac{2\beta_2}{\alpha} - v \qquad (22)$$

$$\lim_{u\to 0} f(u,v) = \infty$$

Since the limit as u approaches 0 is undefined, consider the limit as u approaches u_ϵ where $1 \gg u_\epsilon > 0$. Then

$$\lim_{u\to u_\epsilon} f(u,v) = \sigma \ln(u_\epsilon) - \frac{\beta_2}{\alpha u_\epsilon} - v \qquad (23)$$

The function $\bar{f}(u,v)$ is now determined.

$$\bar{f}(u,v) = \begin{cases} f^+ - v \\ f^- - v \end{cases} = \begin{cases} \sigma\Gamma - \dfrac{2\beta_2}{\alpha} - v & u > a \\ \sigma \ln(u_\epsilon) - \dfrac{\beta_2}{\alpha u_\epsilon} - v & u < a \end{cases} \qquad (24)$$

Figure 4.3 shows a comparison of f and $\bar{f}(u,v)$.

Travelling wave solution

Using the substitution z = x + cτ, the system (17) can be converted into an ordinary differential equation in one variable z. The new system is

$$\begin{aligned} \epsilon^2 D u'' - c\epsilon u' + \mu - \beta_1 u + \bar{f}(u,v) &= 0 \\ \delta_1 c v' &= \bar{f}(u,v) \end{aligned} \tag{25}$$

where

$$\bar{f}(u,v) = \begin{cases} f^- - v & u<a \\ f^+ - v & u>a \end{cases} \tag{26}$$

In order to remove the explicit dependence on u, define z so that u(0)=a and define $u(z_1)=a$. Then

$$\bar{f}(u,v) = \begin{cases} f^- - v & z<0 \\ f^+ - v & 0<z<z_1 \\ f^- - v & z>z_1 \end{cases} \tag{27}$$

The solution to the differential equation for v given in

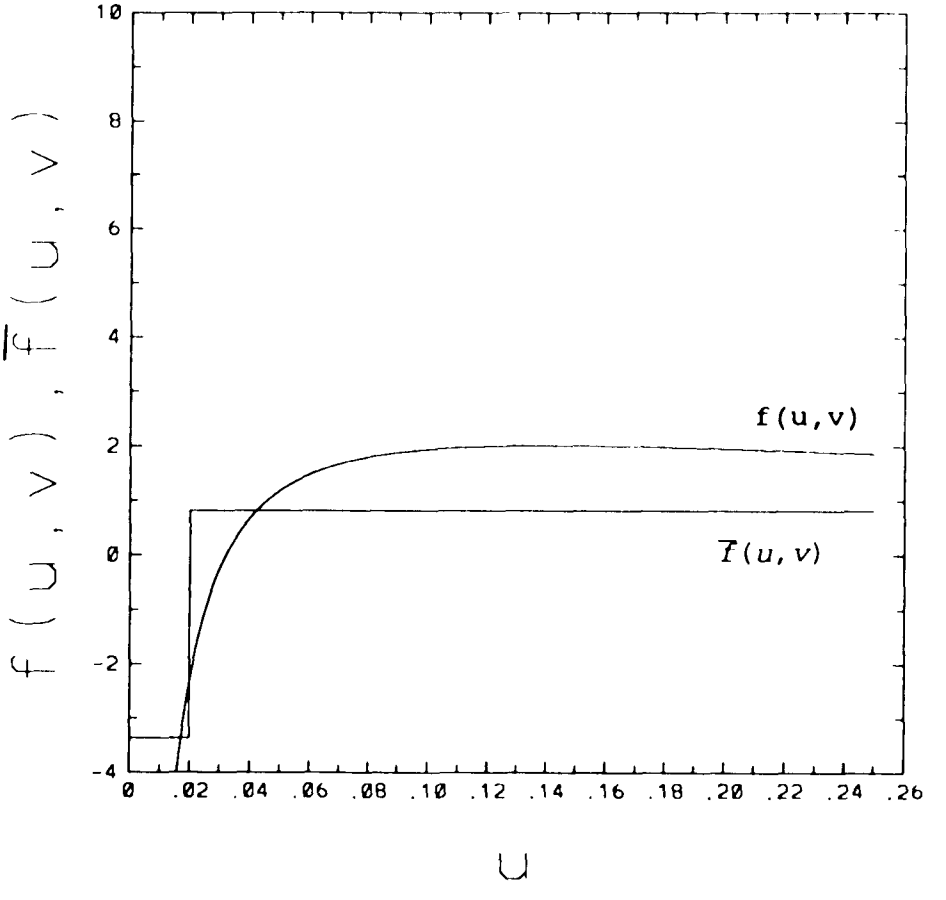

Figure 4.3. The functions f(u,v) and $\bar{f}(u,v)$ are compared. $\bar{f}(u,v)$ is the piecewise linear approximation for f(u,v).

equation (24) is

$$v = \begin{cases} f^- & z<0 \\ (f^- - f^+)e^{\lambda_1 z} + f^+ & 0<z<z_1 \\ ((f^- - f^+)e^{\lambda_1 z} + f^+)(f^- e^{\lambda_1 (z - z_1)}) & z_1<z \end{cases} \qquad (30)$$

where $\lambda_1 = -1/\delta c$. Then the solution for u is

$$u = \begin{cases} f^- + A_2 e^{\lambda_2 z} & z<0 \\ B_0 + B_1 e^{\lambda_1 z} + B_2 e^{\lambda_2 z} + B_3 e^{\lambda_1 z} & 0<z<z_1 \\ C_0 + C_1 e^{\lambda_1 (z-z_1)} + C_3 e^{\lambda_1 z} & z_1<z \end{cases} \qquad (31)$$

where A_2, B_0, B_1, B_2, B_3, C_0, C_1, and C_3 are constants. The constants can be derived using equation 25 and 29.

Case I $0<z<z_1$

Let

$$u = B_0 + B_1 e^{\lambda_1 z}$$
$$v = (f^- - f^+)e^{\lambda_1 z} + f^+ \qquad (32)$$

then

$$B_0 = \frac{\mu}{\beta_1} \qquad B_1 = \frac{f^- - f^+}{\epsilon^2 D\lambda_1^2 + c\epsilon\lambda_1 - \beta_1} \tag{33}$$

Case II $z_1 < z$

Let

$$\begin{aligned} u &= C_0 + C_1 e^{\lambda_1 (z - z_1)} \\ v &= ((f^- - f^+) e^{\lambda_1 z} + f^+)(f^- e^{\lambda_1 (z - z_1)}) \end{aligned} \tag{34}$$

then

$$C_0 = \frac{\mu + f^-}{\beta_1} \qquad C_1 = \frac{f^-((f^- - f^+) e^{\lambda_1 z} + f^+)}{\epsilon^2 D\lambda_1^2 + c\epsilon\lambda_1 - \beta_1} \tag{35}$$

To find the six remaining constants A_2, B_2, B_3, C_3, c, and z_1 constants, the six boundary conditions must be used. The boundary conditions are

$$\begin{aligned} u(0^-) &= u(0^+) = a \\ u(z_1^-) &= u(z_1^+) = a \\ u'(0^-) &= u'(0^+) \\ u'(z_1^-) &= u'(z_1^+) \end{aligned} \tag{36}$$

yielding

$$a = A_2 - f$$
$$a = B_0 + B_1 + B_2 + B_3 \qquad (37)$$

at z = 0, and

$$a = B_0 + B_1 e^{\lambda_1 z_1} + B_2 e^{\lambda_2 z_1} + B_3 e^{\lambda_3 z_1}$$
$$a = C_0 + C_1 + C_3 e^{\lambda_3 z_1} \qquad (38)$$
$$B_1\lambda_1 e^{\lambda_1 z_1} + B_2\lambda_2 e^{\lambda_2 z_1} + B_3\lambda_3 e^{\lambda_3 z_1} = C_1 + C_3\lambda_3 e^{\lambda_3 z_1}$$

If c and z_1 are known then the equations in (35) and (36) form a linear system.

To obtain analytical expressions for the constants, consider the limit as $\epsilon \to 0$. Then $\lambda_2 \to 0$ and $\lambda_3 \to 0$. Let

$$-R = \frac{\lambda_2}{\lambda_3} = \frac{1 + \sqrt{1 + \frac{4\beta_1 D}{c^2}}}{1 - \sqrt{1 + \frac{4\beta_1 D}{c^2}}} \qquad (37)$$

which does not depend on ϵ. The known constants B_0, B_1, C_0, and C_1 become

$$B_0 = \frac{\mu}{\beta_1} \qquad B_1 = \frac{f^- - f^*}{-\beta_1}$$
$$C_0 = \frac{\mu + f^-}{\beta_1} \qquad C_1 = \frac{f^-((f^- - f^*)e^{\lambda_1 z_1} + f^*)}{-\beta_1} \tag{38}$$

Let

$$\overline{B_2} = B_2 e^{\lambda_3 z_1}$$
$$\overline{C_3} = C_3 e^{\lambda_3 z_1} \tag{39}$$

At z = 0, the boundary conditions become

$$a = A_2 - f^-$$
$$a = B_0 + B_1 + B_2 + B_3 \tag{40}$$
$$A_2 = B_2 - B_3 \frac{1}{R}$$

and at $z = z_1$ they become

$$a = B_0 + B_1 e^{\lambda_1 z_1} + \overline{B_2}$$
$$a = C_0 + C_1 + \overline{C_3} \tag{41}$$
$$\overline{B_2} = -\overline{C_3} \frac{1}{R}$$

$\overline{B_2}$ is finite since all other terms in the first equation of (41) are finite which forces $B_2 \to 0$. The boundary conditions a z=0 become

$$\begin{aligned} a &= A_2 - f^- \\ a &= B_0 + B_1 + B_2 + B_3 \\ A_2 &= B_2 - B_3 \frac{1}{R} \end{aligned} \tag{42}$$

Using the new boundary conditions at z=0 (equations (42)), the constants A_2, B_3, and R are found.

$$\begin{aligned} A_2 &= a + f^- \\ B_3 &= \frac{a\beta_1 - \mu + f^- - f^+}{\beta_1} \\ R &= \frac{a\beta_1 - \mu + f^- - f^+}{\beta_1 (a + f^-)} \end{aligned} \tag{43}$$

Now that R is known, c can be found using equation (37).

$$c = \sqrt{\beta_1 D}\left(\sqrt{R} - \frac{1}{\sqrt{R}}\right) \tag{44}$$

Using the boundary conditions at $z=z_1$ the value of z_1 is found to be

$$z_1 = \frac{1}{\lambda_1} \ln\left[\frac{(1+R)(a\beta_1 - \mu) + f^-(f^* - 1)}{-(R+f^-)(f^- - f^*)}\right] \qquad (45)$$

Hence all the constants have been found. Figure 4.4 shows a plot of the solution in the limit as $\epsilon \to 0$. Figure 4.5 shows a plot for the full system solved numerically.

Conclusions

In this chapter, a dimensionless form of the membrane model was studied. It was shown that there is one Hopf bifurcation point for the parameter μ above which oscillations cease. When β_1 decreases below its Hopf bifurcation point oscillations also cease. The behavior of the model is controlled inversely by these two parameters such that increases in one can be offset by decreases in the other and vise versa. Changes in the parameters μ and β_1 away from the Hopf bifurcation in the oscillating regime, approach a homoclinic point.

In previous chapters, numerical simulations have shown that the membrane model (equations 1-6) is a excitable system,

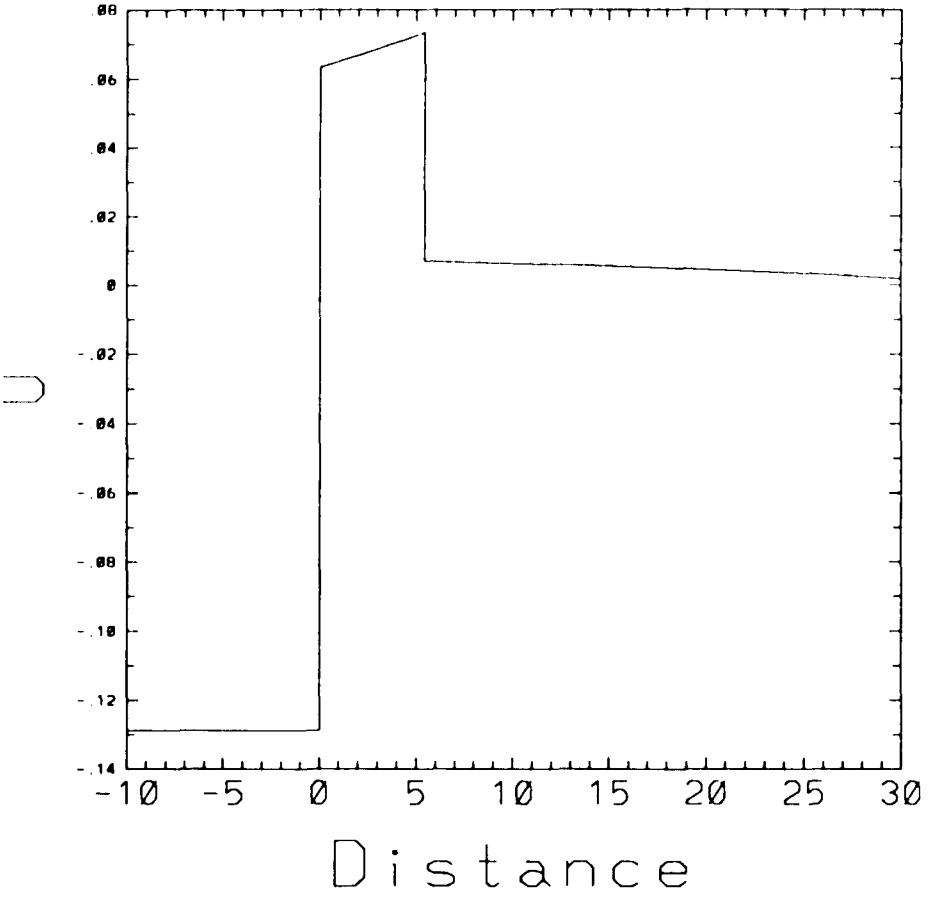

Figure 4.4. A graph for the solution of the piecewise linear solution in the limit as $\epsilon \to 0$. This is an approximation for the full system solved numerically in figure 4.5.

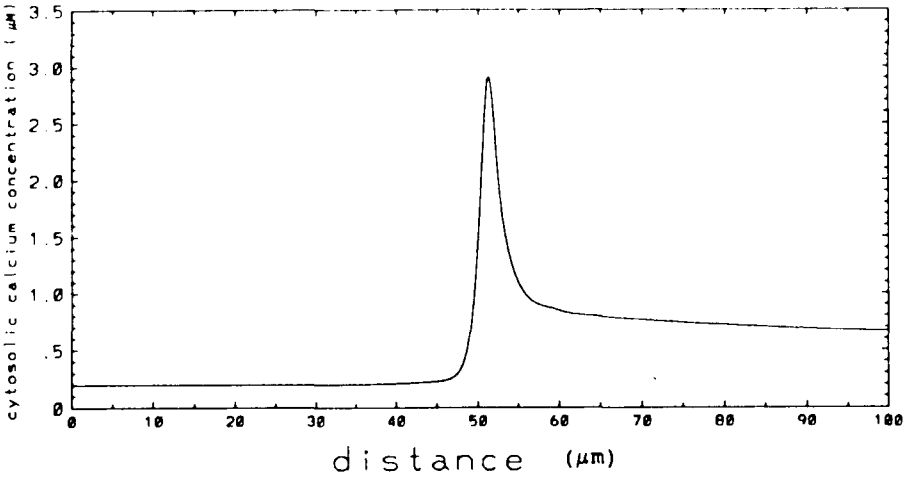

Figure 4.5. The solution of the full system solved numerically in Chapter 3.

that is, when given a sufficient rise in the nonlinear variable $[Ca]_{cyt}$ will support an even larger rise in $[Ca]_{cyt}$. When diffusion is added to the system the system supports a travelling pulse.

In this chapter, a piecewise linear approximation for the spatio-temporal model was proposed. A travelling wave solution was then constructed.

Recently, a mathematical analysis of the model by Goldbeter and co-workers (1990) was performed (Sneyd et al., 1992). Their model also supports travelling wave solutions and is excitable in the temporal case. Their model has two Hopf bifurcation points for their parameter describing calcium entry.

The physiological implication of this difference is that there is a minimum level of calcium entry below which oscillations do not occur. This feature also allows their model to produce changes in frequencies of oscillations with little change in amplitude.

Experimentally, results have been found where the amplitude of oscillations remains relatively constant with changes in frequencies and other results have show that the amplitude increase with decreases frequency of oscillations. Thus, for now both models are validated by the experimental results.

References

Goldbeter, A., G. Dupont, and M. J. Berridge. 1990. A minimal model for signal-induced Ca^{2+} oscillations and for their frequency encoding through protein phosphorylation. *Proc. Natl. Acad. Sci.* 87:1461-1465.

Jafri, M. S., S. Vajda, P. Pasik, and B. Gillo. 1992. A membrane model for cytosolic calcium oscillations: a study using *Xenopus* oocytes. *Biophys. J.* 63:235-246.

Peskin, C. S. 1976. *Partial Differential Equations in Biology*. Courant Institute of Mathematical Sciences. New York. 227 pp.

Sneyd, J., S. Girard, and D. Clapham. 1992. Calcium wave propagation by calcium-induced calcium release: an unusual excitable system. *Bull. Math. Biol.*

Conclusions

This dissertation has investigated the theory behind cytosolic calcium oscillations using numerical and analytical tools. In Chapter One, a basic membrane model was developed to elucidate the mechanism behind cytosolic calcium oscillations. In the model, calcium release into the cytosol causes a rise in cytosolic calcium. This rise precipitates calcium-induced calcium release from the ER through a calcium release channel. The rate of release will increase until it is offset by the action the membrane calcium pumps which reduce the cytosolic calcium concentration to its previous level. The process then repeats itself.

The model predicts that increasing the rate of calcium entry (q) into the cytosol will increase the frequency and decrease the amplitude of the oscillations. The work of my collaborator, Boaz Gillo supported this prediction. A search of the literature showed that a similar result was observed in fibroblasts and cardiac myocytes. The model made the additional prediction, which was not yet reported, that if the level of calcium entry is increased past a certain level the oscillations would cease. This was later confirmed by the publication of new experimental results in *Xenopus* oocytes and pancreatic acinar cells.

Mathematically this observed behavior is a result of a Hopf bifurcation in the parameter for calcium entry (q). As

q increases in the oscillatory parameter space, the Hopf bifurcation point is approached. After passing this point the oscillations cease.

The model also predicts that increasing the concentration of calcium binding proteins results in oscillations with lower frequency and amplitude. Later experimental work observed a similar dependence on buffering in pancreatic acinar cells injected with acetate which acts to bind calcium.

In Chapter Two, the model was enhanced to include the effects of counterions. The only quantitative data for counterion movement comes from electron microprobe analysis which gives the amounts of ions that cross the ER membrane via before and after concentrations. Using the ratio found for the movement of magnesium to the movement of calcium, a conductance was predicted for the counterions. The resulting simulations showed that the counterions caused little change in the calcium oscillations.

The model was able to reproduce qualitatively the experimental observation that the latency period before the oscillations start depends on the level of external agonist dose. The model suggests that calcium entry into the cytosol can account for changes in the latency period. Increases of the calcium entry rate, decreases the period of latency. The concentration of calcium binding can also effect the latency period. The latency period is dependent on the initial conditions. An increased calcium binding protein

concentration will lower the concentration and slow the increase in free calcium causing a longer latency period.

Thapsigargin has been found to be a potent inhibitor of the ER calcium pump. The model reproduces the effects of modulating rate of the calcium pump. When the pump rate (k) out of the cytosol is high there are infrequent spikes of calcium. As the pump rate decreases oscillations occur. Finally, after further decreases in the pump rate the oscillations cease.

Decreasing the pump rate out of the cytosol (but not into the calcium-induced calcium release compartment) has a similar effect as increasing q_{IP} (and q_0). Starting from an oscillating regime, when q_{IP} increases past a Hopf bifurcation point the oscillations cease. There is a homoclinic point at $q_{IP}=0$. The parameter k behaves in the opposite fashion. Decreasing the parameter k past a Hopf bifurcation point results in the end of oscillations. As k increases a homoclinic point is approached. Outside the oscillating region the oocyte is quiescent.

In the oocyte, an increased IP_3 concentration causes an increased calcium influx increases due to release from the IP_3-sensitive store. Thus, the frequency and amplitude of the calcium oscillations can be modulated by the response to hormones and neurotransmitters that evoke IP_3 production. Under natural conditions, the pump rate can be modulated in the oocyte by the amount of ATP present which would modulate

the oscillations. Decreasing the pump rate (k_{pump}) for calcium back into the IP_3-insensitive store of the ER causes peaks in the oscillations with longer recovery times.

Chapter Three predicts the properties of calcium propagation in the oocyte. In addition to signal encoding through the amplitude and frequency of oscillations locally, calcium waves propagate through the oocyte. Complex patterns are measured in the oocyte that have not been observed elsewhere. After a wave of elevated passes a region there is a refractory period in which the cell cannot sustain another wave in the region. In this refractory period the calcium is elevated over the resting calcium level. When the calcium level falls sufficiently the cell can once again support a wave in the region.

The model can simulate the calcium waves that have been observed in the oocyte. Numerical experiments provide some insight into the control of the waves. The model predicts that increasing the total amount of calcium binding protein ($[P_{total}]$) decreases the amplitude and speed of the travelling wave. Increasing rate of calcium entry (q) or decreasing the pump rate out of the cytosol (k) both increase the wave speed according to the simulations. Increasing the pump rate to refill the ER (k_{pump}) is predicted to increases the wave speed.

This model differs from other models in that it posits slightly different physiological principles than the other models. It is unique in its use of the ER membrane potential

that is experimentally indicated. It does not use inhibition of calcium release by diminished calcium binding inside the ER lumen as does the model by Goldbeter and co-workers. Physiological evidence shows that calcium release is independent of calcium ER luminal calcium. The membrane model uses a changes in the electrochemical gradient for calcium to alter the driving force of calcium through the channel. The membrane model also does not rely on oscillations in the IP_3 to cause calcium oscillations as does the molecular model of Meyer and Stryer. Calcium oscillations have been observed in cells loaded with a non-degradable analog of IP_3. It is a two pool model for calcium oscillations that is based upon the mechanism of calcium-dependent calcium release triggered by IP_3 mediated release in response to an agonist.

Mathematically it differs from the other models in that there is only one Hopf bifurcation whereas the other model have two. This enables the membrane model to have a striking dependence of amplitude and frequency on the level of calcium entry. It however makes it difficult to reproduce the signal seen with an exponential decay of IP_3 concentration with time.

The work started in this study will be continued in various directions. One area that must be considered is the effect of calcium influx with a time course other than constant. When a cell is exposed to a dose of

neurotransmitter, the cytosolic concentration of IP_3 is not constant nor is it a simple step change.

Another area that will be studied is to make a whole cell model of calcium oscillations to integrate the different processes in the cell that regulate the cytosolic calcium concentration. The membrane model explicitly models the IP_3-insensitive store of the ER. A completely integrative model would also explicitly model the contributions of the IP_3-sensitive store, the calcium channels in the plasma membrane (if present), mitochondrial calcium uptake, and nuclear calcium regulation.

References

Ambler, S. K., P. Poenie, R. Y. Tsien, and P. Taylor. 1988. Agonist-stimulated oscillations and cycling of intracellular free calcium in individual cultured muscle cells. *J. Biol. Chem.* 263:1952-1959.

Baumann, O., B. Walz, A. V. Somlyo, and A. P. Somlyo. 1991. Electron probe microanalysis of calcium release and magnesion uptake by endoplasmic reticulum in bee photoreceptors. *Proc. Natl. Acad. Sci.* 88:741-744.

Benham, C. D. and T. B. Bolton. 1986. Spontaneous transient outward currents in single visceral and vascular smooth muscle cells of the rabbit. *J. Physiol.* 381:385-406.

Berridge, M. J., P. H. Cobbold, and K. S. R. Cuthbertson. 1988. Spatial and temporal aspects of cell signalling. *Phil. Trans. R. Soc. Lond. B.* 320:325-343.

Berridge, M. J., and R. F Irvine. 1989. Inositol phosphate and cell signalling. *Nature.* 341:197-205.

Blatter, L. A. and W. G. Wier. 1992. Agonist-induced $[Ca^{2+}]_i$ waves and Ca^{2+} release in mammalian vascular smooth muscle cells. *Am. J. Physiol.* 263:H576-H586.

Busa, W. B. and R. Nuccitelli. 1985. An elevated free cytosolic Ca^{2+} wave follows fertilization in eggs of the frog, *Xenopus laevis*. *J. Cell. Bio.* 100:1325-1329.

Cartaud, A., R. Ozon, M. P. Walsh, J. Haiech, and J. G. Demaille. 1980. *Xenopus Laevis* oocyte calmodulin in the process of meiotic maturation. *J. Biol. Chem.* 255:9404-9408.

Charbonneau, M. and R. D. Grey. 1984. The onset of activation responsiveness during maturation coincides with the formation of the cortical endoplasmic reticulum in oocytes of *Xenopus laevis*. *Developmental Biology.* 102:90-97.

Chay, T. R., and J. Keizer. 1983. Minimal model for membrane oscillations in the pancreatic ß-cell. *Biophys. J.* 42:181-190.

Darnell, J., H. Lodish, and D. Baltimore. 1990. *Molecular Cell Biology 2nd ed.* Scientific Americam Books. New York. 1105 pp.

Dascal, N., and R. Boton. 1990. Interaction between injected Ca^{2+} and intracellular Ca^{2+} stores in *Xenopus* oocytes. *FEBS.* 267:22-24.

Dascal, N., B. Gillo, and Y. Lass. 1985. Role of calcium mobilization in mediation of acetylcholine responses in *Xenopus laevis* oocytes. *J. Physiol.* 366:299-314.

Delesse, M. A. 1847. Procede mecanique pour determiner la composition des roches. *Comput. Rend. Acad. Sci.* 25:544-547.

DeLisle S., K. Krause, G. Denning, B. V. L. Potter, and M. J. Welsh. 1990. Effect of inositol trisphosphate and calcium on oscillation elevations of intracellular calcium in *Xenopus* oocytes. *J. Biol. Chem.* 265:11726-11730.

Dumont, J. N. 1972. Oogenesis in *Xenopus laevis* (Daudin). *J. Morphol.* 136:153-180.

Foskett, J. K., C. M. Roifman, and D. Wong. 1991. Activation of calcium oscillations by thapsigargin in parotid acinar cells. *J. Biol. Chem.* 266:2778-2782.

Foskett, J. K. and D. Wong. 1991. Free cytoplasmic Ca^{2+} concentration oscillations in thapsigargin treated parotid acinar cells are caffeine- and ryanodine-sensitive. *J. Biol. Chem.* 266:14535-14538.

Gandhi, C. R., and D. H. Ross. 1988. Characterization of a high-affinity Mg^{2+}-independent Ca^{2+}-ATPase from rat brain synaptosomal membranes. *J. Neurochem.* 50:248-256.

Gardiner, D. M. and R. D. Grey. 1983. Membrane junctions in *Xenopus* eggs: their distribution suggests a role in calcium regulation. *J. Cell Biol.* 96:1159-1163.

Gillo, B., Y. Lass, E. Nadler, and Y. Oron. 1987. The involvement of inositol 1,4,5-trisphosphate and calcium in the two-component response to acetylcholine in *Xenopus* oocytes. *J. Physiol.* 392:349-361.

Girard, S., A. Lückoff, J. Lechleiter, J. Sneyd, and D. Clapham. 1992. Two-dimensional model of calcium waves reproduce⌣ the patterns observed in *Xenopus* oocytes. *Biophys. J.* 61:509-517.

Goldbeter, A., G. Dupont, and M. J. Berridge. 1990. Minimal model for signal induced Ca^{2+} oscillations and for their frequency encoding through protein phosphorylation. *Proc. Natl. Acad. Sci. USA.* 87:1461-1465.

Gottwald, B. A., and G. Wanner. 1981. A reliable Rosenbrock-integrator for stiff differential equations. *Computing.* 26:335-357.

Gray, P. T. A. 1988. Oscillations of free cytosolic

calcium evoked by cholinergic and catecholaminergic agonists in rat parotid acinar cells. *J. Physiol. (London)*. 406:35-53.

Harootunian, A. T., J. P. Y. Kao, and R. Y. Tsien. 1988. Agonist-induced calcium oscillations in depolarized fibroblasts and their manipulation by photoreleased Ins(1,4,5)P_3, Ca^{++}, and Ca^{++} buffer. *Cold Spring Harbor Symposia on Quantitative Biology*. 53:935-943.

Ishide, N., M. Miura, M. Sakurai, and T. Takishima. 1992. Initiation and development of calcium waves in rat myocytes. *Am. J. Physiol*. 263:H327-H332.

Jacob, R., J. E. Merritt, T. J. Hallam, and T. J. Rink. 1988. Repetitive spikes in cytoplasmic calcium evoked by histamine in human endothelial cells. *Nature*. 335:40-45.

Jafri, M. S., S. Vajda, P. Pasik, and B. Gillo. 1992. A membrane model for cytosolic calcium oscillations: a study using *Xenopus* oocytes. *Biophys. J*. 63:235-246.

Joseph, S. K. and J. R. Williamson. 1986. Characteristics of inositol trisphosphate-mediated Ca^{2+} release from permeabilized hepatocytes. *J. Biol. Chem*. 261:14658-14664.

Kuba, K. and Takeshita. 1981. Simulation of intracellular Ca^{2+} oscillations in a sympathetic neurone. *J. Theor. Biol*. 93:1009-1031.

Lai, F. A., H. P. Erickson, E. Rosseau, Q. Liu, and G. Meissner. 1988. Purification and reconstitution of the calcium release channel from skeletal muscle. *Nature*. 331:315-319.

Lakatta, E. G., M. C. Capogrossi, A. A. Kort, and M. D. Stern. 1986. Spontaneous myocardial calcium oscillations: overview with emphasis on ryanodine and caffeine. *Fed. Proc*. 44:2977-2983.

Lavenda, B., G. Nicolis, and M. Herschkowitz-Kaufman. 1971. Chemical instabilities and relaxation oscillations. *J. Theor. Biol*. 32:283-292.

Lechleiter, J. D. and D. E. Clapham. 1992. Molecular mechanisms of intracellular calcium excitability in *X. laevis* oocytes. *Cell*. 69:283-294.

Lechleiter, J., S. Girard, E. Peralta, and D. Clapham. 1991. Spiral calcium wave propagation and annihilation in *Xenopus laevis* oocytes. *Science*. 252:123-126.

Lefever, R. and G. Nicolis. 1970. Chemical instabilities

and sustained oscillations. *J. Theor. Biol.* 30:267-284.

Lin N. Y., Y. F Liu, W. Y. Cheung. 1974. Cyclic 3':5'-nucleotide phosphodiesterase: purification, characterization, and active form of the protein activator from bovine brain. *J. Biol. Chem.* 249:4943-4954.

Meissner, G., E. Darling, and J. Eveleth. 1986. Kinetics of rapid Ca^{2+} release by sarcoplasmic reticulum. effects of Ca^{2+}, Mg^{2+}, and adenine nucleotides. *Biochem.* 25:236-244.

Meissner, G. 1983. Monovalent ion and calcium ion fluxes in sarcoplasmic reticulum. *Molecular and Cellular Biochemistry.* 55:65-82.

Meyer, T., and L. Stryer. 1988. Molecular model for receptor-stimulated calcium spiking. *Proc. Natl. Acad. Sci. USA.* 85:5051-5055.

Mobley, B. A., and B. R. Eisenberg. 1975. Sizes of components in from skeletal muscle measured by methods of stereology. *J. Gen. Physiol.* 66:31-45.

Nathanson, M. H., P. J. Padfield, A. J. O'Sullivan, A. D. Burgstahler, and J. D. Jamieson. 1992. Mechanism of Ca^{2+} wave propagation in pancreatic acinar cells. *J. Biol. Chem.* 267:18118-18121.

Neylon, C. B., J. Hoyland, W. T. Mason, and R. F. Irvine. 1990. Spatial dynamics of intracellular calcium in agonist-stimulated vascular smooth muscle cells. *Am. J. Physiol.* 259:C675-C686.

Oetliker, H. 1982. An appraisal of the evidence for a sarcoplasmic reticulum membrane potential and its relation to calcium release in skeletal muscle. *Journal of Muscle Research and Cell Motility.* 3:247-272.

Ogawa, Y., N. Kurebayashi, A. Irimajiri, and T. Hanai. 1981. Transient kinetics for Ca uptake by fragment sarcoplasmic reticulum from bullfrog skeletal muscle with reference to the rate of relaxation in living muscle. *Adv. Physiol. Sci.* 5:417-435.

Okada, Y., W. Tsuchiya, and T. Yada. 1982. Calcium channel and calcium pump involved in oscillatory hyperpolarizing responses of L-strain mouse fibroblasts. *J. Physiol.* 327:440-461.

Osada, S., S. Saji, T. Nakamura, and Y. Nozawa. 1992. Cytosolic calcium oscillations induced by hepatocyte growth factor (HGF) in single fura-2-loaded cultured hepatocytes:

effects of extracellular calcium and protein kinase C. *Biochem. et Biophys. Acta.* 1135:229-232.

Osipchuk, Y. V., M. Wakui, D. I. Yule, D. V. Gallacher, and O. H. Petersen. 1990. Cytoplasmic Ca^{2+} oscillations evoked by receptor stimulation, G-protein activation, internal application of inositol trisphosphate of Ca^{2+}: simultaneous microfluorometry and Ca^{2+} dependent Cl^- current recording in single pancreatic acinar cells. *EMBO J.* 9:697-704.

Parker, I. and I. Ivorra. 1990. Localized all-or-none calcium liberation by inositol trisphosphate. *Science.* 250:977-979.

Parker, I. and R. Miledi. 1986. Changes in intracellular calcium and in membrane currents evoked by injection of inositol trisphosphate into *Xenopus* oocytes. *Proc. R. Soc. Lond. B.* 228:307-315.

Parker, I., K. Sumikawa, and R. Miledi. 1987. Activation of a common effector system by different brain neurotransmitter receptors in *Xenopus* oocytes. *Proc. R. Soc. Lond.* 231:37-45.

Parker, I. and Y. Yao. 1991. Regenerative release of calcium from functionally discrete subcellular stores by inositol trisphosphate. *Proc. R. Soc. Lond. B.* 246:269-274.

Peskin, C. S. 1976. *Partial Differential Equations in Biology.* Courant Institute of Mathematical Sciences. New York. 227 pp.

Petersen, C. C. H., E. C. Toescu, and O. H. Petersen. 1991. Different patterns of receptor-activated cytoplasmic Ca^{2+} oscillations in single pancreatic acinar cells: dependence on receptor type, agonist concentration and intracellular Ca^{2+} buffering. *EMBO J.* 10:527-533.

Prigogine, I. 1968. *Introduction to Thermodynamics of Irreversible Processes.* 3rd ed. Wiley Interscience. New York.

Rawlings, S. R> D. J> Berry, and D. A. Leong. 1991. Evidence for localized calcium mobilization and influx in single rat gonadotropes. *J. Cell. Biol.* 266:22755-22760.

Robertson, S. P., J. D. Johnson, and J. D. Potter. 1981. The time-course of Ca^{2+} exchange with calmodulin, troponin, parvalbumin, and myosin in response to transient increases in Ca^{2+}. *Biophys. J.* 34:559-569.

Rooney, T. A., D. C. Renard, E. J. Sass, and A. P.

Thomas. 1991. Oscillatory cytosolic calcium waves independent of stimulated inositol 1,4,5-trisphosphate formation in hepatocytes. *J. Biol. Chem.* 266:12272-12282.

Rooney, T. A. and A. P. Thomas. 1991. Organization of intracellular calcium signals generated by inositol lipid-dependent hormones. *Pharmac. Ther.* 49:223-237.

Rooney, T. A., E. J. Sass, and A. P. Thomas. 1989. Characterization of cytosolic calcium oscillations induced by phenylephrine and vasopressin in single fura-2-loaded hepatocytes. *J. Biol. Chem.* 264:17131-17141.

Sagara, Y. and G. Inesi. 1991. Inhibition of the scrcoplasmic reticulum Ca^{2+} transport ATPase by thapsigargin at subnanomolar concentrations. *J. Biol. Chem.* 266:13503-13506.

Schlegal, W., B. P. Winger, P. Mollard, F. Wuarin, G. R. Zahnd, C. B. Wolheim, and B. Dufy. 1987. Oscillations of cytosolic Ca^{2+} in pituitary cells due to action potentials. *Nature (London)*. 329:719-721.

Seifert, P. 1987. Computational experiments with algorithms for stiff ODEs. *Computing*. 163-176.

Sneyd, J., S. Girard, and D. Clapham. 1992. Calcium wave propagation by calcium-induced calcium release: an unusual excitable system. *Bull. Math. Biol.*

Snyder, P. M., K. H. Krause, and M. J. Welsh. 1988. Inositol Trisphophate isomers, but not inositol 1,3,4,5 tetrakisphosphate, induces calcium influx in *Xenopus laevis* oocytes. *J. Biol. Chem.* 263: 11048-11051.

Somlyo, A. V., H. Gonzalez-Serratos, H. Shuman. G. McClellan, and A. P. Somlyo. 1981. Calcium release and ionic changes in the sarcoplasmic reticulum of tetanized muscle: an electron-probe study. *J. Cell Biol.* 90:577-594.

Somogyi, R. and J. W. Stucki. 1991. Hormone-induced calcium oscillations in liver cells can be explained by a simple one pool model. *J. Biol. Chem.* 266:11068-11077.

Stephenson, D. G., I. R. Wendt, and Q. G. Forrest. 1981. Non-uniform ion distribution and electrical potential in sarcoplasmic regions of skeletal muscle fibres. *Nature.* 289:690-692.

Stern, M. D., M. C. Capogrossi, and E. G. Lakatta. 1988. Spontaneous calcium release from the sarcoplasmic reticulum in myocardial cells: mechanisms and consequences. *Cell*

Calcium. 9:247-258.

Swillens, S. and D. Mercan. 1990. Computer simulation of a cytosolic calcium oscillator. *Biochem. J.* 271:835-838.

Takahashi, T., E. Neher, and B. Sakmann. 1987. Rat brain serotonin receptors in *Xenopus* oocytes are coupled by intracellular calcium to endogenous channels. *Proc. Natl. Acad. Sci. USA*. 84:5063-5067.

Tamakatsu, T. and W. G. Wier. 1990a. Calcium waves in mammalian heart: quantification of origin, magnitude, waveform, and velocity. *FASEB*. 4:1519-1525.

Tamakatsu, T. and W. G. Wier. 1990b. High temporal resolution video imaging of intracellular calcium. *Cell Calcium*. 11:111-120.

Tanaka, y., N. Hayashi, A. Kaneko, T. Ito, E. Miyoshi, Y. Sasaki, H. Fusamoto, and T. Kamada. 1992. Epidermal growth factor induces dose-dependent calcium oscillations in single fura-2-loaded helaptcytes. *Hepatology*. 16:179-486.

Taylor, W. C., W. J. Berridge, K. D. Brown, A. M. Cooke, and B. V. L. Potter. 1988. Dl-myo-inositol 1,4,5-trisphosphate mobilizes intracellular calcium in Swiss 3T3 cells and *Xenopus* oocytes. *Biochem. Biophys. Res. Comm.* 150:626-632.

Valko, P. and S. Vajda. 1985. An extended ODE solver for sensitivity calculations. *Comput. Chem*. 8:255-271.

Wakui, M., Y. V. Osipchuk, and O. H. Petersen. 1990. Receptor-activated cytoplasmic Ca^{2+} spiking mediated by inositol trisphosphate is due to Ca^{2+}-induced Ca^{2+} release. *Cell*. 63:1025-1032.

Wakui, M. and O. H. Petersen. 1990. Cytoplasmic Ca^{2+} oscillations evoked by acetylcholine or intracellular infusion of inositol trisphosphate or Ca^{2+} can be inhibited by internal Ca^{2+}. *FEBS*. 263:206-208.

Wakui, M., V. L. Potter, and O. H. Petersen. 1989. Pulsatile intracellular calcium release does not depend on fluctuations in inositol trisphosphate concentration. *Nature*. 339:317-320.

Wolff, D. J., P. G. Poirier, C. O. Brostrom, and M. A. Brostrom. 1977. Divalent cation binding properties of bovine brain Ca^{2+}-dependent regulator protein. *J. Biol. Chem.* 252:4108-4117.

Wrzosek, A., H. Schneider, S. Grueninger, and M. Chiesi. 1992. Effect of thapsigargin on cardiac muscle cells. *Cell Calcium*. 13:281-292.